5-2019

Incorporating Recent Geochemical and Isotopic Constraints in Age Dating the Waters of Hot Springs National Park, Arkansas

Kristina Marie Raley
University of Arkansas, Fayetteville

Incorporating Recent Geochemical and Isotopic Constraints in Age Dating the Waters of Hot Springs National Park, Arkansas

A thesis submitted in partial fulfillment of
the requirements for the degree of
Master of Science in Geology

by

Kristina Raley
Baylor University
Bachelor of Science in Geology, 2014

May 2019
University of Arkansas

This thesis is approved for recommendation to the Graduate Council.

_____
Phillip D Hays, Ph.D.
Thesis Director

_____
Ralph Davis, Ph.D.
Committee Member

_____
John Van Brahana, Ph.D.
Committee Member

Abstract

Mean water age for spring discharge in Hot Springs National Park was calculated as approximately 4,400 years by Bedinger et al (1978) using carbon-14. Their analysis indicated that the water was a mixture of a small portion of cold water that was less than twenty years old with a preponderance of hot water. However, this result includes some error due to Bedinger et al. using general isotopic values for soil dissolved inorganic carbon and mineral carbon instead of obtaining actual values from the study area. A more accurate age calculation for the springs has been made possible by additional geological and geochemical data collected (Bell and Hays, 2007; Kresse and Hays, 2009).An improved age model for the Hot Springs National Park was be developed using the USGS software NETPATH-WIN; this program models the isotopic compositions and net geochemical mass balance reactions along the flowpath. NETPATH-WIN is capable of calculating possible combinations of mass transfers. Rayleigh distillation calculations can also be applied to each model to predict carbon and radiocarbon dates at the end path. Seven different A_0 models will be tested in conjunction with three different geochemical systems with mixing and non-mixing scenarios.

Geochemical, physical, and selected field parameters were collected from 10 cold-water springs, 30 cold-water wells, and 16 thermal springs, primarily by USGS personnel during three sampling events: 1) from January through September 1972; 2) from September 2007 to June 2008; and 3) during June 2018 by the author. Analysis from the 181 model runs that passed a QA/QC check determined that the most applicable most applicable geochemical system scenario and A_0 model for the flow system is the Non-Mixing Alkaline-Earth geochemical system with the Mass Balance (1990) A_0 model that produced a median mass residence time of 4,375 years.

Acknowledgements

The financial assistance provided by the James D. and Donna K. Morrison Geosciences Scholarship and the Matthew Edmonds Geology Award is gratefully appreciated. Ty Johnson of the Arkansas Geological Survey provided his knowledge of the stratigraphy of the Hot Springs area; additionally, his geological map proved to be invaluable to this thesis. I would also like to thank David Parkhurst for kindly responding to email correspondence concerning NETPATH. Kelly Sokolosky provided latitude and longitude coordinates for the thermal springs in Hot Springs National Park, Arkansas. Michael Foust assisted with the creation of the location maps with his knowledge of ArcMap. Erik Polluck and Lindsey Conaway provided laboratory assistance. Dr. Thomas Byl and Aaron Pugh assisted with collected field samples. Joshua Blackstock provided invaluable assistance with planning techniques, finding the latest version of NETPATH, NETPATH-WIN, and field sampling techniques. Julie Rodgers assisted with all formatting issues with Microsoft Word. Finally, I would like to acknowledge Dr. Van Brahana and Dr. Phil Hays for their writing expertise and knowledge of Hot Springs, Arkansas.

Dedication

This report is dedicated to several individuals without whom this thesis would not have happened. First, I would like to thank Dr. Hays and Dr. Van Brahana for being patient and honest with me. I would also like to thank Lisa and Steve Milligan for allowing me to finish my data collection and conduct model runs at their home during the summer of 2018. Last but not least, I would like to thank my support network, which includes my mom, Karen, and my dad, Greg. Thank you, Sean, for volunteering to be a copy editor and to Alicia Harrington for your never-ending support. Also, a thank you to all the lovely ladies at St. Scholastica for thinking of me and being the best cheering squad, a girl could ask for. Finally, this is dedicated to the members of my family who are no longer here but provided great emotional support during this process: Jeanette Bennett, Sister Anne Michelle Raley, and Pepper the Golden Retriever/Labrador mix.

Contents

Figures

Tables

Conversion Factors, Vertical Datum, and Abbreviations

All latitude and longitude coordinates are recorded in NAD27

Temperature in degrees Celsius (°C) may be converted to degrees Fahrenheit (°F) as follows:

°F= (1.8 x °C) + 32

Abbreviations and Acronyms Used in this Report

Ag, Silver

Al, Aluminum

amu, Atomic mass units

As, Arsenic

B, Boron

Ba, Barium

Be, Beryllium

^{12}C, Carbon-twelve

^{13}C, Carbon-thirteen

^{14}C, Carbon-fourteen

Cd, Cadmium

Cl, Chlorine

Co, Cobalt

CO_2, carbon dioxide

Cr, Chromium

Cu, Copper

DIC, Dissolved inorganic carbon

DO, Dissolved oxygen

DOC, Dissolved organic carbon

δD, Deuterium

Eh, Electromotive potential

Fe, Iron

Fl, Fluoride

H, Hydrogen

HNSP, Hot Springs National Park

IM, Initial Member

Li, Lithium

MDa, Arkansas Novaculite

meq, Microequivalents

Mg, Magnesium

mg/L, Milligrams per liter

Mhs, Hot Springs Sandstone

Mn, Manganese

Mo, Molybdenum

MRT, Mean Residence Time

Ms, Stanley Shale

Na, Sodium

NBS-19, National Bureau of Standards

Ni, Nickel

µg/L, Micrograms per liter

µS/cm, Microsiemens per centimeter at 25 degrees Celsius

Obf, Bigfork Chert

$^{o}/_{oo}$, Parts per thousand (per mil)

%, Percent

Pb, Lead

P_{CO2}, Partial pressure of CO_2

p*e*, Negative log of the electron activity

pH, Negative log of the activity of the hydrogen ion

pmc, Percent modern carbon

ppm-v, Parts per million per volume

Sb, Antimony

Se, Selenium

Si, Silica

SO_4^{2-}, Sulfate

Sr, Strontium

$^{87}Sr/^{86}Sr$, Strontium ratio

TDIC, Total Dissolved Inorganic Carbon

TDS, Total dissolved solids

Tl, Thallium

TU, Tritium Units

V, Vanadium

VPDB, Vienna Pee Dee Belemnite

VSMOW, Vienna Standard Mean Ocean Water

Zn, Zinc

Introduction

Hot Springs National Park (HSNP) encompasses the area of resurgence for 44 thermal springs concentrated within the physiographic province of the Ouachita Mountains, in west-central Arkansas (Figure 1). The Ouachita Mountains are structurally composed of complex folds and thrust faults that are approximately orientated east-west, resulting from the Ouachita orogeny (Guccione, 1993).

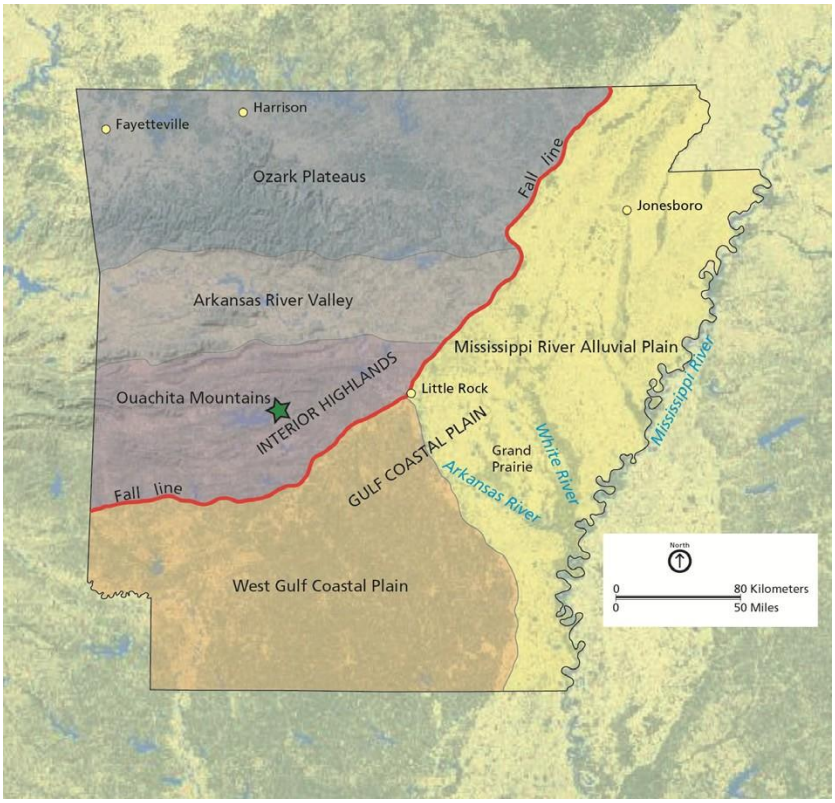

Figure-1: Physiographic provinces of Arkansas with information from Arkansas Geological Survey (2012). Green star denotes the location of Hot Springs National Park. *Graphic credit: Trista L. Thornberry-Ehrlich (Colorado State University) using ESRI National Geographic topographic imagery base layer.*

The regional tectonics of this plate to plate compression dominate existing land surface of the northwestern one-third of the state, long after the last vestiges of mountain building dissipated at the close of the Paleozoic Era (Figure 1). Plate collision compacted sedimentary layers that were transported as terrigenous sediments carried by streams from the north, northeast and south. Another major source of highly siliceous sediments, many of which were transported by a combination of air-fall of volcanic ash and stream transport of ash from island arcs that lay to the south, provided the source material for the 650-foot thick Arkansas Novaculite as well as the Hatton Tuff (Niem, 1971).

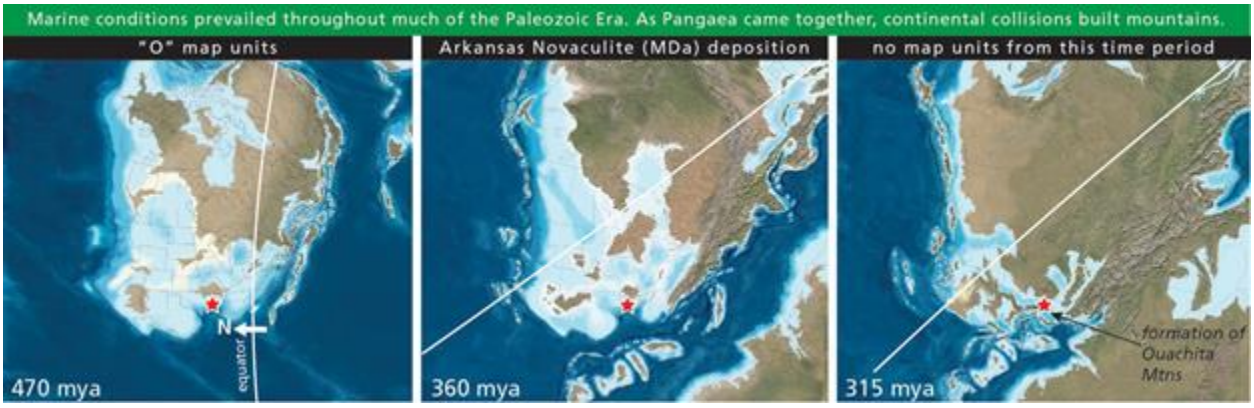

Figure-2. Paleogeography for the area of the Ouachita Mountains and Hot Springs National Park, Arkansas. The maps show deposition of major sediments and the regional tectonics that formed the Ouachita Mountains. The red star represents the approximate locations of HSNP, and the white line represents the approximate location of the equator. The abbreviation "mya" means "million years ago". *Figure modified from Thornberry-Ehrlich, 2013. Graphic compiled by Jason Kenworthy (NPS Geologic Resources Division). Base paleogeographic maps created by Ron Blakely (Colorado Plateau Geosystems, Inc), which are available at http://cpgeosystems.com/index.html.*

Since the Cretaceous Period, the southern segment of the Ouachita orogen is overlain by younger sediments (in the region of southern Arkansas/northern Louisiana) and is not visible at land surface (Viele and Thomas, 1989). The collision of tectonic plates and the resultant

subduction of the southern plate generated thermal metamorphism of rocks near the core of the orogeny (Keller et al., 1977; Thornberry-Erlich, 2013).

On average, the park recently has attracted more than 1.76 million visitors annually since 2000 (Thornberry-Ehrlich, 2013). The springs serve as an important source of drinking water for the town of Hot Springs as well as for park visitors for recreational and therapeutic purposes (Bell and Hays, 2007). The park is notable for being the first national reservation ever created. The United States government set aside the area of the hot springs in 1832 (Haywood and Weed, 1912); it was formally named a national park in 1921 (Harris et al., 2004).

The systematically-fractured strata through which the hot springs flow are mostly Paleozoic sedimentary rocks that have undergone slight thermal metamorphism and at least three episodes of compressional deformation and uplift. Deformation events resulted in a series of thrust faults and also overturned, complexly folded anticlines and synclines trending in a northeast-southwest direction (Bedinger et al., 1979; Bell and Hays, 2007; Thornberry-Ehrlich, 2013). Uplift of these rocks was responsible for systematic jointing. The resulting configuration of the deformed core of the Ouachitas in HSNP is known as the Zig-Zag Mountains (Purdue and Miser, 1923; Bedinger et al., 1979; Kresse and Hays, 2009).

The source of heat and water that create the hot springs was historically a source of contention, although recent studies appear to have resolved the issue in favor of meteoric recharge moving slowly (multiple millennia) downgradient through low-permeability joints and fractures to depths of from 6000 to 8000 feet, gaining heat from the geothermal gradient, until the water reached its maximum temperature at the intersection of recharge pathways with thrust faults and rapidly rising (several days) along faults that are much more permeable than the downgradient portion of the flowpath (Figure-5). This rapid expulsion of the groundwater does

not allow time for reequilibration of temperature as it moves from its hottest to the cold surface environment. Additionally, this hot water is mixed near the distal end of the flow system with cold-water recharge from nearby shallow sources. This interpretation contrasts with the hypothesis of a deep igneous source for heat and water, and is based on geochemistry, stable isotopes, and recently developed methodologies found in the signatures of rock/water interaction. Bedinger et al. (1979) calculated the mean residence time of the spring discharge using carbon-14 (^{14}C) unstable isotope (radionuclides). Additionally, Bedinger et al. (1979) provided tritium (^{3}H) values, which indicated a mixture of old, hot water with fairly young, cold water near the resurgences of the springs at HSNP of local isotopic values in their mixing calculations. The analysis indicated that the water is a mixture of a small portion of water less than twenty years old with a preponderance of hot water giving an averaged, mixed age of 4,400 years old (Bedinger et. al., 1979). However, ^{14}C-age dating performed by Darrell Pennington using an integrated mass-balance model developed in NETPATH-XL to calculate the groundwater dates indicated dates younger than 4,400 years. In order to compliment Pennington's initial findings, performed additional analysis of ^{14}C activity models and mass transfer functions by using the latest data gathered by the U.S. Geological Survey (USGS) and the age modeling software NETPATH-WIN.

Purpose and Scope

There are two major objectives of this thesis. The first is to compile and synthesize select analyses and studies that meet strict QA/QV requirements in the area of Hot Springs National Park since the introduction of the seminal report by Bedinger et al., 1978. This report marked the change from descriptive studies to reports involving sophisticated geochemical analyses and theoretical modeling. Multiple reports and numerous analyses have been generated since 1979,

and they have tended to focus on questions of limited scope. This report expands the scope to that of Bedinger et al., 1979, with the inclusion of the new hydrogeological, geochemical, and isotopic data. The second purpose is to generate a refined estimate of the age of the hot water in the springs of HSNP using the geochemical model NETPATH-WIN developed by the U.S. Geological Survey [USGS] (Plummer et al., 1994; Parkhurst and Charlton, 2008; El-Kadi et al., 2010). Determining the age of the groundwater, which is computed value of the mean duration that the water has been out of contact with atmosphere. Another means of identifying groundwater age is to refer to it as subsurface residence time. This computation provides effective information for management of the park, it provides a timeframe for groundwater circulation, and it informs managers as to whether the springs can be considered as renewable (Clark, 2015). Groundwater that is actively being recharged is considered a sustainable resource, whereas groundwater that is not being actively recharged, such as water from an ancient igneous source, is considered a mineable mixing models that account for local geochemical and isotopic values.

Study Area

HSNP is located within the city limits of Hot Springs and based on recent work by Kresse and Hays (2009), the recharge zone for the hot springs has been extended to the north and east of HSNP. As a result of their finding, the boundary of this study has been expanded to include their expanded area. (Figure-3). On March 4, 1921 HSNP became an officially designated national park. The park encompasses slightly more than 22 square kilometers (km^2) and contains forty-seven hot springs within its boundaries (Hays oral commun., 2018). The study area for this report includes both the recharge zone that is located outside the park and the discharge zone which is located inside the park (Figure-3).

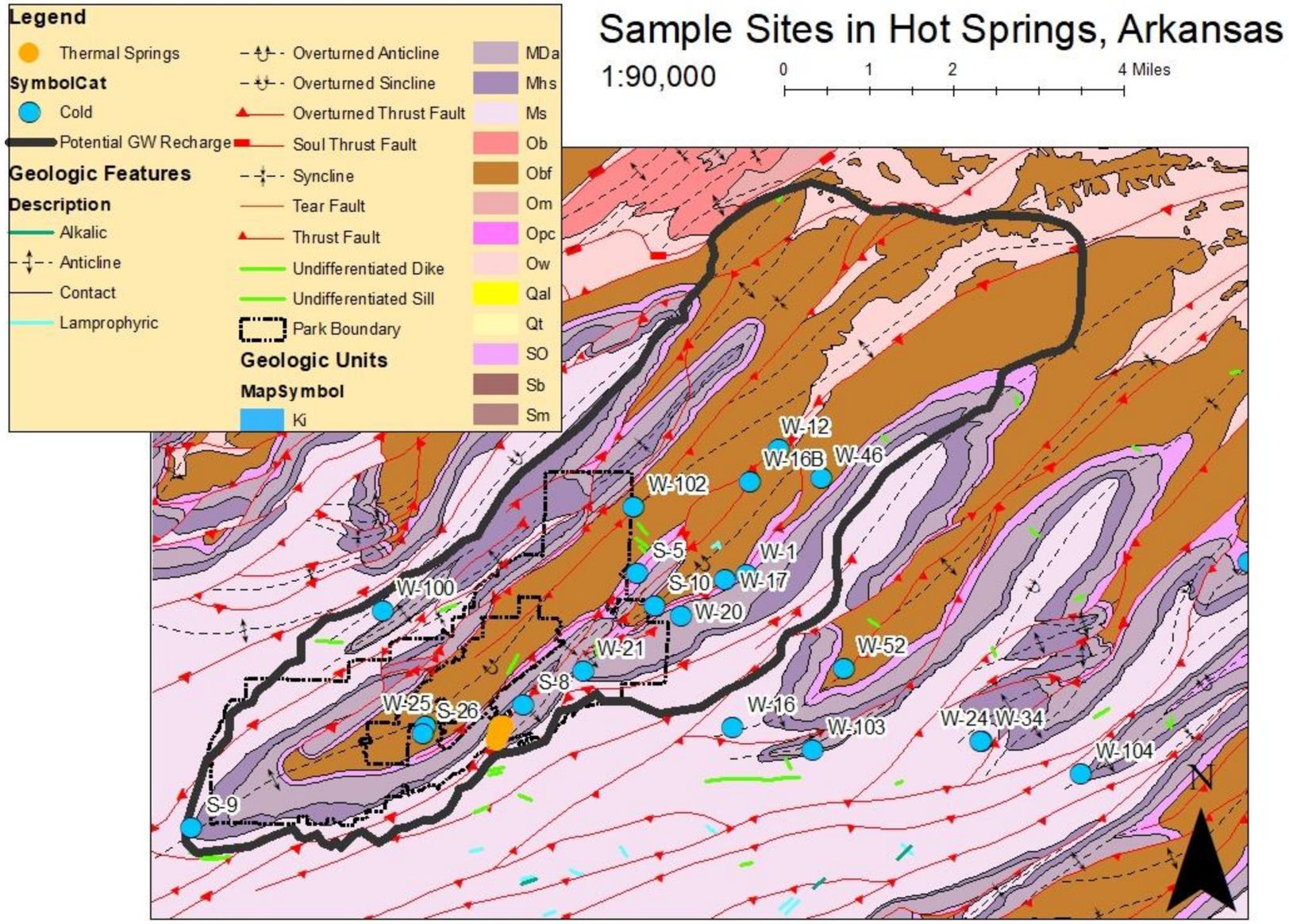

Figure-3: Geologic location map of samples collected in Hot Springs, Arkansas. The dark grey line indicates the potential groundwater recharge boundary. Cold water wells and springs are labeled and are indicated by a blue dot. Thermal springs are indicated by orange dots and are shown in better detail in Figure 4. *ArcMap data was obtained from Dr. Phil Hays and is sourced from Johnson and Hanson (2011)*

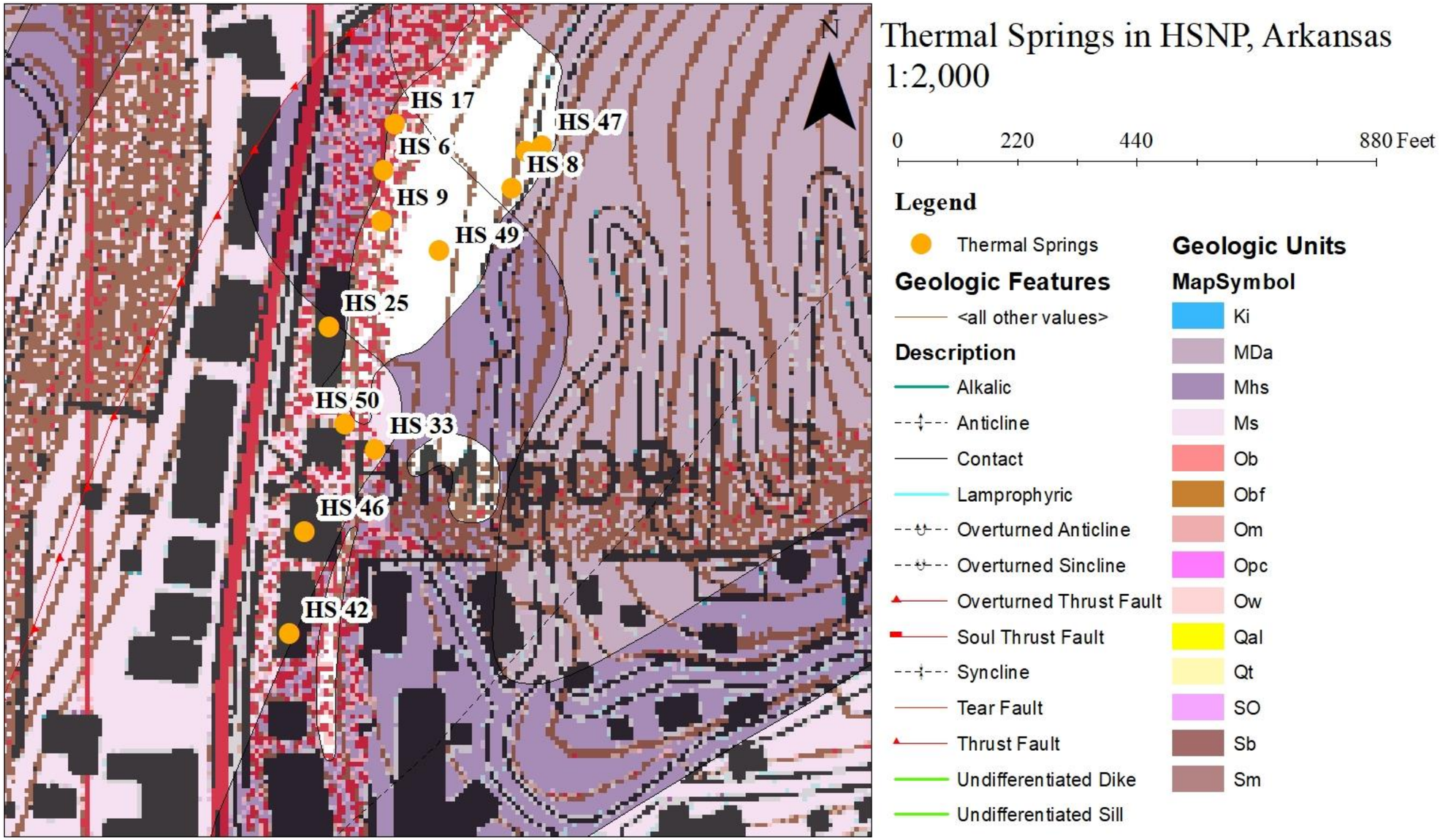

Figure-4: Location map of thermal springs sampled off of Central Avenue in Hot Springs National Park Arkansas. Thermal springs are represented by orange dots. *ArcMap data was obtained from Dr. Phil Hays and is sourced from Johnson and Hanson (2011). Location data was provided by Kelly Sokolosky*.

Geology

Tectonic Setting

The Ouachita Mountains are structurally composed of complex folds and thrust faults lying south of the valley of the Arkansas River (Figure-1); these folds and thrusts resulted from the collision between the ancient continents of Llanoria and Laurasia during the late Pennsylvanian and Permian periods (Guccione, 1993). This collision compacted sedimentary layers of mud, sand, and quartz crystals together to form layers of shale, sandstone, and chert (Guccione, 1993). The strata that make up the flow path for the springs are mostly Paleozoic sedimentary rocks that have undergone at least three episodes of compressional deformation; these deformation events resulted in a series of thrust faults and also overturned complexly folded anticlines and synclines trending in a northeast-southwest direction (Bedinger et al., 1979; Bell and Hays, 2007; Darrell Pennington written commun., 2009; Thornberry-Ehrlich, 2013).

Stratigraphy

The formations that the waters are currently hypothesized to pass through include the Womble Shale, Bigfork Chert, Missouri, Polk Creek Shale, Arkansas Novaculite, Hot Springs Sandstone, and the Stanley Shale [Figure-4] (Purdue and Miser, 1923; Albin, 1965; Bedinger et al., 1979; Bell and Hays, 2007; Yeatts, 2006).

The Womble Shale is the oldest unit in in the hydrogeological model. This unit is assumed to range in thickness from 500 to 1200 ft (Purdue and Miser, 1923; McFarland, 2004; Johnson written commun., 2018). The Womble is predominately black, hard, argillaceous shale with interlaying thin beds of sandstone and limestone; the sandstone occurs in several areas, is well-cemented, and ranges in thickness of 6 inches to 3 feet (Purdue and Miser, 1923). The

limestone layers are hard, compact lentils that are 20 ft or more in thickness and are mostly found in the northwest section of the district, interspersed with numerous quartz veins (Purdue and Miser, 1923; Yeatts, 2006). Limestone and calcite veins are found near the top of the unit while the shale near the "contact with the Big Fork Chert is sooty and graphitic and thus possibly contains high amounts of carbon" (Johnson written commun., 2018).

The Bigfork Chert overlies the Womble Shale; the Formation consists of thin-bedded, dark to light gray cryptocrystalline chert interbedded with black siliceous shale, sandstone, calcareous siltstone, and dense blue gray limestone; additionally, parts of the Formation contain small quantities of disseminated calcite and pyrite" (Purdue and Miser, 1923; Johnson and Hanson, 2011). The thickness of the unit for the Hot Springs mapping area is assumed to be 750 ft (Johnson written commun., 2018). Numerous amounts of straight, glossy-surfaced joints oriented in all directions is found in the Big Fork Chert (Purdue and Miser, 1923). The joints are often filled with quartz veins and a little bit of calcite (Purdue and Miser, 1923). The sandstone in this unit is fine grained and thin-bedded (Purdue and Miser, 1923). Limestones were found near the top of the unit (Johnson written commun., 2018). Additionally, Tripoli was "found throughout the unit where entire beds were composed of it"; this is significant since Tripoli is the "product of weathered calcareous chert" (Johnson written commun., 2018). Limestone fragments are also found in the olistromes (debris flows) that occur in this unit (Johnson written commun., 2018). This unit is thinly-interbedded and has disharmonic folding (Purdue and Miser, 1923; Johnson and Hanson, 2011).

The Missouri Mountain Shale and the Polk Creek Shale "were mapped together in the Zigzag Mountains because the Blaylock Sandstone is not deposited here dividing the two" (Johnson written commun., 2018). The thicknesses of these two units range from 200 to 250 ft

and the “thicknesses are trusted” due to the formations being in “contact with the rigid Arkansas Novaculite” (Johnson written commun., 2018). The Polk Creek Shale is composed of black, fissile, and graphitic shale with thin layers of dense black chert and hard quartzitic sandstone (Purdue and Miser, 1923). The Formation itself is intensely crumpled and contains many slickensides and joints (Purdue and Miser, 1923). The Missouri Mountain Shale consists of shale, conglomerate, and thin layers of sandstone and quartzite (Purdue and Miser, 1923). The conglomerate layer contains limestone clasts with a shale matrix (Purdue and Miser, 1923). The sandstone and quartzite layers are hard and three to five inches thick with round grains of quartz (Purdue and Miser, 1923). The shale itself is soft and argillaceous and contains plentiful number of joints which are oriented in all directions (Purdue and Miser, 1923).

The Arkansas Novaculite is a very thick formation with three members: a lower, middle and upper. The lower member is approximately 275 ft thick, the middle member ranges from 0 to 80 ft thick and “can be eroded away locally”; the upper member ranges from 0 to 160 ft thick “and can be eroded away locally” (Johnson written commun., 2018). The lower member is a massively bedded unit with white to dark-gray cryptocrystalline quartz, fine-grained novaculite on thin edges and is interbedded with “gray shales, minor amounts of sandstone and conglomerate near the base” (Johnson and Hanson, 2011). The middle member is composed of “dark-gray to black siliceous shale interbedded with numerous thin beds of dark novaculite” (Johnson and Hanson, 2011). The novaculite beds are generally less than two inches thick in the Zigzag Mountains (Johnson and Hanson, 2011) The Upper Novaculite is composed of “white thin-bedded novaculite interbedded with soft white shale and is typically calcareous and contains thick beds of Tripoli (Johnson and Hanson, 2011; Johnson written commun., 2018). Some areas in the Formation “may be more calcareous than others and tripoli has been noticed to form

primarily in overturned beds" (Johnson written commun., 2018). All three members are brittle and jointed into angular rocks (Purdue and Miser, 1923). Novaculite is a low grade altered microcrystalline chert (Johnson written commun., 2018).

The Hot Springs Sandstone overlays the Arkansas Novaculite (Purdue and Miser, 1923). The thickness is variable from 0 to 450 ft; the unit "is present throughout the Zigzag Mountains and it pinches out to the south" (Johnson, written commun., 2018). "There are a few anomalously thick areas of this unit and the unit is also associated with more faulting and tighter folding due to the increased rigidity" (Johnson written commun., 2018). This unit consists "of medium to fine-grained, sub-angular to sub-rounded quartzarenite" with quartzite located in some places in the unit (Johnson and Hanson, 2011). There is some conglomerate at its base and shale and siltstone at the top (Purdue and Miser, 1923; Johnson and Hanson, 2011). The conglomerate clasts are composed of novaculite with a sandy matrix (Purdue and Miser, 1923). The sandstone layers are hard and quartzitic, with joints in various directions (Purdue and Miser, 1923).

Finally, the Stanley Shale is composed "predominantly of grayish-black to brownish-gray shales, with lesser amounts of thin to massive-bedded, fine-grained, gray to brownish-gray, micaceous, feldspathic sandstone, dark-green to black tuff and black chert" (Johnson and Hanson, 2011) The weathered sandstone is "generally more porous" for this unit (Johnson and Hanson, 2011). At the contact with the Hot Springs Sandstone, the "clean sandstones are interbedded with shale and sandstone in the Stanley" (Johnson and Hanson, 2011). Both the sandstone layers and the shale layers contain joints in all directions and are filled with quartz veins (Purdue and Miser, 1923). There are also "significant calcite veins within the unit in some

areas usually around faulting" (Johnson written commun., 2018). The thickness of the unit is speculated to be 1500 ft (Johnson written commun., 2018).

Table-1: Lithostratigraphy of HSNP, modified from Johnson written commun. 2018

System	Unit	Character of rocks	Maximum thickness in Hot Springs area[1] (ft)
Mississippian	Stanley Shale	Greyish-black to brownish grey shales with interbedded thin to massive micaceous, feldspathic sandstone, dark green to black tuff and black chert. Significant calcite veins near faulting.	1500
	Hot Springs Sandstone Member of the Stanley Shale	Quartzarenite sandstone with quartzite located in some places with a conglomerate base and shale and siltstone at the top	0 - 450
	Arkansas Novaculite	Massive and interbedded with cryptocrystalline quartz, novaculite, shales, sandstones, and conglomerate. The upper member is tripolitic and all members are highly fractured	275
Devonian			
Silurian	Missouri Mountain Shale	Shale, conglomerate and thin layers of sandstone and quartzite. Lots of joints	200 - 250
Ordovician	Polk Creek Shale	Black, fissile, graphitic shale with thin layers of dense black chert and hard quartzitic sandstone	
	Bigfork Chert	Thin-bedded dark to light gray cryptocrystalline chert interbedded with siliceous shale and subordinate amounts of calcareous siltstone and dense blue-gray limestone. Highly fractured. Limestone found near top; Tripoli found throughout	750
	Womble Shale	Black, hard, agrillaceous shale with interlaying beds of sandstone and limestone. Limestone and calcite veins are found near the top. Contact is sooty and graphitic.	500 - 1,200

[1]Ty Johnson, Arkansas Geological Survey, written commun., 2018

In summary, the stratigraphic column of HSNP are silica-based units (sandstones, chert, and novaculites) and shale-based units with interlaying layers of limestone and calcite. All units, except the Womble Shale, experienced considerable compressional deformation and contain a

widespread distribution of joints; therefore, groundwater flow is controlled by secondary porosity with primary porosity being negligible (Kresse and Hays, 2009).

Groundwater Flow

The ability of groundwater to flow through strata depends on a rock's permeability and porosity. Porosity of rocks is the amount of pore space of said rock; in other words, the part of the rock that is "devoid of material" (Fetter, 2001). Sedimentary rocks may have primary porosity—porosity originally present after sediment deposition—and secondary porosity—porosity created by diagenetic process porosity (Fetter, 2001). Primary porosity is reduced after burial by compaction and lithification; the essential takeaway is that the "primary porosity of a sedimentary rock" (i.e. porosity through pore space) "will be less than that of the original sediment" (Fetter, 2001). Groundwater can also travel through rock via the secondary porosity. This refers to openings in rocks created by faults, joints, fractures, and dissolution

Permeability is a measurement of the capability of a material to transfer fluid that is controlled by the size and conductivity of pores (Palmer, 2007). The greater the effective diameter of pores the higher the permeability (Fetter, 2001). The porosity of sedimentary rocks is dependent on grain-size sorting, shape, and what material composes the matrix of the rock (Fetter, 2001).A rock's permeability and porosity characteristics determine whether the unit is classified as an aquifer, i.e. a rock that has high permeability and high porosity, or a confining unit, i.e. a rock that has relatively low permeability and low porosity. The stratigraphic units of the study area are highly fractured, contain many joints, and have a reverse fault running through them thus allowing water to flow through the rocks via secondary porosity.

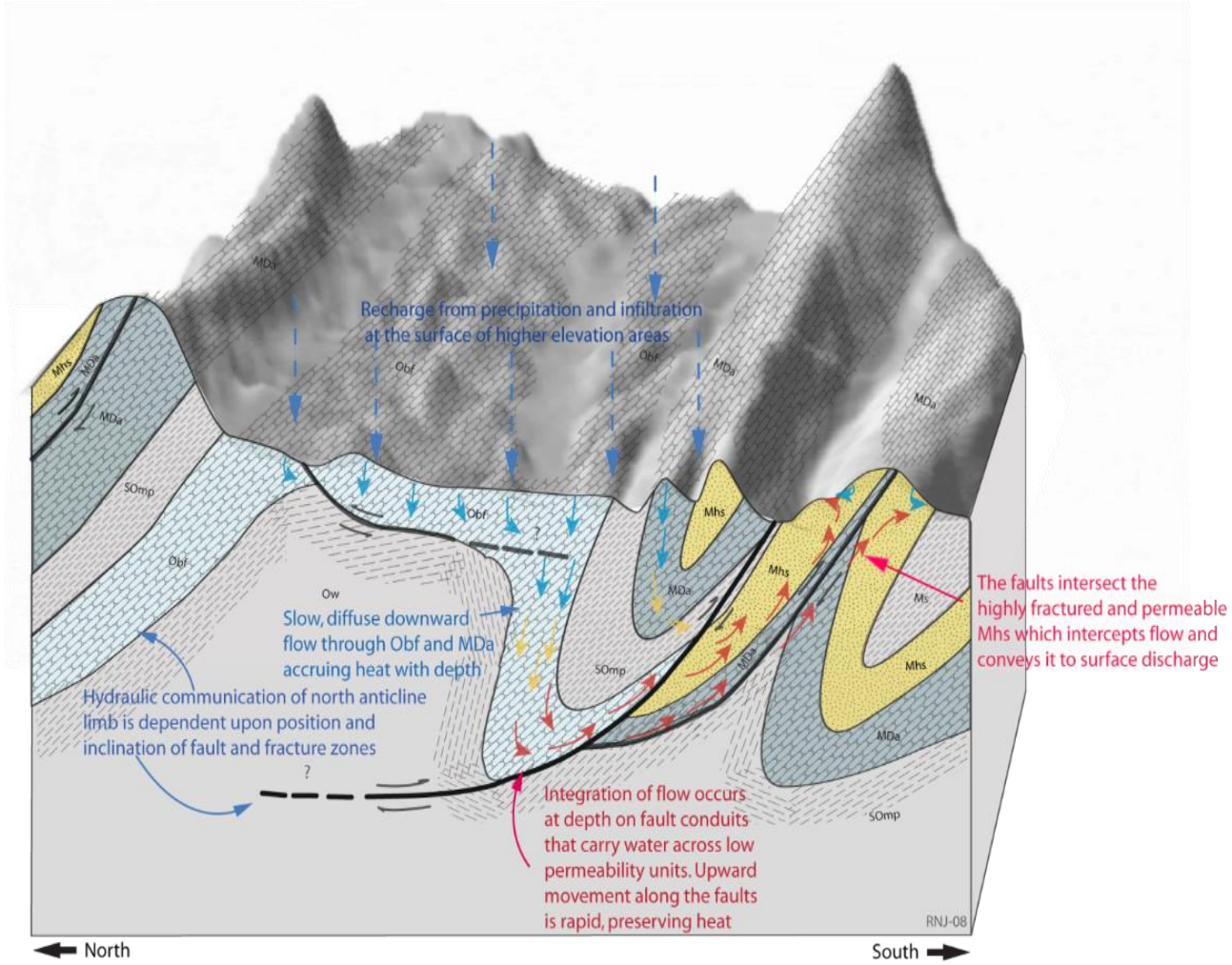

Figure-5: Conceptual model of the thermal groundwater flow for HNSP, Arkansas. Meteoric recharge enters the Bigfork Chert and the Hot Springs Sandstone and slowly flows downgradient, heated from the geothermal gradient during descent to depth. When the waters reaches a thrust fault, it flows upward very rapidly. (Source: *P.D. Hays, written commun., 2018)*

Hydrogeology

Past studies of the hot springs system concluded that the discharge from the hot springs is meteoric in origin; precipitation enters the highly fractured Bigfork Chert and Arkansas Novaculite in the anticlinal valley tens of miles west, north, and northeast of the discharge area for the hot springs (Bedinger et al., 1979; Bell and Hays, 2007). Once in the ground the waters travel down to an estimated depths of 4,500 ft to 7,500 ft with an estimated geothermal gradient ranging from 0.006 ºC/ft to 0.01 ºC/ft the water is heated as it descends until the flow path reaches the conduits created by thrust faults (Haywood, 1912; Bryan, 1922; Bedinger et al., 1979; Yeatts, 2006; Bell and Hays, 2007; Thornberry-Ehrlich, 2013). The hot waters resurge "from the plunging crestline of a large overturned anticline between the traces of two thrust faults that are parallel to the axis of the anticline" (Kresse and Hays, 2009; Darrell Pennington written commun., 2009). The thermal waters discharge in the Hot Springs Sandstone and are confined by shales in the southwest, southeast, and northwest sections of the park (Yeatts, 2006). The cold-water component is derived from precipitation that enters the ground and flows to the hot springs via "shallow northeast trending faults, joints and fractures" (Bedinger et al., 1979; Yeatts, 2006; Bell and Hays, 2007). Yeatts (2006) concluded that "the lower member of the Arkansas Novaculite is probably the primary aquifer of shallow groundwater flow". Additional cold-water recharge sources include "vertical infiltration through fill material, lateral infiltration from Hot Springs Creek, and shallower flow paths from the thermal water recharge zone" (Yeatts, 2006; Darrell Pennington written commun., 2009). The recharge area for the shallow ground-water (i.e. the cold-water component) is "bounded on three sides by low-permeability barriers and extends approximately to the topographic divide"; these barriers create a recharge

area of approximately 0.14 mi^2 (Yeatts, 2006; Darrell Pennington written commun., 2009). (See Figure-5 for a visual explanation on the flow model for the hot springs system).

Previous Studies

There have been a variety of studies done in HSNP soon after the park first opened. This paper will merely go over the researched highlights of various studies. Early research came to the following conclusions: that the source of the spring discharge was of meteoric origin, that the recharge area occurred in the Bigfork Chert located in the anticlinal valley between the Sugarloaf and West Mountains, and that a fault system (along with fractures and joints) would be required for the groundwater to discharge at the Hot Springs Sandstone (Purdue and Miser, 1923; Bedinger et al., 1979; Darrell Pennington written commun., 2009). The next big breakthrough came in Bedinger et al's comprehensive study of the hot springs. Bedinger's group used the stable isotope analysis of deuterium and oxygen-18 concentrations to determine the chemical concentrations of the discharge of the hot springs are "not significantly different from those of the cold ground waters" (Bedinger et al., 1979). The deuterium and oxygen-18 values, the other geochemical data, flow measurements, and study of the geologic structure of the region hot-springs water is of local meteoric origin" *(*Bedinger et al., 1979*)*. In addition to the study's previously mentioned age dating, mathematical modeling was used to test the flow path and deduced that the groundwater was slowly heated after coming into contact with high temperature rocks (Bedinger et al., 1979). Bedinger et al (1979) used the global value of $0^0/_{00}\ \delta^{13}C$ for mineral carbon and $-24^0/_{00}\ \delta^{13}C$ for soil carbon (referred to as plant Carbon in Bedinger et al (1979). Bedinger et al's (1979) ^{14}C and tritium analyses indicated the springs were a mixture of hot water around 4,400 years old with a cold-water component less than 20 years old.

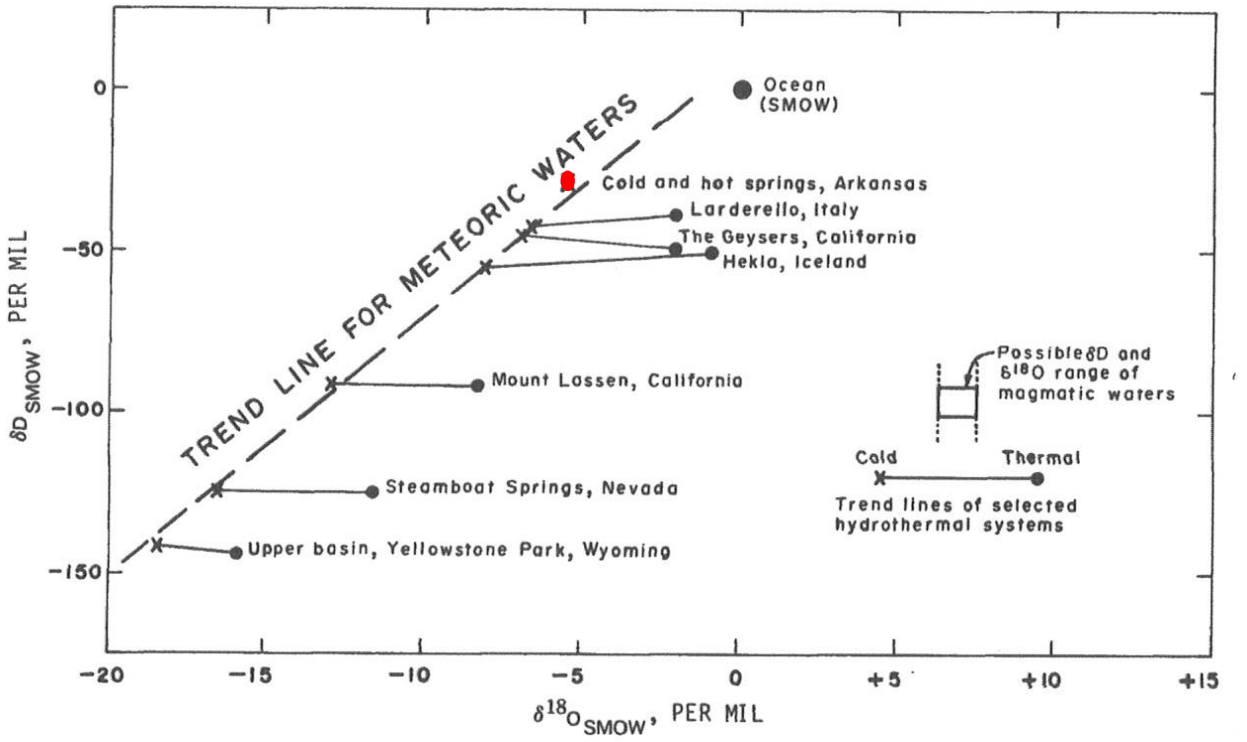

Figure-6: Comparison of isotopic composition of waters from the cold and hot springs of Arkansas and of hydrothermal waters elsewhere (after White and others, 1973).

Bell and Hays (2007) used water-quality, water-temperature, isotopic and radiochemical data to support the importance of the cold-water component of the hot springs. The binary mixing models that used silica and total dissolved solids employed by Bell and Hays indicated that cold-water recharge from storm events contributes an estimated 10 to 35 percent of the discharge issuing from the springs (Bell and Hays, 2007; Darrell Pennington written commun., 2009). Temperature modeling indicated that 1 to 35 percent of the discharge from various hot springs originated from cold-water recharge (Bell and Hays, 2007; Darrell Pennington written commun., 2009). Yeatts (2006) noted that the cold-water component "enters the ground-water system as locally derived recharge and flows along shallow northeast trending faults, joints, and fractures to the thermal springs". "The thermal springs are bounded on the southwest, southeast, and northwest by shale barriers" (Yeatts, 2006). Yeatts (2006) postulated that "the lower member of the Arkansas Novaculite" is the "primary aquifer of shallow ground-water flow". The

groundwater levels determined the flowpath to be towards Hot Springs Creek (Yeatts, 2006). The flow path indicated by said dye trace was concluded to be "along the western boundary contact with the Stanley Shale or along northeast-trending fractured lineaments" (Yeatts, 2006). The size of the shallow cold-water recharge zone was estimated to range from 0.10 to 0.20 mi^2 with the recharge zone being "bounded on three sides by low-permeability barriers and extends approximately to the topographic divide" (Yeatts, 2006). Yeatts (2006) performed a rhodamine dye trace starting on "Hot Springs Mountain, about 1,000 ft east of Central Avenue" and was "detected above background levels at several thermal recovery sites over a period of several weeks" (Yeatts, 2006). Yeatts postulated that the flowpath of the dye trace "to the thermal springs is probably along the western boundary contact with the Stanley Shale or along northeast-trending fractured lineaments" (Yeatts, 2006). The dye's presences verified that the collection sites "is part of the recharge area and that surface waters enters the ground-water system at some point along the pathway of the rhodamine dye" (Yeatts, 2006).

Kresse and Hays (2009) characterized the water quality and geochemistry for the shallow groundwater system and provided a basis of comparison to the geochemistry of the hot springs by sampling fifteen shallow wells, two cold-water springs, and ten hot springs. Kresse and Hays (2009) concluded that the hydrogeochemistry of the hot springs is the result of the rock/water interactions in the shale formations in the deeper sections of the of the flow path; the low strength ionic waters enter the ground through the quartz formations, travel through the upper formations and "are modified by passage through shale formations present at depth" (Kresse and Hays, 2009). Mixing curves that used strontium, lithium, and manganese data indicated that the shale formations were more significant than the quartz formations for much of the dissolved species content comprising the overall geochemistry (Kresse and Hays, 2009). In exception to

the general geochemistry, mixing model analysis for Sr geochemistry indicated that thirty-five percent of the strontium came from the shale formations while the other sixty-five percent were contributed from the quartz formations (Kresse and Hays, 2009). This analysis implies that the quartz formations are overall more significant in the contribution of Sr^{2+}. Therefore, the quartz formations are implied to be more significant for Ca^{2+} production as Sr^{2+} ions chemically behave similar to Ca^{2+} ions (Zachry oral commun, 2016; Hays written commun., 2018).

Darrell Pennington used the geochemical and isotopic data collected by Bell and Hays (2007) and Kresse and Hays (2009) in the integrated mass-balance model NETPATH-XL which is discussed in greater detail in the methodology chapter of this thesis. Fifteen cold-water springs with a median temperature of 18.55°C represented the initial end members and ten hot-water springs with a median temperature of 61.25°C represented the final end members in the flow path (Darrell Pennington, written commun., 2009). Physical and geochemical parameters for the mass-balance calculations included temperature, pH, conductivity, silica, strontium, and major cations and anions (Darrell Pennington written commun., 2009). Rayleigh distillation calculations were used for ^{14}C, ^{13}C, and $^{87}Sr/^{86}Sr$ for each geochemical system calculated mass transfer NETPATH ; each model also used nine samples collected by the USGS from HSNP to determine median and mean source values for soil CO_2 and mineral carbon and were input into the model in place of global average values (Darrell Pennington written commun., 2009). Initial ^{14}C activity models were derived either from original data or initial end member $\delta^{13}C$ composition (Darrell Pennington written commun., 2009). Four geochemical systems were developed for age calculation based on the groundwater major constituents, observations by Bedinger et al. (1979), and the knowledge of the HSNP geothermal system (Darrell Pennington

written commun., 2009). Forty calculated mass transfer NETPATH runs provided ages ranging from 1281 to 5030 years old (Darrell Pennington written commun., 2009).

Background Theory

Isotope Geochemistry

Each element in the universe is composed of protons, neutrons and electrons. The number of protons distinguishes one element from another, and the number of neutrons, combined with the number of protons, determines the isotope of said element (Clark and Fritz, 1997). An isotope of an element has the same number of protons but has a different number of neutrons (Hoefs, 1987). For example, the element carbon is defined as having six protons and six electrons, and either 6, 7, or 8 neutrons. The sum of the neutrons and the protons gives carbon an atomic mass varying from 12 to 14, of which carbon-twelve (^{12}C) is by far the most prevalent isotope. The isotope carbon-thirteen (^{13}C) contains six protons and seven neutrons, and the isotope carbon-14 (^{14}C) contains six protons and 8 neutrons. Isotopes are categorized into two different groups: stable and unstable (Hoefs, 1987; Clark and Fritz, 1997). ^{12}C and ^{13}C are stable, and ^{14}C is unstable, losing half its mass in 5730 years.

Unstable isotopes, also known as radioactive isotopes or radionuclides, tend to decay to a more stable form at a predictable rate, whereas stable isotopes do not (Clark and Fritz, 1997). Stable isotopes tend to be used as environmental tracers “for the provenance of groundwater” while unstable isotopes are used to measure time and age that the radionuclide has existed in its present form (Clark and Fritz, 1997).

An isotopic ratio is the of the heavy isotope verses the lighter isotopes. Relative abundance of isotopes is expressed as the deviation from a measured standard using delta (δ) notation and values are expressed in per mil ($^{o}/_{oo}$) (Kresse and Hays, 2009):

$$\delta Z_x = (R_x\text{-}R_{std})/\ R_{std} * 1000\ {}^{o}/_{oo}$$

in which

δZ_x is the δ value of sample x

Rx is the sample ratio

Rstd is the standard ratio

Recognizing that several isotopes of one element exist is important when exploring subtleties in chemistry. This is especially true when elements combine with other elements to form molecules. If we examine the molecule carbon dioxide, traditionally written as CO_2, we can mathematically calculate that $^{13}C^{16}O_2$, which has a mass of 45 amu or atomic mass units, is heavier than $^{12}C^{16}O_2$, which has a mass of 44 amu. These differing masses are important since the amount of mass can affect the rates of chemical reactions; this in turn leads to the process of fractionation (Clark and Fritz, 1997).

$$\delta^{13}C_{sample} = \left(\frac{(^{12}C/^{12}C)_{sample}}{(^{13}C/^{12}C)_{reference}} - 1\right) \times 1000\ {}^{o}/_{oo}$$

When calculating isotopic delta values, one must always use a recognized isotopic standard. Isotopic standard values vary depending on the isotope. Isotopic concentrations are expressed as the difference between the sample ratio and the reference ratio over the measured ratio which is expressed using delta (δ) notation (Clark and Fritz, 1997). The isotopic concentrations are expressed in parts per thousand or permil (${}^{o}/_{oo}$). A positive δ- ${}^{o}/_{oo}$ value indicates that the sample has more of the heavy isotope as compared with a standard whereas a negative δ- ${}^{0}/_{00}$ indicates that the sample has less of the heavy isotope as compared with a standard.

The distribution of isotopes in a system is controlled by the fractionation of isotopes during physical/chemical reactions and by the distillation of isotopes from the “reactant reservoir

as the reaction proceeds" (Clark, 2015). The basic idea behind fractionation is that chemical and physical reactions tend to favor the heavier isotopes occupying more stable molecular bond locations over the lighter isotopes. For example, when precipitation condenses and falls from a cloud, said precipitation a greater proportion of heavier isotopes of water as compared with the source vapor of the cloud. Thus, the remaining vapor that makes up the cloud is depleted in the heavier isotope while becoming enriched with the lighter isotope. This process of isotopes becoming either enriched or depleted until the reactant reservoir is used up (i.e. the reaction comes to completion) is the process of distillation, more commonly known as Rayleigh distillation (Clark, 2015).

Carbon Isotope Geochemistry

Carbon has two naturally occurring stable isotopes: ^{12}C with a 98.89 % abundance and ^{13}C with a 1.11% abundance (Faure, 1986; Clark and Fritz, 1997). While the most well-known reference standard for carbon was PDB, NBS standards are more commonly utilized for interlaboratory calibration today (Hoefs, 1987) ^{14}C, also known as radiocarbon, is a radioactive isotope that has a half-life of 5,730 years and is considered a useful tool in hydrogeology to date groundwater when sufficient time has passed since recharge for initial ^{14}C activity to decline (Clark and Fritz, 1997). Since radiocarbon is naturally found in the upper atmosphere and is formed from cosmogenic radiation. It has also been made and added to the atmosphere artificially by the testing of weapons and by nuclear reactors. Measured ^{14}C activities referenced to the international standard known as "percent modern carbon" (pmc) and is defined as ninety-five percent of the ^{14}C activity in the 1950s NBS oxalic acid standard (Clark and Fritz, 1997). The standard is the activity of a specific wood that was grown in 1890 is a fossil-carbon dioxide-free environment (Clark and Fritz, 1997). ^{14}C fractionates during organic and inorganic phase

changes and reactions similar to stable isotopes (Clark and Fritz, 1997). Carbon is analyzed as CO_2 gas by mass spectrometers (Faure, 1986).

Strontium Isotope Geochemistry

Strontium (Sr^{2+} in its ionic form) is a soluble, reactive trace metal that is commonly found in most groundwaters (Kresse and Hays, 2009). This alkaline metal behaves similarly to calcium in various chemical reactions and has the potential to replace calcium in carbonate and sulfate minerals. Strontium has four naturally occurring isotopes: ^{84}Sr, ^{86}Sr, ^{87}Sr, and ^{88}Sr and analysis of strontium is reported as $^{87}Sr/^{86}Sr$ ratios. The reference strontium carbonate standard provided by the National Institute of Standards and Technology is $^{87}Sr/^{86}Sr = 0.70100$ (Clark and Fritz, 1997). Strontium isotopic ratios are interesting to analyze as strontium isotopes themselves are not subject to fractionation.

Additionally, their isotopic signatures are determined only by the concentration of Sr^{2+}(Clark and Fritz, 1997) Strontium ratios are significant to hydrogeological investigations due to different rocks of differing ages tend to have pointedly different strontium ratios (Clark and Fritz, 1997). As groundwater moves through conduits in the rock, the water leaches off minerals containing strontium from the surrounding rock and adds the rock's strontium ratio signature to the groundwaters dissolved Sr^{2+} concentration (Clark and Fritz, 1997; Kresse and Hays, 2009). Analyzing the strontium concentration in groundwater samples can lead to the identification of recharge sources, transport pathways, and mixing. Since strontium is found in carbonates and the mixing model is concerned with locating all sources of carbon, Sr^{2+} can be used as a proxy to determine the mixing sources of lithologic carbon in the system.

Carbon Sources

Carbon is one of the most abundant elements on Earth and can be located in many organic and inorganic sources and fractionated by a variety of processes as displayed in Figure-5 (Faure, 1986). In Figure-5 ^{14}C travels through its pathway from the atmosphere where it is collected by plants which then leads it to the soil and finally to the ground (Darrell Pennington written commun., 2009). Carbon is located in the atmosphere in the form of gaseous CO_2, ultimately sourced from volcanic and crustal exhalation, the combustion of fossil fuels, and respiration. Additionally, atmospheric weapons testing and nuclear power plants emitted additional radiocarbon into the atmosphere while thermonuclear bomb testing emitted enough nitrogen-14 to make ^{14}C. The average atmospheric carbon concentration is 360 ppm-v (parts per million per volume) with a $\delta\ ^{13}C$ value of -6.4 $^{0}/_{00}$ VPDB (Vienna Pee Dee Belemnite) during preindustrial times; today the $\delta\ ^{13}C$ value is -8.3$^{0}/_{00}$ and is slowly decreasing due to a combination of and inputs of "^{13}C-depleted CO_2 from combustion of fossil fuels and enhanced soil respiration" (Clark and Fritz, 1997; Clark, 2015). The partial pressure of CO_2 in 2014 was noted to be about 400 ppm-v and "has been increasing by about ppm/year over the past decade" (Clark, 2015). The average ^{14}C activities in the atmosphere is 104 pmc in CO_2 and 122 pmc in CH_4, or methane gas, with a $\delta\ ^{13}C$ value of -47$^{0}/_{00}$ (Clark, 2015).

Plants can then collect $^{14}CO_2$ by either photosynthesis or by rainwater that contains $^{14}CO_2$ from the atmosphere (Clark and Fritz, 1997). The fractionation that occurs during photosynthesis enriches the amount of ^{12}C in "biologically synthesized organic compounds" while depleting the amount of ^{13}C (Faure, 1986; Clark and Fritz, 1997). This depletion affects the amount of ^{14}C with a resulting mass effect of ~2.3X ^{14}C with respect to ^{13}C fractionation (Clark and Fritz, 1997; Darrell Pennington written commun., 2009). In summary, the fractionation caused by

photosynthesis creates a 4.3% or a $42.5^{0}/_{00}$ enrichment over the standard 100 pmc (Clark and Fritz, 1997; Darrell Pennington written commun. 2009). Photosynthesis can occur one of two ways depending on whether or not the plant is a C_3 or a C_4 plant. Ninety-five percent of plants can be classified as a C_3 plant; a C_3 plant has an "ineffective step of CO_2 respiration" involved in photosynthesis (Clark, 2015). Due to this inefficiency, the $\delta\ ^{13}C$ of C_3 plants is lower than atmospheric CO_2 at a value of $-27^{0}/_{00}$ with a fractionation of $20^{0}/_{00}$ (Clark, 2015). The remaining five percent of plants are classified as C_4 plants; these plants, which evolved due to "declining atmospheric CO_2 concentrations during the past 15 million years", reduce the amount of CO_2 respiration which leads to a lower fractionation of $-6^{0}/_{00}$ and $\delta\ ^{13}C$ values ranging from -10 to $-14^{0}/_{00}$ (Clark, 2015). The ^{14}C activities of living plants in general is 100 pmc (Clark. 2015). Regardless of how CO_2 enters the plant, eventually the carbon will enter the soil due to plant decay or root respiration. Additional sources of soil carbon include carbon captured in rainwater and bacterial oxidation of soils (Clark and Fritz, 1997).

As a result, the soil zone is home to the larger source of carbon with concentrations ranging between 3000 to 30,000 ppm-v and an average $\delta\ ^{13}C$ value of $-27^{o}/_{oo}$ with ^{14}C activity of 95 pmc (Clark and Fritz, 1997; Clark, 2015). The amount of CO_2 that dissolves into groundwater is dependent on the following four factors: the geochemistry of the recharge area, the partial pressure of CO_2 (P_{CO2}), the weathering reactions taking place in the soil zone of the recharge area, and the temperature and pH of the water (Clark and Fritz, 1997; Darrell Pennington written commun., 2009). Weathering reactions in soils is mostly dependent on the oxidation of organic materials in the soil with organically derived CO_2 driving weathering reactions (Clark, 2015). This process combined with hydration of CO_2 generates carbonic acid (Clark, 2015). The concentration of CO_2 derived solely from the respiration of soil organic carbon ranges from

3,000-10,000 ppm-v in contrast to today's atmospheric CO_2 concentration of 400 ppm-v (Clark, 2015). Weathering reactions are constrained in modern times to the soil horizon thanks to the development of plant and animal species as well as the reduction of atmospheric CO_2 concentrations; in contrast, Earth's atmosphere contained higher concentrations of CO_2 during the Precambrian period and early Paleozoic era which allowed for geochemical weathering before plants and soils before plants and soils developed (Clark, 2015).

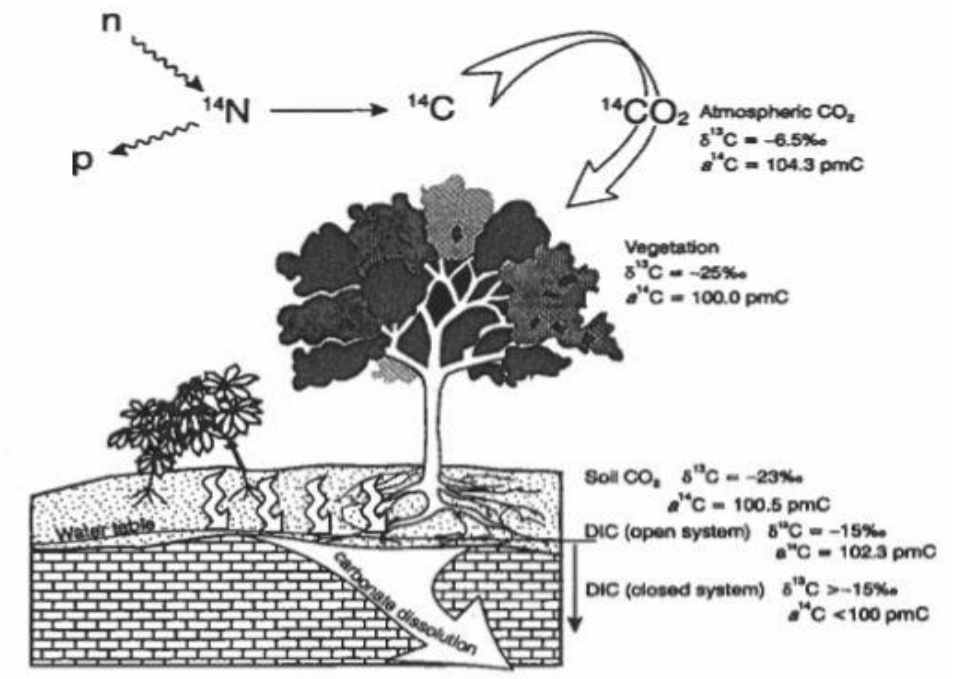

Figure-7: The pathways and associated fractionation of 14C and 13C in CO2 during groundwater dissolution, respiration in soils, and photosynthesis. *Reproduced from Clark and Fritz 1997.*

Carbon is classified into two categories after dissolution into groundwater: dissolved organic carbon (DOC) and dissolved inorganic carbon (DIC); the fractionation path of the dissolved soil carbon and mineral carbon is shown in Figure-7. If the dissolved soil ^{14}C remains with the groundwater along the flowpath and does not dilute, then the decay of ^{14}C could be easily used to calculate the age of the water; however, this scenario rarely happens as dilution

along the flow path is much more common (Clark and Fritz, 1997; Darrell Pennington written commun., 2009).

Mineral carbon has an average $\delta\ ^{13}C$-value of 0 $^{o}/_{oo}$ with a ^{14}C activity of 0 pmc and is obtained via the dissolution of calcite from limestones, exchange with the aquifer matrix, or through the diffusion of ^{14}C into the aquifer matrix (Hoefs, 1987; Clark and Fritz, 1997; Darrell Pennington written commun., 2009; Clark, 2015).

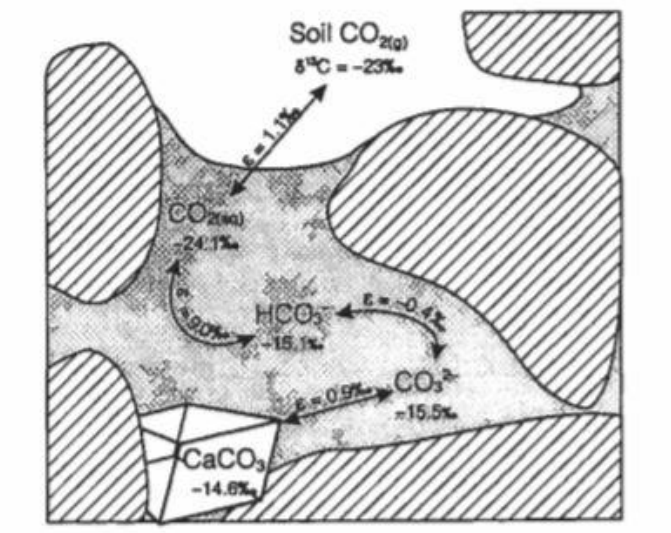

Figure-8: Conceptual drawing of ^{13}C fractionation during equilibrium exchange of carbon between CO_2 gas, DIC, and calcite at 25°C. Enrichment is supposed to be -1.1 per mil between soil CO_2 and aqueous CO_2. Conditions of geochemical equilibrium and calcite saturation are assumed for isotopic equilibrium*; reproduced from Clark and Fritz 1997*

Groundwater Dating

Whereas the words “dating or age” normally refer to the elapsed time span related to a single specific date or age since the object was formed, that is not the meaning for groundwater. Groundwater does not truly have an “age”, due to the fact that waters from different recharge

$$a_t{}^{14}C = q \times a_o{}^{14}C \times e^{-\lambda t} \qquad \text{Equation 1}$$

in which

$a_t{}^{14}C$ is the ^{14}C activity of DIC in groundwater after accounting for dilution

q is the dilution factor

$a_o{}^{14}C$ is the percent modern ^{14}C in the soil

λ is the decay constant

Figure-9. Equation describing the relation between the activity of carbon-14 of dissolved inorganic carbon in groundwater, the dilution factor, the percent modern carbon-14 in the soil, and the decay constant of carbon-14.
[Source of equation 1: Zhu and Murphy (2000)]

sources with different "ages" converge together and mix (Clark and Fritz, 1997). Therefore, a more meaningful phrase than "age" of water is the "mean residence time" (MRT) of water.

A complication arises when attempting to determine the MRT of groundwater because tritium, a radioactive isotope of hydrogen, is the only datable component of the water molecule (Clark and Fritz, 1997), and tritium has a relatively short half-life of 12.43 to12.5 years, and relatively low abundance in waters, making it useful for dating waters of up to 40 years (Hoefs, 1980; Unterweger et al., 1980; Clark and Fritz, 1997; Solomon and Cook; 2010) . Geoscientists instead often determine the MRT of the water by dating dissolved constituents (Clark and Fritz, 1997). The exact approach to dating varies with the relative MRT of the water sample (Clark, 2015). ^{14}C-age dating is a popular tool for waters ranging from 1,000 to 45,000 years (Zhu and Murphy, 2000). The difficulty that arises from ^{14}C-age dating comes from all the different sources of carbon that can mix with the groundwater at various points in its flow path,

which leads to a need for corrections to yield an accurate apparent ^{14}C age (Zhu and Murphy, 2000). While a simple algebraic equation can be used to calculate error (see Figure-9), it is a flawed method due to not being able to account for more than two carbon sources, where isotopic exchange occurs, if isotopic exchange occurs, what mass-transfer reactions occur, and what are the dominant major ground water constituents (Zhu and Murphy, 2000).

Inverse mass-balance modeling is another tool used to calculate ^{14}C ages; this method "deduces the mass transfer reactions taking place between two observation points along a flowpath that may have been responsible for the chemical and isotopic evolution in ground water" (Zhu and Murphy, 2000). Inverse mass-balance models can be tailored to each site's "geology, mineralogy, petrographic observations, and knowledge of mineral dissolution kinetics" of said site's aquifer (Zhu and Murphy, 2000). The following hydrological assumptions of this method are taken directly from Zhu and Murphy (2000):

(1) Inter-aquifer mixing is insignificant

(2) A chemical steady state prevailed during the time considered

(3) Dispersion and diffusion do not significantly affect solution chemistry

(4) The two water analyses from the 'initial' and 'final' wells should represent packets of water the flow along the same path.

Creating ^{14}C Data Models With NETPATH-WIN Software

NETPATH-WIN is a program developed by the Water Resources Division of the United States Geological Survey (USGS) that uses inverse geochemical mass-balance modeling techniques to determine the net geochemical mass-balance reactions that can occur between the initial and final members in a hydrologic system (Plummer et al., 1983; Plummer 1985;

Parkhurst and Plummer 1993; Plummer et al., 1994; Glynn and Brown, 1996; Nordstrom 2007; Parkhurst and Charlton, 2008; Darrell Pennington written commun., 2009; El-Kadi et al., 2010). NETPATH-WIN defines a net geochemical mass-balance reaction as a model (Plummer and Parkhurst, 1991).; a model is "the masses of a set of plausible minerals and gases" (phases) "that must enter or leave the initial solution in order to exactly define a set of selected elemental and isotopic constraints observed in a final (evolutionary) water" (Plummer and Parkhurst, 1991). A simplified version of a model according to Plummer and Parkhurst (1991) is

Initial water + "Reactant Phases" → *Final water + "Product Phases"*

The constraints used in the models can vary from elements, to redox states, or a particular isotope; the constraints are included to restrain the phases that can be added or removed from the final water (or final member) (Plummer and Parkhurst, 1991). The models are additionally capable of determining the radiocarbon ages of dissolved carbon in waters if sufficient chemical and isotopic data are available by using the generalized isotope evolution model of Wigley and others (1978) (Plummer and Parkhurst, 1991; Parkhurst and Charlton, 2008; Darrell Pennington written commun., 2009). NETPATH-WIN uses the techniques developed by Plummer and others, 1983; Plummer 1985; Parkhurst and Plummer, 1993; Glynn and Brown, 1996; Nordstrom, 2007) to build geochemical and isotopic reaction models from collected isotopic and geochemical data (Parkhurst and Charlton, 2008). The program can calculate mixing proportions between two to five initial sources (which can be single sourced waters or mixed waters) and can calculate the myriad of possible combination of phase changes that can account for the geochemical and isotopic composition of the initial and final waters. After each combination (or model) is created, NETPATH-WIN determines $\delta^{13}C$, ^{14}C (pmc), $\delta^{15}N$, and the $^{87}Sr/^{86}Sr$ ratio of

the final end member (i.e. the waters that discharge at the springs) using Rayleigh distillation techniques (Plummer and Parkhurst, 1994).

Methodology

Data Collection

Geochemical, physical, and selected field parameters were collected from 10 cold-water springs, 30 cold-water wells, and 16 thermal springs, primarily by USGS personnel during three sampling events: 1) from January through September 1972; 2) from September 2007 to June 2008; and 3) during June 2018 by the author. Location of these springs and wells are presented in Figures 3 and 4. Analyses were conducted at USGS laboratories, except where described below. Data from the USGS analyses are available online at https://waterdata.usgs.gov/nwis, specifying Arkansas as the state, and Garland as the county. All data are also included in Appendix A of this thesis to facilitate verification for those readers interested in details of samples, and those who would like to conduct additional modeling. Field and lab methodology for USGS projects are documented in Kresse and Hays (2009).

Sampling protocols and analyses for strontium-87/strontium-86 ratios ($^{87}Sr/^{86}Sr$) for selected sites were provided by Dr. Jay Banner, Jackson School of Geosciences, University of Texas, Austin, and the stable isotope ($\delta^{13}C$ for DOC and DIC) for the June 2018 sampling event) were provided by Erik Pollock, University of Arkansas Stable Isotope Lab (UASIL). Water samples obtained for the June 2018 sampling event were filtered in field and stored in 25 mL glass vials without headspace. They were transported chilled to the UASIL and were measured on a Gas bench II headspace sampling unit connected to a Delta V Advantage IRMS (Pollock, written commun. 2019). According to Erik, the samples were introduced into He flushed exetainers containing H_3PO_4 and were allowed to react (Pollock, written commun. 2019). The

evolved CO_2 was then sampled for isotope analysis; the samples were standardized to the VPDB scale using standards NBS-19, UASIL 22 and UASIL 23 (Pollock, written commun. 2019). All utilized equipment was from Thermo Sci. in Bremen, Germany (Polluck, written commun. 2019). Latitude and longitude coordinates were recorded with GPS location phone app by Acceleroto in WGS 1984.Appendix A additionally contains water chemistry data collected by Bedinger et al. (1979) for the sampling event conducted in 1972. The dataset is divided into two parts: cold-water wells and thermal springs.

Quality Assurance and Quality Control

The measure of accuracy of field and lab determinations of water-quality parameters presented in Appendix A is assessed by the quality assurance and quality control (QA/QC) that are imposed by specific standards. The standards used for the analyses in this thesis are those used by the USGS (Wilde et al., 1998a-d).

DB-WIN

Geochemical modeling involved multiple programs that facilitate components of mass balance, radionuclide decay, stable-isotopic calculations related to environmental constraints, and mixing, among others. The physical parameters selected for the mass balance calculations include temperature (°C), pH, and conductivity (µS/cm). Isotopic parameters include δD, $\delta^{18}O$, Tritium in Tritium Units (TU), $\delta^{13}C$ (per mil vs VPDB), ^{14}C (pmc), and $^{87/86}Sr$. Geochemical parameters include the following major cation and anions and associated elements measured in milligrams per liter (mg/L): dissolved oxygen (DO), Calcium (Ca^{2+}), Magnesium (Mg^{2+}), Sodium (Na^{+}), Field Alkalinity as $CaCO_3$, Sulfate (SO_4^{2-}), Chlorine (Cl^{-}), Fluoride (Fl), Silica (Si), Aluminum (Al^{3+}), Barium (Ba^{2+}), Boron (B), Iron (Fe), Lithium (Li^{+}), Manganese (Mn),

and Sr^{2+}. Potassium was excluded as a major cation due to its nondetectable concentration. Silica (Si) is going to be an important constituent due to the sheer amount of chert, quartz, and novaculites found in the stratigraphic section. Strontium is another important constraint since "Sr^{2+} behaves similarly to Ca and loves carbonates" (Hays oral commun., 2009). Therefore, Sr^{2+} is a great proxy to determine how the carbon is interacting within the system. Distribution of carbonates was determined by cross-referencing the stratigraphic descriptions provided by Purdue and Miser (1923) and Johnson and Hanson (2011).

The dataset was input into a Microsoft Excel file and was saved as a .csv file format in order to be read in DB Spreadsheet, an external data editor for DB-WIN. DB-WIN is "a database program to enter and edit chemical and isotopic data" (Plummer et al., 1994). The units milligrams per liter (mg/L) were for concentrations. The other units that DB and NETPATH read are as follows: "temperature in °C; density in grams per cubic centimeter (g/cm^3) (default is 1.0); Eh in volts; tritium in tritium units (TU); ^{14}C of TDIC in percent modern carbon (pmc); $^{87}Sr/^{86}Sr$ as the mole ratio; and all other stable-isotope data in per mil" (Plummer et al., 1994).

DB-WIN has two different options for calculating individual ion activity coefficients: Extended Debye-Hückel and Davies (Plummer et al., 1994). Debye-Hückel was chosen since "activity coefficients of Ca^{2+}, Mg^{2+}, Na^{+}, Cl^{-}, SO_4^{2-}, and HCO_3^{-} are always calculated from the extended Debye-Hückel equations of Truesdell and Jones (1974)" in WATEQFP, the program built into DB that "performs a complete charge balance analysis based on the temperature, pH, and chemical speciation" (Plummer et al., 1976; Plummer et al.,1994).

The formula for Extended Debye-Hückel is as follows (Truesdell and Jones, 1974)

$$log\gamma = \frac{-Az^2\sqrt{I}}{1 + Ba\sqrt{I}} + bI$$

in which

A, *B* are constants depending only on the dielectric constant, density, and temperature

z is the ionic charge

I is the ionic strength (defined as half the sum of the products of the molality and the square of the charge of all ions in the solution)

a hydrated ion size that must be estimated from experimental data

b is the effect of the decrease in concentration of solvent in concentrated solutions

There are four options in DB-WIN for how total dissolved inorganic carbon (TDIC) is to be specified. Option four, "the usual field titration alkalinity expressed as $CaCO_3$, rather than as HCO_3", was selected (Plummer et al., 1994). For p*e* (the negative log of the electron activity) calculation choices, option 0, Redox ignored, was chosen. In this scenario, p*e* "is set to 100 and oxidation-reduction is ignored" (Plummer et al., 1976). Once the data are read from the spreadsheet, DB Spreadsheet is able to create a .LON file, which can be then read by DB-WIN. DB-WIN then can create a file named CHECK which lists the percent error of the charge balance calculation for each well (Plummer et al., 1994).

The equation for Percent Charge Imbalance is taken from Plummer et al. (1994)

$$Percent\ Charge\ Imbalance\ = \frac{\sum meq_{cations} - \sum meq_{anions}}{\sum meq_{cations} + \sum meq_{anions}} \times 100$$

in which,

meq is milliequivalents per kilogram H_2O

The output files include a file with the extension PAT, which contains all the chemical and isotopic data for use by NETPATH" (El-Kadi et al., 2010). To create an output file on DB-WIN, you need to run the program WATEQFP (Plummer et al., 1976), which results can be seen in the produced .OUT file. When running WATEQFP a default Eh of zero volts was assumed since Fe and Mn data were available but Eh data were not (Plummer et al., 1994). Any site with more than five percent charge imbalance error produced by the CHECK file and the .OUT file was eliminated from dataset. This resulted in a total of ten thermal wells and three cold springs that passed the percent charge imbalance inspection.

NETPATH-WIN

One of the key concepts in NETPATH is to mentally visualize the starting points, the ending points, and the complete hydrogeologic environment from start to finish. Inasmuch as one can assume that cold-water springs have a fairly shallow pathway (several hundreds of feet deep), they can serve as an excellent proxy for the geochemical and geophysical condition for the initial members, as well as a mixing end-member. Likewise, end members can be represented by the hot-water springs, insofar as it can be assumed that the water has traveled slowly down the flowpath and acquired heat through slow geothermal equilibration.

Rayleigh distillation calculations are invoked for every geochemical system run for $\delta^{13}C$, ^{14}C (pmc), and $^{87}Sr/^{86}Sr$ ratio and are solved "using the general case of *N* non-fractionating inputs and *M* fractionating outputs considered by Wigley and others (1978, 1979). The limitations of the Rayleigh distillation equations are discussed in Plummer et al. (1994). Another caveat of NETPATH is that the program "is not capable of determining where along the overall flow path that mixing (and mineral-water reaction takes place)" (Plummer et al., 1994). For calculated mass transfer NETPATH runs that involving mixing cases with Rayleigh distillation calculations "NETPATH assumes that all mixing occurs at the initial condition, followed by subsequent mineral-water reaction" (Plummer et al., 1994). Due to this limitation, great care must be exercised when evaluating mixing models.

NETPATH calculates the adjusted ^{14}C age is according to the following equation in Plummer et al., (1994)

$$\Delta t(years) = \frac{5730}{\ln 2} \ln\left(\frac{A_{nd}}{A}\right)$$

in which,

Δt is change in time in years

A_{nd} is the adjusted ^{14}C value calculated at the final well by accounting for reaction effects to the initial ^{14}C

A is the measured ^{14}C content in the final water, entered in DB

This equation is dependent on the initial ^{14}C value at the initial well, A_0.

Table-2: Representative dissolved chemical compositions of groundwater samples used for modeling. [Concentrations are in mg/L, unless otherwise specified. Full dataset is provided in Appendix A. Sample locations are shown in Figures 3 and 4]. Sp, spring; W, well; HS, hot spring

Well Name	Bratton 2 (W-34)	Thornton (W-16)	Greer 3 (W-52)	ARKSCr	HSSSCr	Hale Sp. (HS-25)	Rector Sp. (HS-9)
Stratigraphic Unit	STNL	STNL	BGFK	ARKS	HSSS	HSSS	HSSS
Temp (°C)	20.4	18.7	17.9	20.4	33.77	62.5	62.1
pH (field)	7.4	6.3	5.6	7.1	6.72	7.1	7.5
Diss. 0_2	0.6	1	0.5	0	1.49	n/a	n/a
Alkalinity (Field) as $CaCO_3$	149	78	16	109	109	132	131
Tritium (TU)	3.22	38.64	25.76	1.3	9.66	n/a	0
Ca	44.7	27.16	6.11	34.7	36.7	45.3	44.7
Mg	5.92	4.01	0.288	2.8	2.14	4.83	4.79
Na	14.3	10.83	1.46	2.9	4.16	3.92	3.88
K	n/a	n/a	n/a	1.5	0.867	n/a	n/a
Cl	2.57	2.86	1.22	2.3	3.18	1.83	1.77
SO_4	11.5	22.71	3.6	5.31	4.78	7.48	7.53
F	0.18	0.21	<0.1	0.2	0.18	0.13	0.13
SiO_2	18.3	31.3	10.8	13	22.2	39.7	39.8
B	0.015	0.01	0.004	0.011	0.011	0.01	0.011
Ba	0.15	0.02	0.01	0.01	0.01	0.14	0.08
Li	0.006	0.017	0.0004	n/a	n/a	0.004	0.005
Sr	0.325	0.209	0.019	0.08	0.083	0.106	0.107
Fe	0.158	0.2164	1.22	1.2	<0.02	0.02	<0.006
Mn	0.07	1.12	0.02	0.13	<0.0003	0.23	0.001
Sp. Cond. Field (µS/cm)	295	235	38	247	233	302	311
$\delta^{13}C$ TDIC	-12.7	-17.37	-22.14	-23.7	-23.7	-14.73	-13.24
$\delta^{14}C$ (pmc)	23.67	66.1	78.6	98.9	98.9	35.72	36.99
δD ($^0/_{00}$)	n/a	-28.1	-31.3	-30	-29.4	-29	-28.2
$\delta^{18}O$ ($^0/_{00}$)	n/a	-4.88	-5.63	n/a	-5.58	-5.54	-5.52
$^{87}Sr/^{86}Sr$	0.71	0.714	0.711	0.712	0.712	0.712	0.712
Al	0.003	0.002	0.005	0	<0.02	0.003	0.002
Charge Balance Error (%)	2.01	4	4.81	-2.97	-1.59	0.75	0.3
WATEQF (%)	0.9	2.1	1	-4.4	-3.6	-0.2	-0.6

Table-2: Representative dissolved chemical compositions of groundwater samples used for modeling Concentrations are in mg/L, unless otherwise specified. Full dataset is provided in Appendix A. Sample locations are shown in Figures 3 and 4, and Plates 1 and 2]. Sp, spring; W, well; HS, hot spring (Cont.)

Well Name	Crystal Sp. (HS-8)	(HS-49)	New Sp. (HS-47)	Quapaw Sp. (Hs-42)	Boiler House N. (HS-6)	Fordyce Sp. (HS-46)
Stratigraphic Unit	HSSS	HSSS	HSSS	HSSS	HSSS	HSSS
Temp (°C)	61.9	61.8	61.3	61.2	57.9	57.4
pH (field)	7.5	7.4	7.2	7	6.3	7.2
Diss. 0_2	n/a	n/a	n/a	n/a	n/a	n/a
Alkalinity (Field) as $CaCO_3$	132	128	138	127	132	132
Tritium (TU)	1.923	n/a	n/a	n/a	n/a	n/a
Ca	44.8	44.4	45.9	45.2	45.32	45.4
Mg	4.78	4.72	4.88	4.84	4.82	4.83
Na	3.88	3.75	3.91	3.95	3.91	4.01
K	n/a	n/a	n/a	n/a	n/a	n/a
Cl	1.84	1.84	1.84	1.93	1.86	1.86
SO_4	7.49	7.25	7.32	7.79	7.53	7.46
F	0.13	0.14	0.13	0.14	0.13	0.14
SiO_2	39.6	40.8	39.7	39.8	39.89	40.4
B	0.011	0.011	0.011	0.011	0.011	0.011
Ba	0.14	0.11	0.14	0.14	0.09	0.14
Li	0.005	0.005	0.005	0.005	0.005	0.005
Sr	0.105	0.098	0.106	0.106	0.105	0.108
Fe	<0.006	<0.006	<0.006	0.018	<0.006	0.014
Mn	0.21	0.14	0.21	0.22	<0.0002	0.22
Sp. Cond. Field (µS/cm)	284	290	316	286	302	297
$\delta^{13}C$ TDIC	-13.8	-14.02	-13.3	-14.03	-13.87	-13.86
$\delta^{14}C$ (pmc)	38.28	44.77	36.21	36.56	36.3	35.58
δD ($^0/_{00}$)	-28.3	-29.7	-29.5	-28.9	-28.6	-28.6
$\delta^{18}O$ ($^0/_{00}$)	-5.56	-5.55	-5.61	-5.52	-5.56	-5.49
$^{87}Sr/^{86}Sr$	0.712	0.712	0.712	0.712	0.712	0.712
Al	0.002	0.013	0.002	0.003	0.002	0.002
Charge Balance Error (%)	0.18	1.13	-0.72	2.39	0.57	0.89
WATEQF (%)	-0.8	0.2	-1.7	1.4	-0.4	0

NETPATH considers nine possible methods of defining A_0: (1) Original Data, (2) Mass Balance (1990), (3) Vogel, (4) Tamers, (5) Ingerson and Pearson, (6) Mook, (7) Fontes and Garnier, (8) Eichinger, and (9) User-defined (Plummer et al., 1994). A very brief description of each method will be discussed. Further information regarding these models can be found in Plummer et al. (1994). Original data uses the ^{14}C content of DIC of the initial water defined in DB as a value of A_{oTDIC}. The mass balance method used by Plummer et al. (1990) is made on the initial water composition assuming the reaction of pure water with calcite, dolomite, gypsum, and CO_2 gas; the default ^{14}C values for CO_2 gas and carbonates is assumed to be 100 pmc and 0 pmc respectively (Plummer et al., 1994). Tamers (Tamers, 1967, 1975; Tamers and Scharpenseel, 1970) is comparable to the mass balance (1990) method except that the mass balance (1990) is only performed on CO_2 gas and carbonates; the respective default ^{14}C values for CO_2 gas and carbonates is 100 pmc and 0 pmc (Plummer et al., 1994). Vogel (Vogel 1967; Vogel and others, 1970; and Vogel and Ehhalt, 1963) always assigns A_{oTDIC} as 85 pmc. Ingerson and Pearson (1964) assumes a "carbonate dissolution model to estimate A_{0TDIC} based on ^{13}C data for the inorganic carbon system" (Plummer et al., 1994). Mook (1972, 1976, 1980). Both the Tamers (1975) model and the Ingerson and Pearson (1964) model assumes "a simple mixing between CO_2 in the soil and solid carbonate minerals with no other sources and no sinks of carbon in the system" (Kalin, 2000).

Fontes and Garnier (1979), and Eichinger (1983) assume "that the carbon isotopic equilibrium occurs in one or more steps in the evolution of the recharge water"; more specifically the Fontes and Garnier (1979) model is an extension to the Tamers (1975) model and "describes the exchange of TDIC with either the gas phase or the solid phase" (Plummer et al., 1994; Kalin, 2000). Mook (1980) specifically "assumes isotopic equilibrium between soil gas

and aqueous species in an open system" or in other words "isotopic exchange of all carbon species" occurs "in the soil zone including the dissolved carbonate" (Plummer et al., 1994; Kalin, 2000). Fontes and Garnier (1979) "consider a two-stage evolution of recharge waters accounting for dissolution and isotopic exchange of carbonate minerals with CO_2 in the unsaturated zone and isotopic exchange with the carbonate rocks in the saturated zone" (Plummer et al., 1994). Eichinger (1983) is similar to "that of Ingerson and Pearson with modification for equilibrium isotopic exchange" (Plummer et al., 1994). One important note is that Eichinger (1983) "should only be used for isotope exchange with the solid phase" (Kalin 2000). The initial A_0 value in User-defined is defined in NETPATH by the user (Plummer et al., 1994). This method is disregarded in calculations.

An important modification to consider when evaluating A_o values is that NETPATH modifies the values calculated from literature models as they only consider the DIC. NETPATH's modification is found in Plummer et al. (1994) and is as follows:

$$A_{oTDC} = \frac{A_{oTDC} m_{TDIC} + {}^{14}C_{CH_4} m_{CH_4} + {}^{14}C_{DOC} m_{DOC}}{m_{TDC}}$$

in which

TDC is Total Dissolved Carbon

TDIC is Total Dissolved Inorganic Carbon

DOC is Dissolved Inorganic Carbon

m is the molal concentration of the subscripted quantity in the initial water.

For our calculations there will be some degree of error for $\delta^{13}C$ since DOC and methane values were not quantified (Darrell Pennington written commun., 2009).

Table-3: Local isotopic values used for sources and ground-water samples. Groundwater samples were calculated by invoking Rayleigh distillation calculations, and source values were loaded into NETPATH-WIN to replace default values. [*** = assumed value]**

	$\delta^{13}C$ (per mil vs VPDB)	**^{14}C (pmc)**
Carbonate Rocks (Median)	2.681	0*
Soil OM = CO_2 (Median)	-24.01	100*
Cold Wells (Median)	-20.785	78.2
Hot Springs (Median)	-13.83	36.715

Source $\delta^{13}C$ (per mil vs VPDB) and ^{14}C (pmc) values for local soil carbon dioxide and mineral carbonates were collected and determined by the USGS during previous sampling events. For local soil carbon dioxide, nine samples obtained from lysimeter data were obtained for $\delta^{13}C_{VPDB}$ values. ^{14}C (pmc) values were assumed to be 100 (pmc) due to soils theoretically having access to pure organic carbon. Eight total sources for local mineral carbonates were sampled for $\delta^{13}C_{NBS\text{-}19}$ and all values were converted into $\delta^{13}C_{VPDB}$. ^{14}C (pmc) value was assumed to be zero since ^{14}C is found in living matter and rocks are not classified as living matter. All source values can be seen in Appendix A of this report. The median source values were inputted into NETPATH-WIN instead of the default (global isotopic average) values.

NETPATH offers the Mook (1980, 1986) and Deines et al (1974) sets of fractionation factors for inorganic carbon-13. The Mook (1980, 1986) set was chosen for all of the following model calculations discussed in the Results chapter of this report. Since NETPATH does not "consider the uncertainty in the analytical data and how this uncertainty affects modeling results", model validity is instead determined by a three-step process of percent error and geological interpretation (Plummer et al., 1994). Percent error was performed between the observed and the calculated $\delta^{13}C$ values; all models higher than 15% error were eliminated.

Geochemical System Designs

Constraints and phases must be selected for every calculate mass transfer run performed by NETPATH. In NETPATH a constraint is defined either as a chemical element, an expression of electron conservation, or a conservation of a particular isotope of an element (Plummer, Prestemon, and Parkhurst, 1994). The purpose of a constraint in the model is "to constrain the masses of selected phases (minerals and gases) that can enter or leave the aqueous solution" (Plummer et al., 1994). An important point to note is that "the constraints selected for the model will determine the number and types of phases that need to be selected to solve the modeling problem" (Plummer et al., 1994). A "phase" is defined in NETPATH as "any mineral or gas that can enter or leave the aqueous solution along the evolutionary path" (Plummer et al., 1994). Another important point to note is that "selected phases should be known to occur in the system, even if in trace amounts" (Plummer et al., 1994). Every phase must be marked in one of four ways: (1) dissolution only, (2) precipitation only, (3) dissolution or precipitation allowed, or (4) isotopic exchange (Plummer et al., 1994).

Three geochemical systems were created based upon hydrogeochemical analysis of the water samples collected, geological interpretation of the structural and stratigraphic geology of

the study area, and the previous geochemical observations provided in Bedinger et al (1979) and Kresse and Hays (2009): Alkaline-Earth, Basics, and Alkaline-Earth-plus-Sodium systems. These systems and their associated constraints and phases are listed below in Table-4 while the associated table used to create the. LON and .PAT files to be inputted into NETPATH-WIN can be seen in Appendix B. Each system was tested for mixing and non-mixing calculations.

Hydrogeochemical analysis for each of the stratigraphic formations showed that silica, bicarbonate, and calcium ions had the highest concentrations. Bicarbonate and calcium are commonly found in carbonate deposits while silica is commonly found in various rock types discussed earlier. Therefore, each system developed was based on the idea that carbon and silica are constraints. Since magnesium and strontium concentrations are found in each water sample, reactions accounting for not only the mineral calcite (CaCO3) But for dolomite [$CaMg(CO_3)_2$] and strontianite ($SrCO_3$). Mg^{2+} and Sr^{2+} ions are smaller than Ca^{2+} ions and love to replace Ca^{2+} in the crystal lattice (Zachry oral commun, 2016; Hays written commun., 2018). Insofar as the waters in HSNP all are meteoric in origin, CO_2 gas was chosen as a phase for each system. All three systems are based on a carbonate groundwater system and all associated reactions produced from water/rock interaction from mineral carbonates (Darrell Pennington written commun., 2009) the Basics geochemical system is the simplest system only accounting for silica and carbon for the constraints and the associated carbonate minerals and silica in the phases.

` The Alkaline-Earth and Alkaline-Earth-plus-Sodium systems were the geochemical systems utilized by Bedinger et al. (1979) for radiocarbon age determinations (Darrell Pennington written commun., 2009). The Alkaline-Earth geochemical system is an expanded version of the Basics system that accounts for all the cations associated with dolomite, strontianite, and calcite as constraints. The Alkaline-Earth-plus-Sodium geochemical system was

based on observations made by Bedinger et al (1979). They noted that there was a significant difference in the sodium concentrations between the thermal springs and the cold springs and wells without a difference between the carbonate, sulfate, or chloride concentrations (Bedinger et al, 1979). Bedinger et. al (1979) concluded that the presence of the sodium is most likely the result of cation exchange between Na^+ and Ca^{2+} with a clay mineral being the likely culprit. The clay mineral illite was chosen as a phase in this system to represent the Ca^{2+}/Na^+ exchanges that took place because this clay is the most likely represent the appropriate clay phase for the age at which the exchange occurs (Hays oral commun., 2009; Darrell Pennington written commun., 2009). Na^+ was additionally added as a necessary constraint for this system while Ca^{2+}/Na^+ exchange was added as a phase.

Table-4: Constraints and phases applied to each geochemical system. (*Reproduced from Darrell Pennington, written commun., 2009)*

System Name	Constraints	Phases	Transfer
Basics	Carbon	CO_2-Gas	dissolution
	Silica	Calcite	both diss. & prec.[2]
		Dolomite	both diss. & prec.
		Stronite[1]	both diss. & prec.
		Siilca	both diss. & prec.
Alk. Earth	Carbon	CO_2-Gas	dissolution
	Magnesium	Dolomite	both diss. & prec.
	Strontium	Stronite	both diss. & prec.
	Calcium	Calcite	both diss. & prec.
	Silica	Silica	both diss. & prec.
Alk. Earth + Na	Carbon	CO_2-Gas	dissolution
	Silica	Silica	both diss. & prec.
	Calcium	Calcite	both diss. & prec.
	Magnesium	Dolomite	both diss. & prec.
	Strontium	Stronite	both diss. & prec.
	Sodium	Ca/Na Exchange	both diss. & prec.
		Illite	both diss. & prec.
		NaCl	both diss. & prec.

[1] "Stronite" is short for Strontianite

[2] Abbreviated for both dissolution & precipitation

Results

Statistics

The following subsections of this report utilize box plots to illustrate data ranges. The following description explains how to read a box plot. The red line represents the median/second quartile (Q2) (Covington written commun., 2017). The bottom and top parts of the box are the limits of the first and third quartiles (i.e. Q1 and Q3). Q1 and Q3 combined are referred to as the interquartile range (IQR) (Covington written commun., 2017) The dotted lines are the whiskers of the plot; they show the" full range of the data so long as there are not substantial outliers (Covington written commun., 2017)". If the data extend farther than 1.5IQR above and below Q1 and Q3, "the whiskers instead show Q1 and Q2 ±1.5IQR (Covington written commun, 2017)". "If points fall outside of this maximum range allowed for the whiskers, then these are treated as outliers and plotted as individual points (Covington written commun., 2017)".

Water Chemistry

Shallow-groundwater chemistry in HSNP varied considerably amongst the groundwater-bearing formations sampled—Stanley Shale (Ms), Bigfork Chert (Obf), Arkansas Novaculite (MDa) and Hot Springs Sandstone (Mhs). The Mhs has the largest range of calculated total dissolved solids (TDS) at 131.3 mg/L then followed by Ms at 116.8 mg/L, MDa at 32.5 mg/L, ending with Obf at 16.5 mg/L. This trend is continued with the formations' median TDS values with Mhs being the highest at 130.7 mg/L, followed by Ms at 90.5mg/L, MDa at 23.0 mg/L, and once again ending with Obf as the smallest median value at 10.1 mg/L. The formations are largely dominated by bicarbonate (HCO_3^-) and calcium concentrations range and median values (see Figures 10A and 10B). Silica (Si) and sulfate (SO_4^{2-}) range and medians have the next

largest concentrations followed by magnesium (Mg^{2+}), sodium (Na^{+}) and chloride (Cl^{-}) range and medians. Trace amounts of other elements are present including hydrogen (H^{+}), aluminum (Al), arsenic (As), boron (B), cobalt (Co), copper (Cu), iron (Fe), lead (Pb), lithium (Li), manganese (Mn), nickel (Ni), selenium (Se), strontium (Sr^{2+}), and zinc (Zn). Additionally, trace amounts of uranium, radium, radon and barium are present, thus giving a radioactive quality to the waters. A complete list of all trace elements and their concentrations can be found in Appendix A: Geochemical data. Box and whisker plots were created for major cations, major anions, and silica concentrations for the water samples and were categorized according to which geological formation they were sampled from in order to characterize the hydrogeochemistry of said formations (see Figures 10A and 10B).

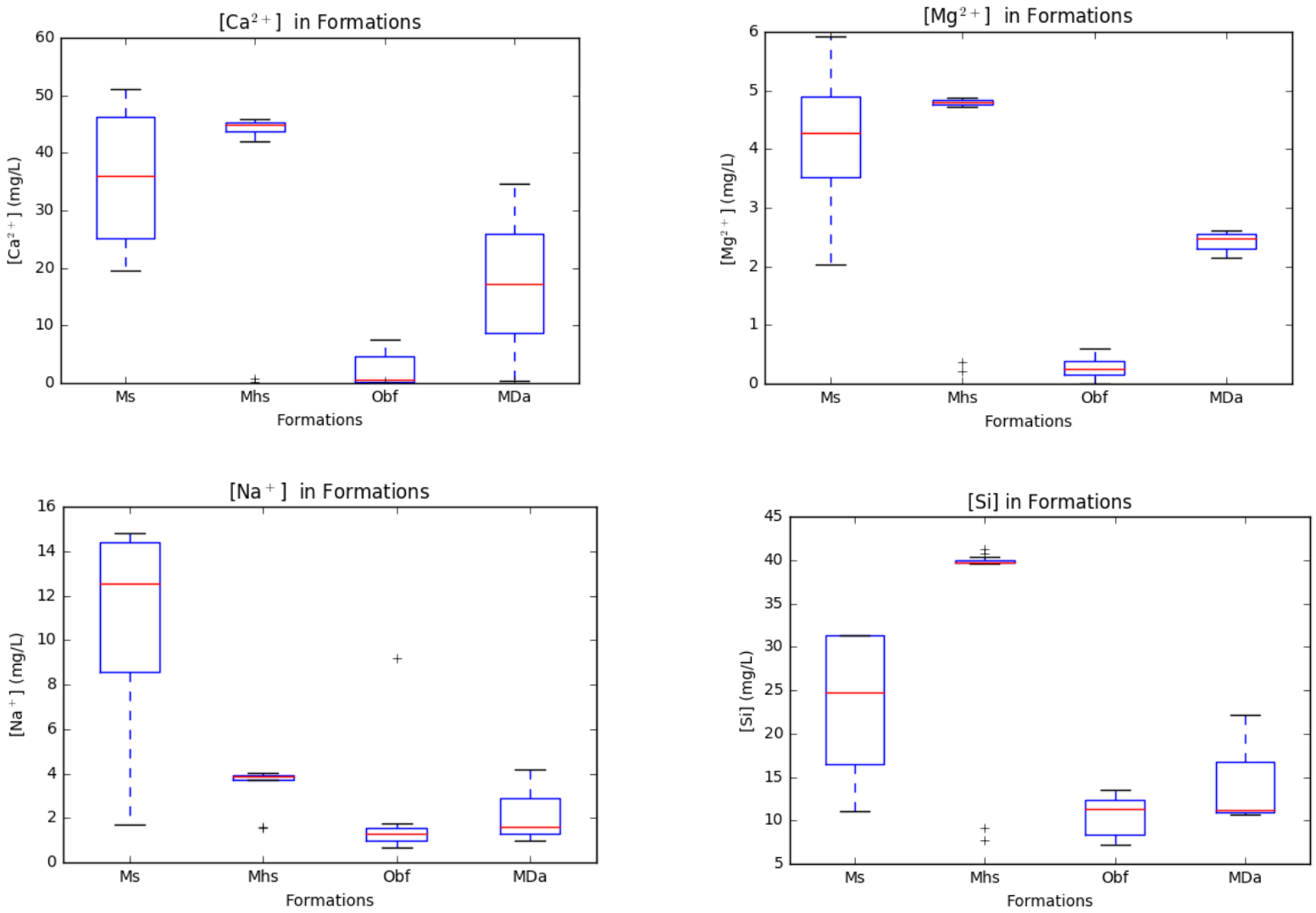

Figure-10A: Major cation and silica concentrations box and whisker plots of the Stanley Shale, Arkansas Novaculite, Bigfork Chert and Hot Springs Sandstone.

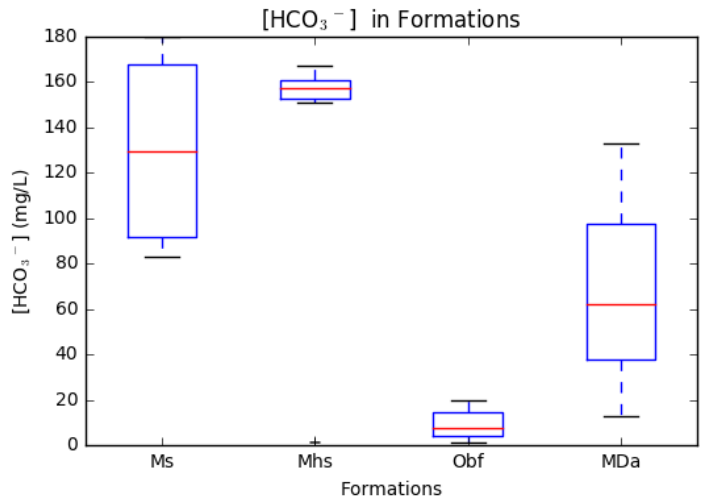

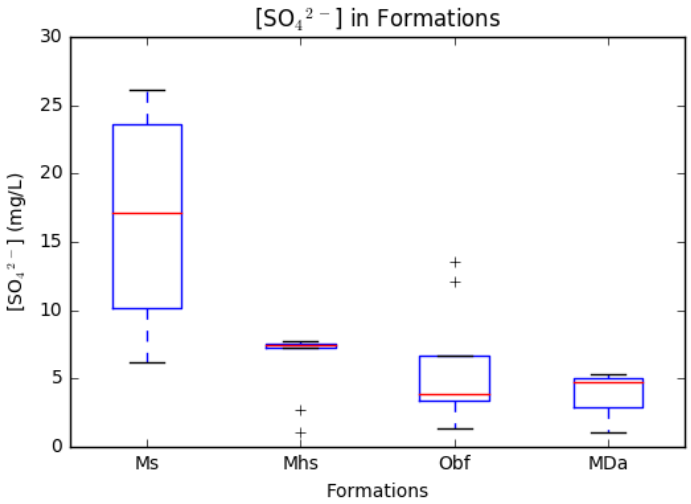

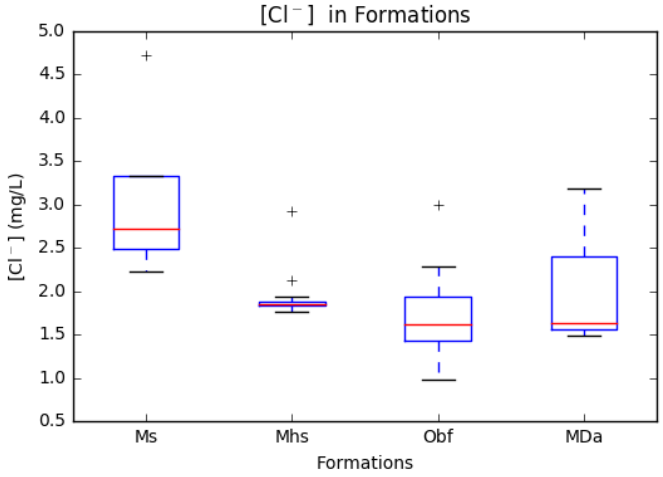

Figure-10B: Major anion concentrations box and whisker plots of the Stanley Shale, Arkansas Novaculite, Bigfork Chert and Hot Springs Sandstone.

Mineral Mass Transfer

The calculated mass transfer NETPATH runs can be separated into two different sections: non-mixing and mixing. Both non-mixing and mixing have only one final member. Non-mixing has only one initial member (IM) while mixing has two or three initial members. No more than three members we considered due to a recommendation by Plummer, Prestemon, and Parkhurst (1994) that a system having more than three IMs is unrealistic. Both non-mixing and mixing included Basics, Alkaline-Earth, and Alkaline-Earth-plus-Sodium geochemical system calculated mass transfer NETPATH runs as mentioned previously (Table-4 in the geochemical system designs section of Methodology). Additionally, both non-mixing and mixing scenario calculated mass transfer NETPATH runs were conducted with the same source carbonate rocks and soil organic matter values. The calculated mass transfer runs conducted in NETPATH additionally calculate the mass transfers of the compounds related to the geochemical system (Table-5).

A full list of all mass-transfers is available in Appendix C and is organized by being either a non-mixing or mixing scenario and the corresponding geochemical system. The values for each model are mole transfers relative to solution with units of mmol/kg water (Plummer et al., 1994; Parkhurst written commun., 2018). Negative mole transfers indicate the precipitation of either a mineral or exsolution of a gas while positive mole transfers indicate the dissolution of either a mineral or a gas (Plummer et al., 1994; Parkhurst written commun., 2018). “The mole transfers are such that, for the elements included as mole balance equations, the initial solution concentration plus the mole transfers produce the final solution concentration” (Plummer et al., 1994; Parkhurst written commun., 2018). For example, the stoichiometry for calculated mass transfer NETPATH run 52 (i.e. No. 52 in the tables) is the concentration of Bratton 2 plus 0.356

SiO_2 produces the recrystallization of 0.143 calcite plus the recrystallization of 0.045 dolomite plus the recrystallization of 0.0025 strontianite plus 0.203 Ca^{2+}/Na^{+} ion exchange plus 0.046 NaCl and the concentration of Spring 25.

The complete list of all model runs can be found in Appendix C. Figure-11 displays box-and-whisker plots for mixing and non-mixing geochemical systems for each method for calculating A_0. Table 6 displays the median ages for each non-mixing and mixing scenario. The unadjusted radiocarbon (i.e. the initial activity carbon [A_0 TDC]) is reported in pmc while the adjusted radiocarbon is reported in years. The A_0 was calculated and age was determined with the following approaches: Original Data, Mass Balance (1990), Tamers (1975), Ingerson and Pearson (1964), Mook (1972), Fontes and Garnier (1979), and Eichinger (1983). Vogel (Vogel 1967; Vogel and others, 1970; and Vogel and Ehhalt, 1963) was excluded due to the observed $\delta^{14}C$ (pmc) values not being representative of the assigned Vogel value of 85 pmc. More details regarding each approach can be found in the NETPATH-WIN section of Methodology as well as Plummer et al., 1994. Due to the amount of total model runs conducted (181 that passed the 15% error QA/QC determinations), A_0 and adjusted age will be discussed in terms of the median in addition to minimum and maximum values.

Table-5: Representative summary of mineral mass transfer. All results can be seen in Appendix C. Abbreviation key: Cal=Calcite; Dolo= Dolomite; Si=SiO_2; Stro= Strontianite; IL= Illite; EX= Ca^{2+}/Na^{+} ion exchange; Init1= Initial Water 1; Init2= Initial Water2; Init3=Initial Water 3; CO_2 diss.= dissolution of CO_2; con. Ig. = Constraint Ignored; Diss.1,2, &3=dissolution of Initial waters 1, 2, & 3; (F)= constraint was forced

Non- Mixing

				Calculated Mass Transfer (mmol/kg water)							
No.	System	Phases	Notes	CO_2 gas	Calcite	SiO_2	Dolomite	Strontianite	Ca/Na Exchange	Illite	NaCl
5	Basics	Cal, Si			-0.5	0.36					
6	Basics	Dolo, Si				0.36	-0.25				
7	Basics	Stro, Si				0.36		-0.51			
20	Basics	Cal, Si			2.0	0.29					
21	Basics	Cal, Si			2.4	0.45					
4	Basics	Cal, Si			0.7	0.48					
47	Alk. Earth	CO_2, Dolo, Stro, Cal, Si	CO_2 diss./ con. Ig.	-1.08	0.3	0.14	0.03	-0.0012			
41	Alk. Earth	CO_2, Dolo, Stro, Cal, Si	CO_2 diss./ con. Ig.	-0.86	0.4	0.14	0.03	-0.0012			
52	Alk. Earth + Na	Si, Cal, Dolo, Stro, EX, NaCl			-0.1	0.36	-0.04	-0.0025	-0.20		-0.05
57	Alk. Earth + Na	Si, Cal, Dolo, Stro, IL, NaCl			1.3	-11.68	-0.81	-0.0012	3.38		-0.3006
65	Alk. Earth + Na	Si, Cal, Dolo, Stro, EX, IL			1.2	-12.88	-0.90	-0.0012	-0.15	3.72	
66	Alk. Earth + Na	Si, Cal, Dolo, Stro, IL, NaCl			1.5	-14.99	-1.05	-0.0012		4.32	-0.3024
114	Alk. Earth + Na	CO_2, Si, Dolo, Stro, EX, IL	CO_2 diss.	0.03		-3.07	-0.30	-0.0025	-0.22	0.98	

Mixing

				Calculated Mass Transfer (mmol/kg water)										
No.	System	Phases	Notes	Initial Water 1	Initial Water 2	Initial Water 3	SiO_2	CO_2 gas	Dolomite	Strontianite	Calcite	Ca/Na Exchange	Illite	NaCl
123	Basics	Init1, Init2, Si	Diss.1,2 (F)	0.421	0.579		0.429							
125	Basics	Init1, Init2, Si	Diss 1,2	0.649	0.351		0.387							
126	Basics	Init1, Init2, Init3, Si	Diss1,2, &3	0.754	0.246	0.000	0.387							
127	Basics	Init1, Init2, Init3, Si	Diss1,2, &3	0.754	0.246	0.000	0.387							
132	Alk. Earth	Init1, Init2, Co2, Stro, Cal, Si	Diss.1,2 (F), CO_2. diss, con. Ig.	0.419	0.581		0.231	-0.8090		-0.00176	0.1870			
135	Alk. Earth	Init1, Init2, Init3, CO_2, Stro, Cal	Diss.1,2, &3 (F), CO_2 diss	0.806	0.000	0.194	0.380	-0.2499		-0.00183	0.2014			
137	Alk. Earth	Init1, Init2, CO_2, Stro, Cal, Si	Diss.1,2 (F), CO_2 diss, con. Ig.	0.712	0.288		0.338	-0.2316		-0.00171	0.0726			
143	Alk. Earth +Na	Init1, Init2, Si, Dolo, Stro, EX, IL	Diss.1,2 (F)	0.979	0.021		-2.777		-0.265	-0.00246		-0.217	0.896	
146	Alk. Earth + Na	Init1, Init2, Si, Dolo, Stro, EX, NaCl	Diss.1,2 (F)	0.972	0.028		-2.911		-0.276	-0.00249		-0.221		1.259
156	Alk. Earth + Na	Init1, Init2, Si, Dolo, Stro, EX, NaCl	Diss.1,2 (F)	0.707	0.293		0.393		0.023	-0.00148		-0.274		0.261
159	Alk. Earth + Na	Init1, Init2, Cal, Stro, EX, IL, NaCl	Diss.1,2 (F)	0.684	0.316					-0.0014	0.0674	-0.251	0.113	0.228
165	Alk. Earth + Na	Init1, Init2, Init3, Cal, Stro, EX, NaCl	Diss.1, 2, &3 (F)	0.684	0.000	0.316				-0.0014	0.0674	-0.251	0.113	0.228
182	Alk. Earth + Na	Init1, Init2, Dolo, Stro, EX, IL, NaCl	Diss1,2 (F)	0.783	0.217				-0.044	-0.00189		-0.113	0.107	-0.118

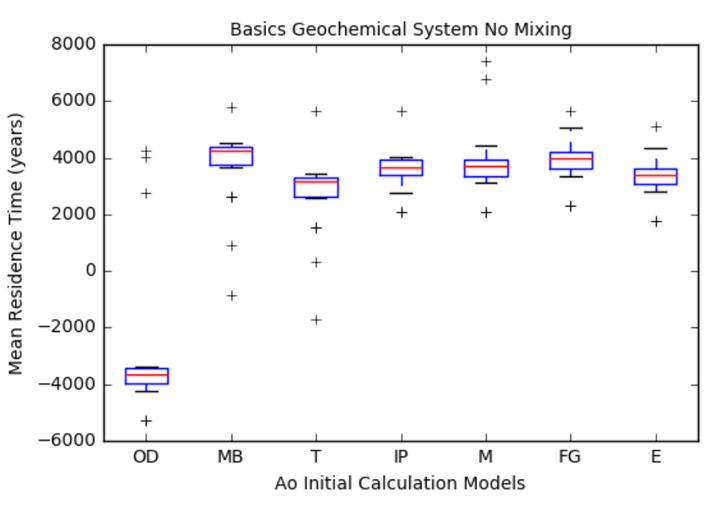

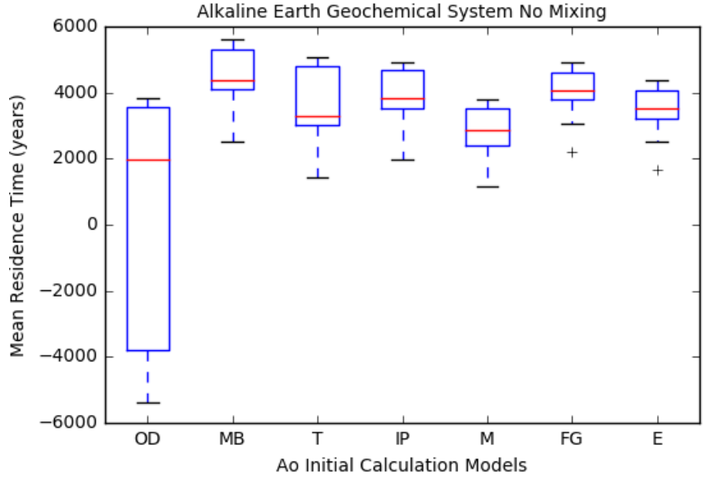

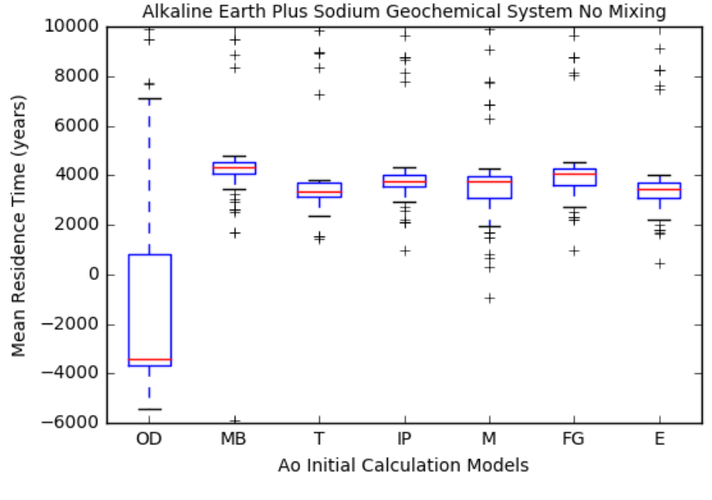

Figure-11: Box and whisker plots of the mean residence time for each geochemical system and each viable model for calculating A_0. Each model is abbreviated on the x-axis is unabbreviated as follows: OD is Original Data, MB is Mass Balance, T is Tamers, IP is Ingerson and Pearson, M is Mook, FG is Fontes and Garnier, and E is Eichinger.

Table-6: Median adjusted ages in years for each geochemical system scenario used and for each viable method for calculating A_o. Color key for the upper table is as follows: bright yellow for Basics, pinkish purple for Alkaline-Earth, and grey for Alkaline-Earth-plus-Sodium. Table condensed from Appendix D.

Median Adjusted Age (years)	Original Data	Mass Balance (1990)	Tamers (1975)	Ingerson and Pearson (1964)	Mook (1972)	Fontes and Garnier (1979)	Eichinger (1983)
Basics Non-mixing	-3671	4236	3152	3685	3710	3968	3378
Alkaline-Earth Non-mixing	1986	4375	3290	3823	2846	4070	3517
Alkaline-Earth-plus-Sodium Non-mixing	-3406	4328	3336	3764	3760	4063	3466
Basics Mixing	-420	5291	4465	4852	4533	5034	4492
Alkaline-Earth Mixing	-1103	4648	3717	4251	3423	4334	3801
Alkaline-Earth-plus-Sodium Mixing	135	4699	3821	4813	4319	4928	4356

Non-Mixing Scenarios

Calculated mass transfer NETPATH runs comprising one IM and one final member are termed non-mixing and represent scenarios for which no mixing occurred. The tested Final Members for the following subsections include Springs 8, 9, 17, 25, 33, 42, 47, and 49. All of these springs are thermal springs found within HSNP and are found in the Hot Springs Sandstone (Figure-4). The tested IMs for the following subsections include wells named Bratton2, Thornton, Greer3, and ARKSCr, HSSSCr (Figure-3). Both Bratton2 and Thornton are wells found in the Stanley Shale while Greer3 is a well found in the Arkansas Novaculite. ARKSCr and HSSSCr are both hypothetical wells created from Arkansas Novaculite and Hot Springs Sandstone well data respectively. Any calculated mass transfer NETPATH run that contained errors or more than 15% between observed $\delta^{13}C$ and computed $\delta^{13}C$ was omitted from the calculated mass transfer NETPATH runs listed in Appendix C. Summary statistics for non-mixing calculated mass transfer runs can be found in Appendix D1. The median adjusted ages for each scenario and A_0 can be found in Table-6.

Basics Geochemical System

The complete list of non-mixing Basics geochemical system scenario calculated mass transfer NETPATH runs (numbers 1 through 30) is available in Appendix C1. Summary statistics for non-mixing Basics calculated mass transfer NETPATH runs can be found in Appendix D1. A box and whisker plot for the mean residence times for each method for calculating A_o for non-mixing Basics models can be found in the top left corner of Figure-11.

The associated phases that passed inspection are combinations of calcite, dolomite, or strontianite with SiO_2. Calculated mass transfer NETPATH runs involving Thornton as an IM

did not yield any results that passed inspection. Greer3 only produced one feasible result when paired with Spring 25 with Ca and SiO_2 as the phases. Likewise, both HSSSCr and ARKSCr both produced one feasible result each when paired with Spring 6 and with Calcite and SiO_2. Bratton2 produced feasible results when paired with Springs 25, 9, 8, 49, 47, 42, 46, 33, and 17 each with the phase combinations calcite & SiO_2, dolomite & SiO_2, and strontianite & SiO_2. The percent error range for observed $\delta^{13}C$ and calculated $\delta^{13}C$ is 0.57% to 14.20%.

The range for the A_0 for Original Data is 23.67 pmc to 98.9 pmc while the median value is 23.67 pmc. The range for the adjusted age for Original Data is -5,277 years to 4,248 years with a median age of -3671 years. The range for the A_0 for Mass Balance (1990) is 61.6 pmc to 94.42 pmc while the median value is 61.6 pmc. The range for the adjusted age for Mass Balance (1990) is -849 years to 5,765 years with a median age of 4,236 years. The range for the A_0 for Tamers (1975) is 54.03 pmc to 92.99 pmc with a median value of 54.03 pmc. The range for the adjusted age for Tamers (1975) is -1,706 years to 5,632 years with a median age of 3,152 years. The range for the A_0 for Ingerson and Pearson (1964) is 57.63 pmc to 98.84 pmc with a median value of 57.63 pmc. The range for the adjusted age for Ingerson and Pearson (1964) is 2,079 years to 5,639 years with a median age of 3,685 years. The range for the A_0 for Mook (1972) is 57.55 pmc to 173.79 pmc with a median value of 57.55 pmc. The range for the adjusted age for Mook (1972) is 2,067 years to 7,434 years with a median age of 3,710 years. The range for the A_0 for Fontes and Garnier (1979) is 59.37 pmc to 118.88 pmc with a median value 59.37 pmc. The range for the adjusted age for Fontes and Garnier (1979) is 394 years to 5,642 years with a median age of 3,968 years. The range for the A_0 for Eichinger (1983) is 55.53 pmc to 102.98 pmc with a median value of 55.53 pmc. The range for the adjusted age for Eichinger (1983) is 1,772 years to 5,129 years with a median age of 3,378 years.

Alkaline-Earth Geochemical System

Calculated mass transfer NETPATH runs 41 and 47 are examples of the non-mixing Alkaline-Earth geochemical system scenarios. The complete list of non-mixing alkaline earth geochemical system scenario calculated mass transfer NETPATH runs (numbers 31 through 47) is available in Appendix C2. Summary statistics for non-mixing Alkaline-Earth model scenarios calculated mass transfer NETPATH can be found in Appendix D1. A box and whisker plot for the mean residence times for each method for calculating A_o for non-mixing Alkaline-Earth models can be found in the center top row of Figure-11.

The only IMs that passed inspection were Thornton and Bratton2. While only Thornton was able to be paired with Spring 25, both Bratton2 and Thornton were able to produce feasible results when paired with Spring 9, 8, 49, 47, 42, 46, 33, and 17. All phases for all combinations included CO_2, dolomite, strontianite, calcite, and SiO_2. The calculations assumed the dissolution of CO_2 and was ignored as a constraint. Percent error values for observed $\delta^{13}C$ and calculated $\delta^{13}C$ ranged 0.25% to 14.50%. The range for the A_0 for Original Data was 23.67 pmc to 66.1 pmc with an average value of 46.13 pmc. The range for the adjusted age for Original Data is -5,377 years to 3,848 years with a median age of 1,986 years. The range for the A_0 for Mass Balance (1990) is 61.6 pmc to 81.91 pmc while the average value is 72.35 pmc. The range for the adjusted age for Mass Balance (1990) is 2,530 years to 5,620 years with a median age of 4,375 years. The range for the A_0 for Tamers (1975) is 54.03 pmc to 76.74 pmc with an average value of 66.05 pmc. The range for the adjusted age for Tamers (1975) is 1,446 years to 5,082 years with a median age of 3,290 years. The range for the A_0 for Ingerson and Pearson (1964) is 57.63 pmc to 75.12 pmc with an average value of 66.89 pmc. The range for the adjusted age for Ingerson and Pearson (1964) is 1,979 years to 4,905 years with a median age of 3823 years. The

range for the A_0 for Mook (1972) is 57.55 pmc to 59.70 pmc with an average value of 58.69 pmc. The range for the adjusted age for Mook (1972) is 1,144 years to 3,812 years with a median age of 2,846 years. The range for the A_0 for Fontes and Garnier (1979) is 59.37 pmc to 75.08 pmc with an average value 67.69 pmc. The range for the adjusted age for Fontes and Garnier (1979) is 2,225 years to 4,901 years with a median age of 4,070 years. The range for the A_0 for Eichinger (1983) is 55.53 pmc to 70.48 pmc with an average value of 63.44 pmc. The range for the adjusted age for Eichinger (1983) is 1,672 years to 4,378 years with a median age of 3,517 years.

Alkaline-Earth-plus-Sodium Geochemical System

. The complete list of non-mixing Alkaline-Earth-plus-Sodium geochemical system model scenarios (numbers 48 through 122) is available in Appendix C3. Summary statistics for non-mixing Alkaline Earth plus Sodium model calculated mass transfer NETPATH can be found in Appendix D1. A box and whisker plot for the mean residence times for each method for calculating A_o for non-mixing Alkaline-Earth-plus-Sodium models can be found in the top right corner of Figure-11.

Bratton2 and Thornton were the only IMs that passed inspection with this geochemical system when paired with Springs 25, 9, 49, 47, 42, 46, 33, and 17. Additionally only Thornton was able to produce results when paired with Spring 8. Interestingly Thornton only had two different combinations of phases:

(1) SiO_2, Calcium, Dolomite, Strontianite, Ca^{2+}/Na^{+} ion exchange, Illite

(2) SiO_2, Calcium, Dolomite, Strontianite, Illite, NaCl

The amount of combinations for the different phases for Bratton2 vary depending on the final member and thus the reader is referred to Appendix C3 for the complete list. The observed $\delta^{13}C$ and calculated $\delta^{13}C$ percent error values ranged 0.3% to 14.0%. The range for the A_0 for Original Data is 23.37 pmc to 66.1 pmc while the average value is 33.85 pmc. The range for the adjusted age for Original Data is -13,823 years to 43,580 years with a median age of -3,406 years. The range for the A_0 for Mass Balance (1990) is 61.6 pmc to 81.91 pmc while the average value is 66.47 pmc. The range for the adjusted age for Mass Balance (1990) is -5,916 years to 51,487 years with a median age of 4,328 years. The range for the A_0 for Tamers (1975) is 54.03 pmc to 76.74 pmc with an average value of 59.48 pmc. The range for the adjusted age for Tamers (1975) is -7,001 years to 50,402 years with a median age of 3,336 years. The range for the A_0 for Ingerson and Pearson (1964) is 57.63 pmc to 75.12 pmc with an average value of 61.83 pmc. The range for the adjusted age for Ingerson and Pearson (1964) is -6,468 years to 50,935 years with a median age of 3,764 years. The range for the A_0 for Mook (1972) is 57.55 pmc to 59.70 pmc with an average value of 58.07 pmc. The range for the adjusted age for Mook (1972) is -6,479 years to 50,924 years with a median age of 3,760 years. The range for the A_0 for Fontes and Garnier (1979) is 59.37 pmc to 75.08 pmc with an average value 63.14 pmc. The range for the adjusted age for Fontes and Garnier (1979) is -6,221 years to 51,182 years with a median age of 4,063 years. The range for the A_0 for Eichinger (1983) is 55.53 pmc to 70.48 pmc with an average value of 59.12 pmc. The range for the adjusted age for Eichinger (1983) is -6,774 years to 50,628 years with a median age of 3,466 years.

Mixing Scenarios

This section is so named due to containing at least two IMs and one final member. The tested final members for the following subsections include Springs 17 and 25 which are the

coldest and warmest of the thermal springs respectively. The tested IMs include Bratton2, Thornton, Greer3, ARKSCr, and HSSSCr. ARKSCr and HSSSCr are both hypothetical wells created from well data from the Arkansas Novaculite and the Hot Springs Sandstone respectively. In this mixing scenario section, each IM is included as a phase and is noted to be dissolved. As was the case for the non-mixing section, any modeling that contained errors or more than 15% error between observed $\delta^{13}C$ and computed $\delta^{13}C$ was omitted from the Calculated mass transfer NETPATH runs listed in Appendix C. The word "errors" refers to modeling results that were left blank in NETPATH WIN even when the calculated mass transfer run was successfully performed. The complete list of non-mixing Alkaline-Earth-plus-Sodium geochemical system model scenarios (numbers 48 through 122) is available in Appendix C3. The complete list of mixing calculated mass transfer NETPATH runs (numbers 123 through 181) is available in Appendix C4. Summary statistics for mixing calculated mass transfer NETPATH runs can be found in Appendix D2. The median adjusted ages for each scenario and A_0 can be found in Table-6.

Basics Geochemical System

The complete list of mixing Basics geochemical system scenario calculated mass transfer NETPATH runs (numbers 123 through 127) is available in Appendix C4. Summary statistics for mixing Basics model runs can be found in Appendix D2. A box and whisker plot for the mean residence times for each method for calculating A_0 for non-mixing Basics models can be found in the bottom left corner of Figure-11.

The phase combinations include SiO_2 and the dissolution of each IM. The range for percent error values for observed $\delta^{13}C$ and calculated $\delta^{13}C$ is 1.69% to 8.62%. The range for the A_0 for Original Data is 33.95 pmc to 50.68 pmc while the average value is 39.75 pmc. The range

for the adjusted age for Original Data is -420 years to 2,133 years with an average age of 587 years. The range for the A_0 for Mass Balance (1990) is 62.26 pmc to 77.74 pmc while the average value is 68.64 pmc. The range for the adjusted age for Mass Balance (1990) is 4,594 years to 5,599 years with an average age of 5,213 years. The range for the A_0 for Tamers (1975) is 55.08 pmc to 73.15 pmc with an average value of 62.43 pmc. The range for the adjusted age for Tamers (1975) is 3,579 years to 5,096 years with an average age of 4,414 years. The range for the A_0 for Ingerson and Pearson (1964) is 64.24 pmc to 75.01 pmc with an average value of 67.54 pmc. The range for the adjusted age for Ingerson and Pearson (1964) is 4,852 years to 5,560 years with an average age of 5,084 years. The range for the A_0 for Mook (1972) is 61.81 pmc to 92.41 pmc with an average value of 69.32 pmc. The range for the adjusted age for Mook (1972) is 4,533 years to 7,858 years with an average age of 5,208 years. The range for the A_0 for Fontes and Garnier (1979) is 65.67 pmc to 77.22 pmc with an average value 70.03 pmc. The range for the adjusted age for Fontes and Garnier (1979) is 5,034 years to 6,373 years with an average age of 5376 years. The range for the A_0 for Eichinger (1983) is 61.5 pmc to 71.22 pmc with an average value of 64.96 pmc. The range for the adjusted age for Eichinger (1983) is 4,492 years to 5,452 years with an average age of 4,761 years.

Alkaline-Earth Geochemical System

The complete list of mixing Alkaline-Earth geochemical system scenario calculated mass transfer NETPATH runs (numbers 128 through 136) is available in Appendix C4. Summary statistics for mixing Alkaline-Earth scenario calculated mass transfer NETPATH runs can be found in Appendix D2. A box and whisker plot for the mean residence times for each method for calculating A_o for mixing Alkaline-Earth models can be found in the bottom center of Figure-11.

The associated phases include strontianite, dolomite, SiO_2. the dissolution of any IMs, and the dissolution of CO_2 gas. The range for percent error values for observed $\delta^{13}C$ and calculated $\delta^{13}C$ is 1.84% to 12.65%. The range for the $A_0$for Original Data is 24.83 pmc to 48.72 pmc while the median value is 31.61 pmc. The range for the adjusted age for Original Data is -3,825 years to 2,239 years with a median age of -1103 years. The range for the $A_0$for Mass Balance (1990) is 62.3 pmc to 73.59 pmc while the median value is 66.35 pmc. The range for the adjusted age for Mass Balance (1990) is 3,779 years to 5,701 years with a median age of 4648 years. The range for the A_0 for Tamers (1975) is 54.85 pmc to 67.44 pmc with a median value of 59.65 pmc. The range for the adjusted age for Tamers (1975) is 2,726 years to 4,974 years with a median age of 3,717 years. The range for the A_0 for Ingerson and Pearson (1964) is 58.37 pmc to 68.82 pmc with a median value of 62.74 pmc. The range for the adjusted age for Ingerson and Pearson (1964) is 3,241 years to 5,338 years with a median age of 4251 years. The range for the A_0 for Mook (1972) is 57.68 pmc to 79.42 pmc with a median value of 58.82 pmc. The range for the adjusted age for Mook (1972) is 3,057 years to 6,522 years with a median age of 3,423 years. The range for the A_0 for Fontes and Garnier (1979) is 60.08 pmc to 73.7 pmc with an average value 64.24 pmc. The range for the adjusted age for Fontes and Garnier (1979) is 3,480 years to 5,905 years with a median age of 4,334 years. The range for the A_0 for Eichinger (1983) is 53.2 pmc to 68.42 pmc with a median value of 60.14 pmc. The range for the adjusted age for Eichinger (1983) is 2,928 years to 5,290 years with a median age of 3801 years.

Alkaline-Earth-plus-Sodium Geochemical System

The complete list of mixing Alkaline-Earth-plus-Sodium geochemical system scenario calculated mass transfer NETPATH runs (numbers 137 through 181) is available in Appendix C4. Summary statistics for mixing Alkaline-Earth-plus-Sodium scenario calculated mass transfer

NETPATH runs can be found in Appendix D2. A box and whisker plot for the mean residence times for each method for calculating A_0 for mixing Alkaline-Earth-plus-Sodium models can be found in the bottom right corner of Figure-11.

The exact phase combinations vary but include the dissolution and inclusion of all IMs, SiO_2, calcite, dolomite, Ca^{2+}/Na^{+} ion exchange, illite, and NaCl. The range for percent error values for observed $\delta^{13}C$ and calculated $\delta^{13}C$ is 0.31% to 14.66%. The range for the A_0 for Original Data is 24.48 pmc to 71.89 pmc while the median value is 37.31 pmc. The range for the adjusted age for Original Data is -3,962 years to 5,416 years with a median age of 135 years. The range for the A_0 for Mass Balance (1990) is 61.86 pmc to 87.71 pmc while the median value is 66.35 pmc. The range for the adjusted age for Mass Balance (1990) is 2,507 years to 7,060 years with a median age of 4699 years. The range for the A_0 for Tamers (1975) is 54.39 pmc to 84.24 pmc with a median value of 59.65 pmc. The range for the adjusted age for Tamers (1975) is 2,173 years to 6,726 years with a median age of 3,821 years.

The range for the A_0 for Ingerson and Pearson (1964) is 58.13 pmc to 93.41 pmc with a median value of 66.41 pmc. The range for the adjusted age for Ingerson and Pearson (1964) is 2,091 years to 6,644 years with a median age of 4,813 years. The range for the A_0 for Mook (1972) is 57.61 pmc to 100.34 pmc with a median value of 63.2 pmc. The range for the adjusted age for Mook (1972) is 421 years to 8,538 years with a median age of 4319 years. The range for the A_0 for Fontes and Garnier (1979) is 59.82 pmc to 83.4 pmc with an average value 68.31 pmc. The range for the adjusted age for Fontes and Garnier (1979) is 488 years to 6,828 years with a median age of 4,928 years. The range for the A_0 for Eichinger (1983) is 55.96 pmc to 78.34 pmc with a median value of 63.38 pmc. The range for the adjusted age for Eichinger (1983) is 1,573 years to 6,126 years with a median age of 4,356 years.

Discussion

Statistical Analysis

The following subsections discuss standard data analysis of the age calculations produced by various calculated mass transfer NETPATH runs. Topics include whether each dataset is skewed, what the best measure of central tendency is for each A_o model, and whether or not each system contains outliers. All number comparisons from here on out will reference both Appendix D and the median values found in Table-6 in Results.

Non-Mixing Basics Geochemical System

The Mass Balance (1990) dataset is negatively skewed while the datasets for Original Data, Tamers (1975), Ingerson and Pearson (1964), Mook (1972), Fontes and Garnier (1979), and Eichinger (1983) are centered around each respective point of central tendency. All seven box plots contain outliers (as shown in Figure-11). The median MRTs for the Basics geochemical system with no mixing can be found in the top yellow row in Table-6. Within the non-mixing Basics geochemical model (in other words only one IM and one final member) there is one negative result with the Original Data model and positive results for the rest. The median MRT for each A_o model is Original Data at -3,671 years; Mass Balance (1990) at 4,236 years; Tamers (1975) is 3,152 years; Ingerson and Pearson (1964) at 3,685 years; Mook (1972) at 3,710 years; Fontes and Garnier (1979) is 3,968 years; and Eichinger (1983) is 3,378 years. All the previously mentioned models produce ages under 4,000 years old with the exception of the Mass Balance (1990) MRT at 4,236 years.

Non-Mixing Alkaline-Earth Geochemical System

The datasets for Original Data, Mass Balance (1990) and Tamers (1975) are bimodal; the Ingerson and Pearson (1964) and Mook (1972) datasets are multimodal; the datasets for Fontes and Garnier (1979) and Eichinger (1983) are negatively skewed. Only the MRT box plots for Fontes and Garnier (1979) and Eichinger (1983) have outliers. The median MRT results for each model are displayed in the second-row pink in Table-6. The median MRT for each A_0 model is Original Data at 1,986 years; Mass Balance (1990) at 4,375 years; Tamers (1975) at 3,290 years; Ingerson and Pearson (1964) at 3,823 years; Mook (1972) at 2,846 years; Fontes and Garnier (1979) at 4,070 years; and Eichinger (1983) at 3,517 years.

Non-Mixing Alkaline-Earth-plus-Sodium Geochemical System

The datasets for Original Data, Mass Balance (1990), Tamers (1975), Ingerson and Pearson (1964), Mook (1972), Fontes and Garnier (1979), and Eichinger are all positively skewed. All MRT box plots contain outliers. The median MRT results for each model are displayed in the third-row grey in Table-6. The median MRTS for each A_0 are as follows: Original Data at -3,406 years; Mass Balance (1990) at 4,328 years; Tamers (1975) at 3,336 years; Ingerson and Pearson (1964) at 3,764 years; Mook (1972) at 3,760 years; Fontes and Garnier at 4,063 years; and Eichinger (1983) at 3,466 years. All values are the same order of magnitude like the previous two geochemical systems.

Mixing Basics Geochemical System

The Original Data dataset is bimodal; the Mass Balance (1990) and Tamers (1975) datasets are centered around their respective values of central tendency; the datasets for Ingerson and Pearson (1964), Mook (1972), Fontes and Garnier (1979) and Eichinger (1983) are

positively skewed. The only MRT box plots with outliers are Mass Balance (1990), Tamers (1975), Mook (1972), Fontes and Garnier (1979), and Eichinger (1983). The median MRT results for each model are displayed in the yellow fourth row in Table-6. The median MRTS are as follows: Original Data at -420 years; Mass Balance (1990) at 5,291 years; Tamers (1975) at 4,465 years; Ingerson and Pearson (1964) at 4,852 years; Mook (1972) at 4,533 years; Fontes and Garnier (1979) at 5,034 years; and Eichinger (1983) at 4,492 years. The MRT for Original Data is the only value that is both negative and not the same order of magnitude for the other A_o models.

Mixing Alkaline-Earth Geochemical System

The dataset for Original Data is multimodal; the datasets for Mass Balance (1990), Tamers (1975), and Ingerson and Pearson (1964) are bimodal; the datasets for Mook (1972), Fontes and Garnier (1979) and Eichinger (1983) is positively skewed. Only the Mook (1972) MRT box plot has an outlier. The MRT results for each model are displayed in the fifth-row pink rows in Table-6. The MRTS that best match each A_0 best measure of central tendency are as follows: Original Data at -1,103 years; Mass Balance (1990) at 4,648 years; Tamers (1975) at 3,717 years; Ingerson and Pearson (1964) at 4,251 years; Mook (1972) at 3,423 years; Fontes and Garnier (1979) at 4,334 years; and Eichinger (1983) at 3,801 years. All of these MRT values are of the same order of magnitude.

Mixing Alkaline-Earth-plus-Sodium Geochemical System

The dataset for Ingerson and Pearson (1964) is bimodal; the datasets for Original Data, Mass Balance (1990), Tamers (1975), Mook (1972), Fontes and Garnier (1979), and Eichinger (1983) are all centered around each's value of central tendency. The median MRT results for

each model are displayed in the bottom grey row in Table-6. The MRT box plot for Original Data is the only A_0 model that does not have an outlier. The median MRTS are as follows: Original Data at 135 years; Mass Balance (1990) at 4,699 years; Tamers (1975) at 3,821 years; Ingerson and Pearson (1964) at 4,813 years; Mook (1972) at 4,319 years; Fontes and Garnier (1979) at 4,928 years; and Eichinger (1983) at 4,356 years. The MRT for Original Data A_0 model is the only value that is both negative and not the same order of magnitude when compared to other models.

A_o Model Analysis

Negative Age Results

Each A_o model tested produced negative MRTs for non-mixing scenarios. More specifically Original Data produced negative MRTS for all geochemical systems; both Mass Balance (1990) and Tamers (1975) produced one negative MRT each for the Basics and Alkaline- Earth-plus-Sodium geochemical systems; Ingerson and Pearson (1964), Mook (1972), Fontes and Garnier (1979), and Eichinger (1983) produced one negative MRT each only for the Alkaline-Earth-plus-Sodium geochemical systems. Mook (1972) additionally produced one negative MRT for the Alkaline-Earth geochemical system. One interesting observation from the results posted in Appendix C3 is that calculated mass transfer NETPATH 117 (Alkaline-Earth-plus-Sodium geochemical system) produced only negative MRTs for all A_o models. In that run the amount of silica and dolomite recrystallized was much higher compared to other phases produced in similar calculated mass transfer NETPATH runs. Likewise, there was a greater amount of dissolution of illite.

For mixing scenarios, Original Data is the only A_0 model that produced negative MRTs. Another noteworthy observation is that Original Data is the only A_0 model that contains either a negative value for median MRT or average MRT both for non-mixing and mixing scenarios. The negative MRTs produced by Mass Balance (1990), Tamers (1975), Ingerson and Pearson (1964), Mook (1972), Fontes and Garnier (1979) and Eichinger (1983) appear to just be outliers when especially compared to the other 179 to 180 positive MRTs produced by these same A_0 models. Since a negative MRT result is infeasible and as the Original Data A_o model produced 120 negative MRTs out of a total 181 MRTs a closer look is warranted. For non-mixing Original Data produced the following results: The Basics geochemical system produced 3 positive MRTs with 27 negative MRTs; the Alkaline-Earth geochemical system produced 9 positive MRTs with 8 negative MRTs; the Alkaline-Earth-plus-Sodium geochemical system produced 20 positive MRTs with 55 negative MRTs. As a whole for every single positive MRT created you would get two negative MRTs to follow. Only shale IMs produced negative MRTs for the Original Data A_0 model for the non-mixing Basics geochemical system scenario.

For mixing Original Data produced the following results: The Basics geochemical system produced 2 positive MRTs with 3 negative MRTs; the Alkaline-Earth geochemical system produced 3 positive MRTs and 6 negative MRTs; the Alkaline-Earth-plus-Sodium geochemical system produced 24 positive MRTs and 21 negative MRTs. The ratio of getting a positive MRT to a negative MRT is about one to one. The positive MRTs seem like outliers for the non-mixing Basics geochemical system scenario. Interestingly for the non-mixing Alkaline-Earth geochemical system inputs from Thornton produce the positive MRTs while inputs from Bratton2 produce the negative MRTs. The only notable observations for non-mixing Alkaline-Earth-plus-Sodium is that as a whole the phases involved in producing positive results are two

different combinations: (1) silica, calcite, dolomite, strontianite, illite, and NaCl; (2) silica, calcite, dolomite, strontianite, Ca^{2+}/Na^{+} exchange, and illite. There really does not appear to be any noteworthy observations for mixing since about all possible IMs were involved. Instead of looking closely at all the results produced from the Original Data model a step back might be warranted to look at the model as is. Original Data is defined by Plummer, Prestemon, and Parkhurst (1994) uses the ^{14}C content of DIC defined for the initial water in DB for the value of A_{oTDIC}. The Vogel (1967) A_0 model was initially discarded due to simply defining the A_{0TDIC} as 85 pmc. Original Data likewise may be too simple by just using a single value for A_{0TDIC} without any further consideration. As the rest of the A_o models produce an overwhelming majority of feasible, positive MRT results I therefore find it more likely that the Original Data model is an ineffective model to apply to this flow model. Likewise, all these negative MRTS produced by the Original Data model indicates a complex flow system.

Outliers

Outside of negative age results, other outliers produced by calculated mass transfer NETPATH runs include modeling ages are mostly incongruent with available data. One good example of a calculated mass transfer NETPATH run that produced too high of an age is run number 91 which produced the following ages: Original Data at 11,320 years; Mass Balance (1990) at 19,227 years; Tamers (1975) at 18,142 years; Ingerson and Pearson (1964) at 18,675 years; Mook (1972) at 18,664 years; Fontes and Garnier (1979) at18,922 years; and Eichinger (1983) 18,369 years. Another good example of a calculated mass transfer NETPATH run that produced ages that were mostly to small is Run 72 with the following ages produced: Original Data at -99 years; Mass Balance (1990) at 1,674 years; Tamers at 11,136 years; Ingerson and

Pearson at 959 years; Mook at -941 years; Fontes and Garnier at 955 years; and Eichinger (1983) at 432 years.

Overall this author would conclude that there are twelve outlier calculated mass transfer NETPATH runs produced out of 181 runs total (12 out of 75 for just non-mixing Alkaline Earth Plus Sodium) which passed the 15% error QA/QC determinations; these include run numbers 64, 66, 72, 73, 91, 100, 105, 108, 113, 117, and 122. Interestingly enough all of these calculated mass transfer NETPATH runs occur for non-mixing Alkaline-Earth-plus-Sodium with runs 64, 66, 72, 73, 104, 105, 113, and 122 using Thornton as an IM and runs 91, 100, 108 and 117 using Bratton2 as an IM. What all these calculated mass transfer NETPATH runs have in common outside of their geochemical system with the exception of runs 72 and 113 is that the rest of this group uses the same combination of phases: phase combination of the dissolution of calcite and illite with the precipitation of silica, dolomite, strontianite, and NaCl. Both run 72 and 113 account for the precipitation of strontianite and Ca^{2+}/Na^{+} exchange with the dissolution of illite; however, each run handles calcite, silica, and dolomite differently.

A visual interpretation of the flow path is handy when attempting to reconcile whether either of these combinations of phases is feasible. As seen in Figure-5 the flow path begins with the Obf and travels to interact with the Ow contact. This contact is sooty and graphitic and contains limestone and calcite veins (Johnson written commun., 2018). The flow path then continues moving up the thrust faults while coming into contact with the Missouri Mountain Shale and Polk Creek Shale, MDa, and Mhs. The upper member of the MDa is tripolitic and is thus another source of $CaCO_3$ (Johnson written commun., 2018). Since illite's chemical formula is $K_{0.65}Al_{2.0}[Al_{0.65}Si_{3.35}O_{10}](OH)$ and Thornton's initial Al^{3+} concentration is 0.002 mg/L compared to Spring 25's concentration of 0.003 mg/L, the dissolution of illite should be

occurring in the scenarios in which Thornton is the IM. Thornton likewise should be dissolving calcite as its initial Ca^{2+} concentration is 27.16 mg/L compared to Spring 25's 45.3 mg/L. NaCl likewise is fine to precipitate based on Thornton's Na^{+} and Cl^{-} concentrations. However based on the initial amounts of silica in the shales, 18.3 mg/L for Bratton2 and 31.3 mg/L for Thornton, the final amounts of silica in the thermal springs (39.7 mg/L for Spring 25), and all the quartz the flow path is coming into contact with can only lead one to the following conclusion: the dissolution of silica should be taking place along the flowpath instead of precipitation. Therefore, the phase combination of the dissolution of calcite and illite with the precipitation of silica, dolomite, strontianite, and NaCl combination of phases is flawed and should be disregarded.

A general observation for these phases is that they tend to have higher values when compared to other calculated mass transfer NETPATH runs produced with the same initial and final members in the Alkaline-Earth-plus-Sodium geochemical system. However, this is not an ironclad rule as there are some calculated mass transfer NETPATH runs that have lower values compared to other similar runs. Overall having ten outliers out of 75 calculated mass transfer NETPATH runs with the same phase combinations seems to indicate that particular combination produces infeasible results. Neither the Basics or Alkaline-Earth geochemical systems for non-mixing produced these kinds of outliers nor did any system for mixing produce any spectacularly consistent high or low numbers for any calculated mass transfer NETPATH run.

A_0 Assessment

When comparing median and average adjusted ages in years for each geochemical system for non-mixing and mixing scenarios, the Mass Balance (1990) model generally produced the greatest ages, followed by Fontes and Garnier (1979), Ingerson and Pearson (1964), Eichinger (1983) and Mook (1972) are about tied, and Tamers (1975). All values are in the same order of

magnitude and range from 2,806 years to 5,853 years. To try to select which activity model is the most accurate for this flow system, the author would start by choosing to discard both Tamers (1975) and Ingerson and Pearson (1964) since these models assume "a simple mixing between CO_2 in the soil and solid carbonate minerals with no other sources and no sinks of carbon in the system" (Kalin, 2000). There are multiple sources of carbonates located in the stratigraphic layers of the Mhs, Obf, the Missouri Mountain Shale and the Polk Creek Shale, the MDa, and the contact at the top of the Womble Shale (Purdue and Miser, 1923; Johnson and Hanson, 2011; Johnson written commun., 2018); therefore as there are multiple carbon sources both the Tamers (1975) and Ingerson and Pearson (1964) models are ineffective for this flow system. Mook (1980) is only applicable if all isotopic exchange is happening at the surface before entering the ground (Plummer et al., 1994; Kalin, 2000; this is highly unlikely due to all the different carbonate sources in the lithology.

The Eichinger (1983) model should only be applied for isotopic exchange with the solid phase (Kalin, 2010). This model alone does not account for all the calculated mass transfer NETPATH runs which utilized CO_2 gas was utilized as a phase. After eliminating the Original Data, Tamers (1975), Ingerson and Pearson (1964), Mook (1972), and Eichinger (1983) as the least applicable A_0 models for the flow system the only two left are Fontes and Garnier (1979) and Mass Balance (1990). As previously stated, Fontes and Garnier (1979) considers a two-stage evolution of recharge waters accounting for dissolution and isotopic exchange of carbonate minerals with CO_2 in the saturated zone and isotopic exchange with carbonate rocks in the saturated zone (Plummer et al., 1994). If there are more than two stages of evolution, then the Fontes and Garnier (1979) model can be considered inaccurate. By contrast Mass Balance (1990) should provide the most accurate determination of A_0 if all known sources and sinks of carbon

during between the recharge point and the discharge point are identified in calculations (Plummer et al., 1983; Parkhurst and Plummer, 1993; Kalin, 2010). Given all the inputted local sources for $\delta^{13}C$ for soil organic matter carbon and carbonates, the Mass Balance (1990) model should currently be the most accurate A_0 model.

Calculated Mass Transfer Analysis

The following are observations from the phases utilized in each run's calculated mass transfer. An important note to remember from NETPATH is that "negative mole transfers indicate the precipitation of either a mineral or the exsolution of a gas while positive mole transfers indicate the dissolution of either a mineral gas (Plummer et al., 1994). When a mineral is precipitated in a groundwater system it is because the water is supersaturated with respect to that mineral; conversely water is able to dissolve a mineral as long as it is undersaturated with respect to that mineral. As it is impractical to talk about each calculated mass transfer NETPATH run separately, general observations for each geochemical system for non-mixing and mixing will be discussed instead. As a result, since not all phases are used in each calculated mass transfer NETPATH run, some of these observations may be potentially flawed. All observations were determined from values in Appendix C. A summary of these observations can be found in Table 7.

Non-Mixing Basics Geochemical System

Beginning with non-mixing Basics, which contained only a combination of three phases at a time, silica is always used in each mass transfer as indicated by the blue color in Table-7. Whenever dolomite or strontianite is utilized, the mass transfer values are always negative which indicates a precipitation of each mineral. Calcite is almost always having negative occurrences

with the exception of three calculated mass transfer NETPATH runs which occur with Greer3, HSSSCr, and ARKSCr as the IMs. So, calcite is being precipitated (and is saturated) with a shale IM and is being precipitated (and is undersaturated) with a quartz IM. This is viable with Greer3, ARKSCr, and HSSSCr having Ca^{2+} concentrations of 6.11 mg/L, 34.7 mg/L and 36.7 mg/L respectively while Spring 25 has a Ca^{2+} concentration of 45.3 mg/L. Meanwhile the shale IM Bratton2 has a Ca^{2+} concentrations of 44.7 mg/L so it would be feasible for Bratton2 calculated mass transfers to be precipitating calcite. As mentioned in the results portion calculated mass transfers involving Thornton as an initial member did not pass inspection and need not to be discussed here. Likewise, ARKSCr and HSSSCr only phase combination in the non-mixing Basics scenario is the dissolution of calcite and silica.

So, under this system the flow system is supersaturated with dolomite and strontianite and is undersaturated in respect to silica. As previously mentioned under this flow system, the dissolution of silica should most definitely be occurring. Dolomite's chemical formula is $CaMg(CO_3)_2$; Bratton2's and Spring 25's Mg^{2+} concentrations are 5.92 mg/L and 4.83 mg/L respectively. Since Bratton2's concentration is higher than Spring 25, which again is the hottest thermal spring and can therefore be implied to be the spring that contains water that has traveled to the maximum depth of the flow system, the precipitation of dolomite is feasible for this flow system. Strontianite ($SrCO_3$) behaves similarly to dolomite in which Bratton2 and Spring25's Sr^{2+} concentrations are 0.325 mg/L and 0.106 mg/L; therefore, there precipitation of $SrCO_3$ is feasible since the IM concentration is larger than the final member concentration.

Non-Mixing Alkaline-Earth Geochemical System

Next with non-mixing Alkaline-Earth which all contain the same combinations of the phases CO_2, dolomite, strontianite, calcite, and silica. All CO_2 and strontianite occurrences are

negative while all SiO_2 occurrences are positive as indicated respectively by the yellow and blue colors in Table 7. Almost all calcite occurrences are positive with the exclusion of calculated mass transfer NETPATH runs 36 and 46. Both calculated mass transfer NETPATH runs have comparatively smaller calcite occurrences at -0.042 mg/L and -0.022 mg/L when compared to the standard 0.401 mg/L. Dolomite has 9 positive occurrences and 8 negative occurrences which tend to correspond with the IM used; negative occurrences appear when Bratton2 is the IM and positive occurrences appear when Thornton is the IM. Bratton2, Thornton, and Spring 25's Mg^{2+} concentrations are 5.92 mg/L, 4.01 mg/L, and 4.83 mg/L/ As stated in the previous section, the precipitation of dolomite is feasible with Bratton2 as the IM since Bratton2 has a larger Mg^{2+} concentration than Spring 25, Likewise, the dissolution of dolomite is feasible with Thornton as the IM since Thornton has a smaller Mg^{2+}concentration than Spring 25's

So, for each calculated mass transfer NETPATH run, strontianite is precipitation, CO_2 gas is being produced, and silica is being dissolved. Thus, the flow system is supersaturated with CO_2 and strontianite and is undersaturated regarding silica. Calcite is being dissolved for a majority of the calculated mass transfer NETPATH runs while dolomite is being precipitated with Thornton as the IM and being dissolved with Bratton2 as the IM. As state in the previous section, the precipitation of $SrCO_3$ and the dissolution of silica and calcite are feasible based on IM and final member concentrations. The production of CO_2 gas is feasible as calcite is being dissolved as water travels down the flow path and comes into contact with several carbonates especially at the Obf and Womble Shale contact.

Non-Mixing Alkaline-Earth-plus-Sodium Geochemical System

Finally, the last geochemical system for non-mixing scenarios is Alkaline-Earth-plus-Sodium. All possible phases include CO_2, calcite, SiO_2, dolomite, strontianite, Ca^{2+}/Na^{+}

exchange, illite, and NaCl. All CO_2 gas occurrences are positive, so CO_2 is always being dissolved when involved in a calculated mass transfer NETPATH run. Strontianite and Ca^{2+}/Na^{+} ion exchange occurrences are almost all negative with the exception of one occurrence each: run 117 for strontianite and run 57 for Ca^{2+}/Na^{+} exchange. Dolomite is similar with almost all occurrences being negative with the exception of two positive occurrences which occur in runs 78 and 113. In almost all cases dolomite, strontianite and Ca^{2+}/Na^{+} exchange is being precipitated; this likewise implies that the flow system is supersaturated in regard to dolomite, strontianite, and Ca^{2+}/Na^{+} exchange. The precipitation of dolomite and strontianite is feasible as discussed in the previous section; both Bratton2 and Thornton have higher Na^{+} concentrations than Spring 25 at 14.3 mg/L, 10.8 mg/L and 3.92 mg/L respectively. Ca^{2+} exchanging with Na^{+} is more likely with Thornton being an IM than Bratton2 based on initial concentrations.

SiO_2, calcite, and NaCl are less clear cut with their positive to negative occurrence ratios at 24 positive to 40 negative, 24 positive to 38 negative, and 20 positive to 25 negative respectively. Based on higher IM concentrations compared to final member concentrations: SiO_2 and calcite are feasible to dissolve while NaCl is feasible to precipitate.

Illite is a little clearer with its ratio of 52 positive to 12 negative; in more situations than not illite is being dissolved than it is being recrystallized; thus, the flow system is more than not undersaturated regarding illite. Besides silicon, oxygen, and hydrogen, illite's main components are potassium and Al^{3+}. Potassium was undetectable in measurements and aluminum concentrations remain consistent across all initial members and final members. Therefore, the likelihood of illite's feasibility of dissolution or precipitation is hazy.

Mixing Basics Geochemical System

For Mixing Basics SiO_2 is the only used phase other than three IMs and all occurrences are positive (as indicated by the color blue in Table 7) which indicates that it is being dissolved; this indicates that the flow system is undersaturated with respect to silica. The silica concentrations are the same value at 0.387 mg/L, thus indicating that its being dissolved in all scenarios. Two calculated mass transfer NETPATH runs have three IMs while the rest of the calculated mass transfer NETPATH runs just use two. However, when three members are utilized the third member is practically non-existent as it has a concentration of 0.000 mg/L. The only pattern for IMs is that the shale IM Bratton2 tends to have a significantly larger concentration than the quartz IMs. For example, calculated mass transfer NETPATH runs 124 has a Bratton2 concentration of 0.754 mg/L while Greer3 has a concentration of 0.246 mg/L. However, calculated mass transfer NETPATH run 123 does not follow this trend as Bratton2 has an initial concentration of 0.421 mg/L while Greer3 has an initial concentration of 0.579 mg/L. Since there were only five calculated mass transfer NETPATH runs that passed inspection it is difficult to state if this is indeed an outlier. As stated previously silica indeed should be dissolving.

Mixing Alkaline-Earth Geochemical System

Next for Mixing Alkaline-Earth when a third IM is used it has an actual concentration amount and the second IM has a concentration of 0.000 mg/L. the calculated mass transfer NETPATH runs that involved this scenario had Bratton2 as IM 1, Thornton as IM 2, and Greer3 as IM 3. The only obvious patterns involving the IMs is that quartz IMs (Greer3 and HSSSCr) has a smaller concentration compared to Bratton2 or Thornton; this is displayed in calculated mass transfer NETPATH run 128 with Bratton2 having a concentration of 0.970 mg/L and silica

Table-7: Calculated Mass Transfer Observations for each geochemical system for non-mixing and mixing. The top row displays all phases utilized. Abbreviation key: CO_2 (g)= Carbon Dioxide gas; Cal= Calcite; SiO_2= Silica; Dolo= Dolomite; Stro= Strontianite; IL= Illite; EX= Ca^{2+}/Na^{+} ion exchange; (+)= positive occurrences; (-)= negative occurrences; (0)= zero value; n/a= not applicable; light blue color= all occurrences for this particular phase were all positive; light yellow color= all occurrences for this particular phase were all negative. How to read: if a space has a numerical value inside, it will list how many positive occurrences there were for that particular phase in that geochemical system followed by how many negative occurrences there were.

Phases	CO_2 (g)	Cal	SiO_2	Dolo	Stro	EX	IL	NaCl
Basics Non-mixing	n/a	3(+), 9(-)	30(+)	0(+), 9(-)	0(+), 9(-)	n/a	n/a	n/a
Alkaline-Earth Non-Mixing	0(+), 17(-)	15(+), 2(-)	17(+), 0(-)	9(+),8(-)	17(-)	n/a	n/a	n/a
Alkaline-Earth-Plus-Sodium Non-Mixing	12(+), 0(-)	24(+), 38(-)	24(+), 40(-)	2(+), 65(-)	1(+), 57(-)	1(+), 61(-)	52(+), 12(-)	20(+), 25(-)
Basics Mixing	n/a	n/a	5(+), 0(-)	n/a	n/a	n/a	n/a	n/a
Alkaline-Earth Mixing	0(+), 9(-)	6(+), 0(-)	7(+), 0(-)	0(+), 3(-)	0(+), 9(-)	n/a	n/a	n/a
Alkaline-Earth Plus Sodium Mixing	3(+)	14(+), 17(-)	18(+), 12(-), 1(0)	2(+), 22(-), 1(0)	34(-)	33(+), 8(-)	27(+), 1(-), 1(0)	18(+), 9(-)

Greer3 having a concentration of 0.029 mg/L. Likewise, Thornton normally has a smaller concentration that Bratton2; the exception for this is calculated mass transfer NETPATH run 132 with Thornton having a concentration of 0.581 mg/L and Bratton2 having a concentration of 0.419 mg/L. The following is a list for the phase occurrences: CO_2, dolomite, and strontianite are all negative (as indicated by the color blue in Table 7). Calcite and SiO_2 are all positive as indicated by the color yellow in Table 7. In summary, CO_2 gas is being produced, calcite and silica are being dissolved, and dolomite and strontianite are being recrystallized. In other words, the flow system is supersaturated regarding CO_2, dolomite, and strontianite and is undersaturated regarding calcite and silica. The phase transfers behave similarly to the non-mixing Alkaline-Earth scenarios and just like that section the phase occurrences of CO_2, dolomite, strontianite, calcite and SiO_2 are feasible.

Mixing Alkaline-Earth-plus-Sodium Geochemical System

The simplest phases to reconcile for Mixing Alkaline-Earth-plus-Sodium are CO_2 gas at all occurrences positive and strontianite at all occurrences negative as indicated respectively by the colors blue and yellow in Table 7. The rest of the phases have the following occurrence ratios: calcite at 14 positive to 17 negative; silica at 18 positive to 12 negative to 1 value at zero; dolomite at 2 positive to 22 negative to one zero value, Ca^{2+}/Na^{+} ion exchange at 33 positive to 8 negative; illite at 27 positive to 1 negative to 1 value at zero; and NaCl at 18 positive and 9 negative. In summary, CO_2 is being dissolved and is undersaturated in the flow system while strontianite is being recrystallized and is supersaturated in the flow system. A majority of the calculated mass transfer NETPATH runs accounts for the dissolution of illite and the recrystallization of dolomite with the transfer of Ca^{2+}/Na^{+} ions. NaCl has a 2 to 1 chance of dissolution to precipitation, calcite has a 14 to 17 chance of dissolution to precipitation and has a

3 to 2 chance of dissolution to precipitation. There are six calculated mass transfer NETPATH runs (145, 161-165) that utilize three IMs: Bratton2 is IM 1, Thornton is IM 2, and Greer3 is IM 3. calculated mass transfer NETPATH runs 145, 161, 162, 163, and 165 had a 0.000 mg/L concentration for the second IM; run 164 had concentrations for all three IMs but has a 0.000 mg/L concentration for SiO_2. One pattern for IMs is that the quartz IMs ARKSCr and HSSSCr have a smaller concentration than Bratton2; one such example is calculated mass transfer NETPATH run 180 with Bratton2 at 0.651 mg/L and ARKSCr at 0.349 mg/L. Bratton2 generally tends to have a higher concentration when paired with Thornton; one example includes calculated mass transfer NETPATH run 168 with Bratton2 at 0.934 mg/L and Thornton at 0.066 mg/L When Bratton2 and Greer3 are paired together there really is not a general pattern as the two rotate on having the largest concentration. When Thornton and Greer3 are paired together it is almost a half and half mixture at 0.454 mg/L and 0.546 mg/L concentrations respectively.

Hydrogeochemical System Scenario Assessment

Although the mixing scenario runs were calculable in NETPATH as a whole they are unlikely to occur in reality based on their locations displayed in Figure-3 in which Bratton2 is W-34, Thornton is W-16, and Greer3 is W-52 (ARKSCr and HSSSCr are hypothetical wells whose concentrations are based on similar wells and thus do not have actual, associated locations). However, the fact their calculations were geochemically possible with addition of other phases instead of just a mixing of initial waters displays how the final geochemistry of the end members is obtained through rock/water interaction as was previously theorized by Kresse and Hays (2009).

While the Basics scenario did provide results, the geochemical system may be too simple as the only constraints are just carbon and silica while CO_2 gas never was utilized as a phase.

The purpose of a constraint in the model is "to constrain the masses of selected phases (minerals and gases) that can enter or leave the aqueous solution" (Plummer et al., 1994). A "phase" is defined in NETPATH as "any mineral or gas that can enter or leave the aqueous solution along the evolutionary path" (Plummer et al., 1994). Given these definitions of constraints and phases along with what is leaving (precipitation) and entering (dissolution) the flow system, the author would state there are probably more constraints on the flow system than just carbon and silica. Therefore, even though the Basics geochemical system is a good starting place, it is probably not the most realistic geochemical system for this flow system.

Likewise, the concentrations of Na^+, Cl^-, Ca^{2+}, Mg^{2+}, SO_4^{2-}, and other listed concentrations in Appendix B change between the initial members and the final members that are not accounted for in the Basics geochemical system and should therefore be disregarded. While the Alkaline-Earth-plus-Sodium scenario did account for changes in the Na^+ concentrations, it is problematic for the following reasons:

1. This is the only system significant outliers outside of negative values appear
2. Has the least consistent mass transfer calculations
3. Potassium was undetectable in measurements and since potassium is a major component in illite, the author remains uncertain to declare the precipitation/dissolution of illite feasible.

The Alkaline-Earth geochemical system has the most consistent mass transfer calculations in terms of utilized phases and accounts for the changing concentrations of Mg^{2+} and Sr^{2+}. Therefore, the most appropriate geochemical system scenario and A_0 model is the Non-Mixing Alkaline-Earth geochemical system with the Mass Balance (1990) A_0 model that produced a median mass residence time of 4,375 years.

Study Strengths and Weaknesses

Mathematically there are a few factors that could influence calculations. In DB-WIN the chosen parameters were:

1. TDIC is specified as "the usual field titration alkalinity expressed as $CaCO_3$, rather than HCO_3^-
2. p*e* was "set to 100 and oxidation-reduction" was ignored (Plummer et al., 1994)
3. Extended Debye-Hückel (Truesdell and Junes, 1974) was selected instead of Davies (Plummer, Prestemon, and Parkhurst, 1994) for calculating individual ion activity

In NETPATH calculations there is the lack of data regarding DOC. Since total dissolved carbon includes total dissolved inorganic carbon and dissolved organic carbon the lack of this data can lead to a flawed age result. Second is the decision to use the Mook (1980, 1986) set of fractionation factors instead of the set by Deines et al (1974). Modeling wise selecting just the precipitation or the dissolution of a phase could have yielded fewer modeling results and potentially could have refined the modeling processes. Another weakness is that NETPATH itself assumes that all mixing occurs at the initial condition followed by subsequent mineral-water reaction and "is not capable of determining where along the overall flow path that mixing (and mineral-water reaction takes place)" (Plummer et al., 1994). Lastly NETPATH does not "consider the uncertainty in the analytical data and how this uncertainty affects modeling results" (Plummer et al., 1994).

This study used local isotopic values for $\delta^{13}C$ for mineral carbonates and soil carbon. Whether or not this study can be considered better that Bedinger's results is difficult to say.

There were definitely ages produced that are less than the average value of 4,400 years calculated by Bedinger et al (1979). Likewise, there are also ages produced that were older than 4,400 years. The author would argue that a strength of this report is how extensive the testing was with seven different A_0 models and three different geochemical systems under both non-mixing and mixing scenarios. Additionally, the utilized data has a percent charge balance less than 5%.

Future Recommendations

This author of this report would recommend the collection of more cold-spring and well major cation and anion concentrations, accessory element concentrations, pH, temperature, alkalinity, dissolved oxygen, δD, $\delta^{18}O$, ^{14}C and $\delta^{13}C$ TDIC data. The collection of this data for wells in the Womble Shale is especially important since there is only one data point in the dataset listed in Appendix A, and it remains lacking in ^{14}C pmc. Furthermore, future modeling accounting for DOC data would lead to a further refinement of mean residence time calculations. A further study recommendation would be to model the cold-water component with the hydrogeochemical flow model. acknowledges that the hot springs are a mixture of hot water and cold-water. The modeling only talks into account the initial point at the recharge zone to the final member discharged at the hot springs. Further modeling of the exact proportions of a hot water component and the cold-water component using this research as a spring board is recommended. Since this study only used IMs collected near the surface and waters from the hot springs it did not consider any mixing from the local cold component in the age calculations. A further study recommendation would be to model the cold-water component with the hydrogeochemical flow model.

Conclusions

Hot Springs National Park (HSNP) is located within the Ouachita Mountains, in west-central Arkansas. These mountains are structurally composed of complex folds and thrust faults that are approximately orientated east-west, resulting from the Ouachita orogeny (Guccione, 1993). The systematically-fractured strata through which the hot springs flow are mostly Paleozoic sedimentary rocks that have undergone slight thermal metamorphism and at least three episodes of compressional deformation and uplift. Deformation events resulted in a series of thrust faults and also overturned, complexly folded anticlines and synclines trending in a northeast-southwest direction (Bedinger et al., 1979; Bell and Hays, 2007; Thornberry-Ehrlich, 2013). The stratigraphic column of HSNP are silica-based units (sandstones, chert, and novaculites) and shale-based units with interlaying layers of limestone and calcite. All units, except the Womble Shale, experienced considerable compressional deformation and contain a widespread distribution of joints; therefore, groundwater flow is controlled by secondary porosity with primary porosity being negligible (Kresse and Hays, 2009). The thermal springs are meteoric in origin with recharge moving slowly (multiple millennia) downgradient through low-permeability joints and fractures to depths of from an estimated depth of 4,500 ft to 7,500 ft with an estimated geothermal gradient ranging from 0.006 ºC/ft to 0.01 ºC/ft the water picks up heat until the flow path reaches the conduits by thrust faults (Haywood, 1912; Bryan, 1922; Bedinger et al., 1979; Yeatts, 2006; Bell and Hays, 2007; Thornberry-Ehrlich, 2013). The hot waters resurge “from the plunging crestline of a large overturned anticline between the traces of two thrust faults that are parallel to the axis of the anticline” and are mixed near the distal end of the flow system with cold-water recharge from nearby shallow sources (Kresse and Hays, 2009; Darrell Pennington written commun., 2009).

Mean water age for spring discharge in Hot Springs National Park was calculated as approximately 4,400 years by Bedinger et al (1978) using carbon-14. Their analysis indicated that the water was a mixture of a small portion of cold-water that was less than twenty years old with a preponderance of hot water. However, this result includes some error due to Bedinger et al. using general isotopic values for soil dissolved inorganic carbon and mineral carbon instead of obtaining actual values from the study area. Additionally, the study did not account for the potential loss of carbon that can occur as water travels along its flowpath. As precipitations falls from the atmosphere it collects atmospheric carbon dioxide, soil-gas carbon dioxide from plant decay, and inorganic carbon from soil and bedrock during infiltration and recharge. ^{14}C-age dating performed by Pennington using an integrated mass-balance model developed in NETPATH-XL to calculate the groundwater dates indicated dates younger than 4,400 years by using additional geological and geochemical data collected (Bell and Hays, 2007; Kresse and Hays, 2009). In order to compliment Pennington's initial findings, I performed a refined analysis of ^{14}C activity models and mass transfer functions by using the latest data gathered by the U.S. Geological Survey (USGS) and the age modeling software NETPATH-WIN.

Source isotopic values were collected for mineral carbon and soil organic matter, which were 2.681 $^{0}/_{00}$ $\delta^{13}C_{VPDB}$ and -24.01$^{0}/_{00}$ $\delta^{13}C_{VPDB}$ respectively; respective ^{14}C (pmc) values were assumed to be 0 pmc and 100 pmc. Geochemical, physical, and selected field parameters were collected from 10 cold-water springs, 30 cold-water wells, and 16 thermal springs, primarily by USGS personnel during three sampling events: 1) from January through September 1972; 2) from September 2007 to June 2008; and 3) during June 2018 by the author. The physical parameters selected for the mass balance calculations include temperature (°C), pH, and conductivity (µS/cm). Isotopic parameters include δD, δ^{18}O, Tritium in Tritium Units (TU), δ^{13}C

(per mil vs VPDB), ^{14}C (pmc), and $^{87/86}Sr$. Geochemical parameters include the following major cation and anions and associated elements measured in milligrams per liter (mg/L): dissolved oxygen (DO), Calcium (Ca^{2+}), Magnesium (Mg^{2+}), Sodium (Na^{+}), Field Alkalinity as $CaCO_3$, Sulfate (SO_4^{2-}), Chlorine (Cl^{-}), Fluoride (Fl), Silica (Si), Aluminum (Al^{3+}), Barium (Ba^{2+}), Boron (B), Iron (Fe), Lithium (Li^{+}), Manganese (Mn), and Sr^{2+}. Potassium was excluded as a major cation due to its nonexistent concentration value.

An improved age model was developed using the USGS software NETPATH-WIN; this program models the isotopic compositions and net geochemical mass balance reactions along the flowpath. NETPATH-WIN is capable of calculating every possible combination of mass transfers. Rayleigh distillation calculations were also applied to each model to predict carbon and radiocarbon dates at the end path. Three geochemical systems were tested in NETPATH along with seven different initial ^{14}C activity models; the A_0 models tested were Original Data, Mass Balance (1990), Tamers (1975), Ingerson and Pearson (1964), Mook (1980) and Eichinger (1983). The Basics Geochemical model had carbon and silica as constraints with the following as phases: CO_2 gas, calcite, dolomite, strontianite, and silica. Alkaline-Earth had the same phases as the Basics geochemical system but included the constraints carbon, magnesium, strontium, calcium, and silica. The Alkaline-Earth-plus-Sodium geochemical system had the same constraints and phases as the Alkaline-Earth system with sodium added as a constraint and Ca/Na ion exchange, illite, and NaCl being added to the total list of phases. All three geochemical systems were tested with just one IM paired with a hot springs member for a non-mixing scenario; likewise, each geochemical system was tested with multiple IMs for a mixing scenario. In order to conduct calculated mass transfer NETPATH runs in NETPATH-WIN, the dataset was first inputted into a Microsoft Excel file and was imported over to DB

Spreadsheet, the external data editor for DB-WIN; all data must first be imported to DB-WIN in order to be imported into NETPATH. The following units were chosen in DB-WIN: milligrams per liter (mg/L) was chosen as the units for concentrations; "temperature in °C; density in grams per cubic centimeter (g/cm^3) (default is 1.0); Eh in volts; tritium in tritium units (TU); ^{14}C of TDIC in percent modern carbon (pmc); $^{87}Sr/^{86}Sr$ as the mole ratio; and all other stable-isotope data in per mil" (Plummer, Prestemon, and Parkhurst, 1994). Extended Debye-Hückel was chosen as the option for calculating individual ion activity coefficients. Total dissolved inorganic carbon was chosen to be specified as "the usual field titration alkalinity expressed as $CaCO_3$, rather than as HCO_3" (Plummer, Prestemon, and Parkhurst, 1994). The redox ignored scenario was selected for the negative log of the electron activity (p*e*). Any site with more than five percent charge imbalance error produced by the CHECK file and the .OUT file was eliminated from dataset. This resulted in a total of 10 thermal wells and three cold-springs that passed the percent charge imbalance inspection.

After performing the calculated mass transfer NETPATH runs percent error was performed between the observed and the calculated $\delta^{13}C$ values; all models higher than 15% error were eliminated. Due to time constraints the mixing modeling scenarios were not as thoroughly tested as the non-mixing scenarios. After performing a QA/QC check, a total of 181 calculated mass transfer NETPATH runs passed initial inspection with non-mixing Basics at 30 calculated mass transfer NETPATH runs, non-mixing Alkaline-Earth at 17 calculated mass transfer NETPATH runs, non-mixing Alkaline-Earth-plus-Sodium at 75 calculated mass transfer NETPATH runs, mixing Basics with calculated mass transfer NETPATH 5 runs, mixing Alkaline-Earth with calculated mass transfer NETPATH 9 runs, and mixing Alkaline-Earth-plus-Sodium with calculated mass transfer NETPATH 45 runs. The Original Data initial ^{14}C activity

model produced 120 negative age results while the rest of the used A_0 models at most produced one to two negative age results; thus, the Original Data A_0 model was deemed as is an ineffective model to apply to this flow system.

Twelve outlier calculated mass transfer NETPATH runs that produced abnormally high ages occurred for the non-mixing Alkaline-Earth-plus-Sodium scenario with ten calculated mass transfer NETPATH runs using the following combination of phases in the mass transfer calculations: silica, calcite, dolomite, strontianite, illite, and NaCl. Since this particular combination produces unrealistic results, it is likely that this is an unrealistic mass transfer for this flow system. Neither the Basics or Alkaline-Earth for non-mixing produced these kinds of outliers nor did any system for mixing produce any spectacularly consistent high or low numbers for any calculated mass transfer NETPATH run.

After investigating the A_0 models and their assumptions involved in their calculations, the most applicable for the flow system were determined to be Mass Balance (1990The Basics geochemical was also deemed to be the least realistic system after analyzing the calculated mass transfers and the major cations and anions found the formations of the stratigraphic column. Likewise, Alkaline-Earth-plus-Sodium system contained outliers while the Alkaline-Earth system contained the most consistent mass transfer calculations. Therefore, the most appropriate geochemical system scenario and A_0 model for the flow system is the Non-Mixing Alkaline-Earth geochemical system with the Mass Balance (1990) A_0 model that produced a median mass residence time of 4,375 years.

For future work the author recommends testing out more calculated mass transfer NETPATH runs with more than one IM since time did not permit in this study. Additional model

of the discharge point of the springs mixed with the cold-water component could lead to understanding the proportions of the mixed product.

Selected References

Albin, D. R., 1965, Water Resources Reconnaissance of the Ouachita Mountains, Arkansas: U.S. Geological Survey Water-Supply Paper 1809-J

Bedinger, M.S., Pearson, F. J., Jr., Reed, J.E., Sniegocki, R.T., and Stone, C.G., 1979, The Waters of Hot Springs National Park, Arkansas-Their Nature and Origin: Geohydrology of Geothermal Systems Geological Survey Professional Paper 1044-C

Bell, R. W. and Hays, P. D., 2007, Influence of Locally Derived Recharge on the Water Quality and Temperature of Springs in Hot Springs, National Park, Arkansas: U.S. Geological Survey Scientific Investigations Report 2007-5004

Bryan, K., 1922, The Hot Water Supply of the Hot Springs, Arkansas, *The Journal of Geology*, Vol. 30, No. 6, p.425-449

Clark, I. D. and Fritz, P., 1997, Environmental Isotopes in hydrogeology, CRC Press

Clark, I., 2015, Groundwater Geochemistry and Isotopes, CRC Press

Eichinger, L. 1983, A Contribution to the Interpretation of ^{14}C Groundwater Ages Considering the Example of a Partially Confined Sandstone Aquifer: *Radiocarbon* 25, p.347-356

El-Kadi, A.I., Plummer, L.N., and Aggarwal, P., 2010, NETPATH-WIN: An Interactive User Version of the Mass-Balance Model, NETPATH. *Groundwater*

El-Kadi, A.I., Plummer, L.N., and Aggarwal, P., 2010, Supporting information to: NETPATH-WIN: An Interactive User Version of the Mass-Balance Model, NETPATH

Faure, G., 1986, Principles of Isotope Geology, Second Edition, John Wiley & Sons

Fetter, C. W., 2001, Applied Hydrogeology, Fourth Edition, Prentice Hall

Fontes H.-Ch. And J.-M. Garnier. 1979. Determination of the Initial ^{14}C Activity of the Total Dissolved Carbon: A Review of the Existing Models and a new Approach. *Water Resources Research* 15, p. 399-413

Fournier, R. O. and Rowe, J.J., 1966, Estimation of Underground Temperatures from the Silica Content of Water from Hot Springs and Wet-Steam Wells. American Journal of Science, v. 264, p.685-697

Fry, B., 2006, Stable Isotope Ecology, Springer-Verlag

Glynn, P.D., and Brown, J.G., 1996, Reactive Transport Modeling of Acidic Metal-Contaminated Groundwater at a Site with Sparse Spatial Information. In *Reactive Transport in Porous Media: General Principles and Application to Geochemical Processes, Reviews in Mineralogy*, vol. 34, Chapter 9. ed. C.I. Steefel, P. Lichtner, and E. Oelkers, 377-Washingotn, DC: Mineralogical Society of America.

Glynn, P.D., and Plummer, L.N., 2005, Geochemistry and the Understanding of Ground-Water Systems: Hydrogeology Journal, v.13, p.263-287

Guccione, M.J., 1993, Geologic History of Arkansas Through Time and Space, University of Arkansas

Hanor, J.S., 1980, Fire in the Folded Rocks: Geology of Hot Springs National Park: Eastern National Park and Monument Association.

Haywood, J.K., and Weed, W. H.,1912, Analyses of the Waters of The Hot Springs of Arkansas and Geological Sketch of Hot Springs, Arkansas, Document 282, 57th Congress, 1st Session, 56 p. Washington, D.C., Government Printing Office

Hoefs, J., 1987, Stable Isotope Geochemistry, Third Edition, Springer-Verlag

Hot Springs NP Annual Recreation Visitors Report, accessed on January 28, 2019 at https://irma.nps.gov/Stats/SSRSReports/Park%20Specific%20Reports/Annual%20Park%20Recreation%20Visitation%20(1904%20-%20Last%20Calendar%20Year)?Park=HOSP

Ingerson, E., and F.J. Pearson, Jr. 1964. Estimation of age and Rate of Motion of Groundwater by the ^{14}C-method, In *Recent Researches in the Fields of Atmosphere, Hydrosphere, and Nuclear Geochemistry*, Sugawara Festival Volume. Ed. Y. Miyake and T. Koyama, p.263-283, Maruzen Co., Tokyo

Johnson, T. C. and Hanson, W. D., 2011, Geologic map of Hot Springs North, Hot Springs South, Fountain Lake, and Lake Catherine Quadrangles Quadrangles, Hot Spring, Saline, and Garland County, Arkansas: Arkansas Geological Survey, Digital Geologic Map, DGM-HSR-003, 1 sheet.

Kalin, R. M., 2010, Radiocarbon Dating of Groundwater Systems. In *Environmental Tracers in Subsurface Hydrology*, Chapter 4. ed. Cook, P.G., and Herczeg, A.L. Kluwer Academic Publishers

Keller, W.D., Viele, G.W., and Johnson, C.H., 1977, Texture of Arkansas Novaculite Indicates Thermally Induced Metamorphism: Journal of Sedimentary Petrology, v. 47, p. 834-843.

Kendall, Carol 2010. USGS Isotope Tracers Project Data and Resource Page, accessed January 28, 2019 at https://wwwrcamnl.wr.usgs.gov/isoig/

Kresse, T. M., and Hays, P.D., 2009, Geochemistry, Comparative Analysis, and Physical Chemical Characteristics of the Thermal Waters East of Hot Springs National Park, Arkansas, 2006-09, U.S. Geological Survey Scientific Investigations Report 2009-5263.

Mook, W.G., 1972, On the Reconstruction of the Initial ^{14}C content of Groundwater from the Chemical and Isotopic Composition. *In* Proceedings of Eighth International Conference on Radiocarbon Dating, v. 1, Royal Society of New Zealand, Wellington, New Zealand, p. 342-352

National Park Service, Hot Springs National Park Maps, accessed March 19, 2019 at https://www.nps.gov/carto/app/#!/maps/alphacode/HOSP

Niem, A.R., 1971, Stratigraphy and origin of tuffs in the Stanley Group (Mississippian), Ouachita Mountains, Oklahoma and Arkansas: unpublished Ph.D. dissertation, University of Wisconsin, Madison, 203 p.

Nordstrom, D.K., 2007, Modeling low-temperature geochemical processes. In *Treatise on Geochemistry*, vol. 5: *Surface and Ground Water, Weathering and Soils*, ed. J.I. Drever, 1-38. New York: Elsevier.

Palmer, A. N., 2007, Cave Geology, Third Edition, Cave Books

Parkhurst, D.L. and Plummer, L.N., 1993. Geochemical models. In *Regional Ground-Water Quality*, Chapter 9, ed. W.M. Alley, 199-225. New York: van Nostrand Reinhold.

Parkhurst, D. L. and Charlton, S. R., 2008, NetpathXL-An Excel® Interface to the Program NETPATH

Pennington, D. W., 2009, Correction of ^{14}C Dates Using an Integrated Mass-Balance Approach at Hot Springs National Park, Arkansas [unpublished manuscript cited as written communication, xx p.]

Plummer, L.N., 1985. *Geochemical modeling: a comparison of forward and inverse methods*. Proceedings First Canadian/American Conference on Hydrogeology, Banff, Alberta, June 1984, ed. B. Hitchon and E.I. Wallick, 149-177. Worthington, Ohio: National Water Well Assoc.

Plummer, L.N., Prestemon, E.C., and Parkhurst, D.L., 1991, An Interactive Code (Netpath) For Modeling Net Geochemical Reactions Along A Flow Path, U.S. Geological Survey Water-Resources Investigations Report 91-4078

Plummer, L. N., Prestemon, E.C., and Parkhurst, D.L., 1994, An Interactive Code (Netpath) for Modeling Net geochemical reactions along a flow path version 2.0, U.S. Geological Survey Water-Resources Investigations Report 94-4169

Plummer, L. N. and Sprinkle, C.L., 2001, Radiocarbon dating of dissolved inorganic carbon in groundwater from confined parts of the Upper Floridian aquifer, Florida, USA. *Hydrogeology Journal* 9, *Issue 2*, p.127-150

Plummer, L.N., Bexfield, L.M., Anderholm, S.K., Sanford, W.E., Busenburg, E., 2004 Interpretation of Radiocarbon Age of Dissolved Inorganic Carbon in Ground Water. Geochemical Characterization of Ground-water Flow in the Santa Fe Group Aquifer System, Middle Rio Grande Basin, New Mexico. U.S. Geological Survey Water-Resources Investigations Report 03-4131

Plummer, L.N., Jones, B.F., and Truesdell, A.H., 1976, WATEQF – A Fortran IV Version of WATEQ, A Computer Program for Calculating Chemical Equilibrium of Natural Waters, U.S. Geological Survey, Water-Resources Investigations Report 76-13

Purdue, A.H., 1910, The Collecting Area of the Waters of the Hot Springs, Hot Springs, Arkansas, The Journal of Geology, v.18, no.3, p.279-285

Purdue A.H, and Miser, H.D., 1923, Hot Springs folio, Arkansas: U.S. Geological Survey Geologic Atlas, Folio no. 215, 12 p

Sharp, Zachary 2007, Principles of Stable Isotope Geochemistry, Prentice Hall

Solomon, D.K, and Cook, P.G, 2010, ^{3}H and ^{3}He. In *Environmental Tracers in Subsurface Hydrology*, Chapter 13. ed. Cook, P.G., and Herczeg, A.L. Kluwer Academic Publishers

Tamers, M.A. 1975. Validity of Radiocarbon Dates on Groundwater. *Geophysical Surveys* 2, p. 217-239

Thornberry-Ehrlich, T.L., 2013, Hot Springs National Park: Geologic Resources Inventory Report. Natural Resource Report NPS/NRSS/GRD/NRR-2013/741. National Park, U.S. Department of the Interior, National Park Service, Fort Collins, Colorado

Truesdell, A.H., and Jones, B.F., 1974, WATEQ, A Computer Program for Calculating Chemical Equilibria of Natural Waters, Journal Research U.S. Geol. Survey, v. 2, no.2, p.233-248

U.S. Department of Health and Human Services, Centers for Disease Control and Prevention, National Institute for Occupational Safety and Health, 2005, NIOSH Health Hazard Evaluation Report, HETA #2004-0094-2978: National Park Service, Hot Springs, Arkansas, 33 p.

Wilde, F.D., Radtke, D.B., Gibs, J., and Iwatsubo, R.T. 1998, Techniques of Water-Resources Investigation—Book 9. Handbooks for Water-Resources Section A. National Field Manual for the Collection of Water-Quality Data: Preparations for Water Sampling. USGS-TWRI book 9, chap. A1., p. 47

Wilde, F.D., Radtke, D.B., Gibs, J., and Iwatsubo, R.T. 1998, TWRI—Book-A2. National Field Manual for the Collection of Water-Quality Data: Selection of Equipment for Water Sampling. USGS-TWRI book 9, chap. A2., p. 94

Wilde, F.D. and Radtke, D.B. 1998, TWRI—Book 9-A6. National Field Manual for the Collection of Water-Quality Data: Field Measurements. USGS-TWRI book 9, chap. A6., variously paginated. 9-A7

Wilde, F.D., Radtke, D.B., Gibs, J., and Iwatsubo, R.T. 1999, TWRI—9-A4. National Field Manual for the Collection of Water-Quality Data: Collection of Water samples. USGS-TWRI book 9, chap. A4., p. 156

Wigley, T.M.L., Plummer, L.N., and Jr., Pearson, F.J. 1978, Mass Transfer and Carbon Isotope Evolution in Natural Water Systems. Geochimica et Cosmochimica Acta 42, p. 1117-1139

Viele, G.W. and Thomas, W.A., 1989, Tectonic synthesis of the Ouachita orogenic belt: in Hatcher, R.D., Jr., Thomas, W.A., and Viele, G.W., eds., The Appalachian-Ouachita Orogen in the U.S. Boulder, Colorado. Geological Society of America, The Geology of North America v, F-2, p.695-728.

Yeatts, D.S. 2006, Characteristics of Thermal Springs and the Shallow Ground-Water System at Hot Springs National Park, Arkansas: U.S. Geological Survey Scientific Investigations Report 2006-5001

Zhu, C. and Murphy, W.M., 2000, On Radiocarbon Dating of Ground Water, Groundwater, Vol. 38, No.6, ProQuest

APPENDIX A

Geochemical Data, Including Authorship of Data, Publication Information, Collection Information, Quality Assessment, and Comments

A1. Hot Springs in Hot Springs National Park

A2. Cold Springs in the Vicinity of Hot Springs National Park

A3. Shallow Wells in the Vicinity of Hot Springs National Park

Appendix A1. Water Quality from Hot Springs in Hot Springs National Park

Well (W), spring (S), or hot spring (HS) number	Latitude (ddmmss)	Longitude (ddmmss)	Name of well or spring	Sampling Date (mm/dd/yyyy)	Well Depth (in feet above LSD)	Geologic Formation	Water Temp (°C)	Water Temp (°F)
HS-6	343056	930311	Hot Spring 6 Boiler House North	9/11/2007			57.9	136.22
HS-8	343056	930309	Hot Spring 8 Crystal	9/12/2007			61.9	143.42
HS-9	343055	930313	Hot Spring 9 Rector	9/11/2007			62.1	143.78
HS-17	343057	930313	Hot Spring 17 ArScenic North	1/25/1972			55.4	131.72
HS-17	343057	930313	Hot Spring 17 ArScenic North	9/11/2007			54	129.2
HS-23	343053	930311	Hot Spring 23 Twin Spring North	1/26/1972			56.2	133.16
HS-25	343052	930313	Hot Spring 25 Hale	9/10/2007			62.5	144.5
HS-33	343051	930309	Hot Spring 33 Upper Display	1/26/1972			57.6	135.68
HS-33	343050	930312	Hot Spring 33 Upper Display	9/13/2007			55.8	132.44
HS-42B	343047	930310	Hot Spring 42 Health Services	1/19/1972			61.3	142.34
HS-42	343048	930313	Hot Spring 42 Quapaw	9/11/2007			61.2	142.16
HS-46	343049	930313	Hot Spring 46 Fordyce	9/10/2007			57.4	135.32
HS-47	343058	930309	Hot Spring 47 New North	9/12/2007			61.3	142.34
HS-48	343058	930308	Hot Spring 48 New South	1/25/1972			60	140
HS-49	343035	930310	Hot Spring 49	1/21/1972			61.8	143.24
HS-49	343054	930312	Hot Spring 49	9/12/2007			61.8	143.24
HS-50	343051	930311	Maurice Hot Spring 50	1/20/1972			53.3	127.94
HS-99	343055	930312	80,000-gallon reservoir 99	1/27/1972			61	141.8

Appendix A1. Water Quality from Hot Springs in Hot Springs National Park--Continued

Well (W), spring (S), or hot spring (HS) number	Silica (mg/L)	Aluminum (mg/L)	Iron total (mg/L)	Calcium (mg/L)	Magnesium (mg/L)	Sodium (mg/L)	Potassium (mg/L)	Alkalinity (field)	Field Bicarbonate (mg/L)	Sulfate (mg/L)	Chloride (mg/L)
HS-6	39.89	0.0021		45.32	4.82	3.91		132	161	7.53	1.86
HS-8	39.6	0.0019		44.8	4.78	3.88		132	161	7.49	1.84
HS-9	39.8	0.0017		44.7	4.79	3.88		131	159	7.53	1.77
HS-17	41	0	0	44	4.6	3.9	1.5		[2] 160	7.8	1.8
HS-17	39.7	0.0017		42	4.81	4.04		124	151	7.6	1.87
HS-23	41	0	0	44	4.6	3.9	1.5		159	8.2	1.9
HS-25	39.7	0.0029		45.3	4.83	3.92		132	161	7.48	1.83
HS-33	42	0	0.04	45	4.8	4	1.5		164	8.2	1.9
HS-33	41.3	0.0041		45.2	4.78	3.7		126	153	7.66	1.82
HS-42	42	0	0.01	45	4.8	4	1.5		159	8.6	1.9
HS-42	39.8	0.0026		45.2	4.84	3.95		127	154	7.79	1.93
HS-46	40.4	0.0016		45.4	4.83	4.01		132	161	7.46	1.86
HS-47	39.7	0.002		45.9	4.88	3.91		138	167	7.32	1.84
HS-48	42	0	0.02	45	4.7	4	1.5		165	8.6	1.9
HS-49	41	0	0.06	44	4.8	3.8	1.5		155	8.2	1.9
HS-49	40.8	0.0133		44.4	4.72	3.75		128	156	7.25	1.84
HS-50	42	0	0	45	4.8	4	1.5		156	9	1.9
HS-99	42	0	0	45	4.8	4	1.5		165	8	1.8

Appendix A1. Water Quality from Hot Springs in Hot Springs National Park--Continued

Well (W), spring (S), or hot spring (HS) number	Zinc (mg/L)	Strontium (mg/L)	Ammonia as NH_4	Fluoride (mg/L)	Nitrate (NO_3)	Ortho-phosphate (PO_4)	Organic Nitrogen a N	Residue on evaporation at 180°C	Sum of constituents	Specific conductance (µmho/cm at 25°C
HS-6	0.0006	0.1054		0.13						302
HS-8	0.00049	0.1045		0.13						284
HS-9	0.00047	0.1067		0.13						311
HS-17	0.05	0.11		0.2	0	0		184	187	266
HS-17	0.0006	0.1024		0.13						290
HS-23	0.03	0.11		0.2	0.2	0.09		185	188	269
HS-25	0.00042	0.1055		0.13						302
HS-33	0.08	0.11		0.2	0	0.02		188	193	269
HS-33	0.0065	0.1014		0.15						298
HS-42	0.02	0.11		0.2	0	0.04		188	191	272
HS-42	0.0012	0.106		0.14						286
HS-46	0.0006	0.108		0.14						272
HS-47	0.00037	0.1064		0.13						297
HS-48	0.06	0.12		0.2	0.1	0		189	196	316
HS-49	0.06	0.11		0.2	0	0.06		184	191	276
HS-49	0.0067	0.0988		0.14						302
HS-50	0.05	0.11		0.2	0	0.04		189	191	284
HS-99	0.04	0.12		0.2	0	0		188	191	311

Appendix A1. Water Quality from Hot Springs in Hot Springs National Park--Continued

Well (W), spring (S), or hot spring (HS) number	pH (units) (field)	Dissolved oxygen (DO)	Deuterium/Protium ratio (per mil)	Tritium pCi/L	$^{18}O/^{16}O$ ratio (per mil)	$^{13}C/^{12}C$ ratio (per mil)	^{14}C (% modern)	$^{87}Sr/^{86}Sr$ ratio	Data Source
HS-6	6.3		-28.6		-5.56	-13.87	36.3	0.71196	Kresse & Hays, 2009
HS-8	7.5		-28.3	0	-5.56	-13.8	38.3	0.71189	Kresse & Hays, 2009
HS-9	7.5		-28.2	0	-5.52	-13.24	37	0.7119	Kresse & Hays, 2009
HS-17	7.7	3.6	-30	3	-5.4	-14.1	36.9		Bedinger et al., 1977
HS-17	7.3		-29.4			-13.51	40	0.7119	Kresse & Hays, 2009
HS-23	7.52	3.9	-28	0.7		-14.2	35.1		Bedinger et al., 1977
HS-25	7.1		-29		-5.54	-14.73	35.7	0.71196	Kresse & Hays, 2009
HS-33	7.13	1.1	-28	0.9	-5.4	-14.6			Bedinger et al., 1977
HS-33	7.2		-30.2		-5.48	-13.42	36.9	0.71191	Kresse & Hays, 2009
HS-42	6.93	0	-28	2.7	-5.4		4.6		Bedinger et al., 1977
HS-42	7		-28.9		-5.52	-14.03	36.6	0.71192	Kresse & Hays, 2009
HS-42	6.93	0	-28	2.7	-5.4		4.6		Bedinger et al., 1977
HS-46	7.2		-28.6		-5.49	-13.86	35.6	0.7119	Kresse & Hays, 2009
HS-47	7.2		-29.5		-5.61	-13.3	36.2	0.7119	Kresse & Hays, 2009
HS-48	7.27	2.4					38.7		Bedinger et al., 1977
HS-49	6.95	0.4	-28	9	-5.6		36.8		Bedinger et al., 1977
HS-49	7.4		-29.7		-5.55	-14.02	44.8	0.71192	Kresse & Hays, 2009
HS-50	7.03	2							Bedinger et al., 1977
HS-99	7.36	3.3	-28		-5.6		30.4		Bedinger et al., 1977

Appendix A2. Water Quality from Cold Springs in the Vicinity of Hot Springs National Park

Well (W), spring (S), or hot spring (HS) number	Latitude (ddmmss)	Longitude (ddmmss)	Name of well or spring	Sampling Date (mm/dd/yyyy)	Well Depth (in feet above LSD)	Geologic Formation	Water Temp (°C)	Water Temp (°F)
S-5	343231	930128	Echo Valley Spring	1/27/1972			20.5	68.9
S-7	343033	925849	Cluster Spring	9/26/1972			20.8	69.44
S-7	343033	925849	Cluster Spring	6/25/2018				
S-8	343110	930253	Happy Hollow Spring	1/24/1972			17.5	63.5
S-9	342954	930701	Music Mountain Spring	9/27/1972			20.9	69.62
S-10	343211	930115	Sleepy Valley Spring	1/28/1972		364BGFK	12	53.6
S-10	343211	930115	Sleepy Valley Spring	9/13/2007		364BGFK	19.2	
S-10	343211	930115	Sleepy Valley Spring	9/13/2007		364BGFK	19.2	66.56
S-11	343105	925720	Mclendon Mineral Spring	9/27/1972			18.6	65.48
S-26	343052	930408	Whittington Avenue Spring	1/24/1972			18	64.4
S-69	343105	925720	Diamond Mineral Spring	1/22/1972			18.8	65.84
S-83	342314	933633	Caddo Gap Spring	6/18/2008		330ARKS	33.77	92.786
S-83	342314	933633	Caddo Gap Spring	6/18/2008		330ARKS	33.77	92.786
S-84	343227	935435	Little Missouri Spring	6/10/2008		330ARKS	23.4	74.12
S-84	343227	935435	Little Missouri Spring	6/10/2008		330ARKS	23.4	74.12

Appendix A2. Water Quality from Cold Springs in the Vicinity of Hot Springs National Park--Continued

Well (W), spring (S), or hot spring (HS) number	Silica (mg/L)	Aluminum (mg/L)	Iron total (mg/L)	Calcium (mg/L)	Magnesium (mg/L)	Sodium (mg/L)	Potassium (mg/L)	Alkalinity (field) as CaCO3	Field Bicarbonate (mg/L)	Sulfate (mg/L)	Chloride (mg/L)
S-5	9.7	0	1.3	67	2.9	1.3	0.6		219	7.2	2
S-7	13	0	0.66	42	2.5	4.6	1.7		147	11	2.7
S-7											
S-8	8.4	0	0	0.2	0.3	1.3	0.2		[2] 1	1.4	2.3
S-9	2.6	0.08	0.04	11	1.4	2.4	1		[2] 29	8.6	4.7
S-10	11	0.4	2.1	3.7	1	1.3	0.8		[2] 2	14	2.1
S-10	12.5	50.7		7.57	0.579	1.45			10	13.55	2.28
S-10	12.5	0.051		7.57	0.579	1.45		8	10	13.55	2.28
S-11	11	0	1	40	1.4	1.7	1		145	7.2	1.6
S-26	9.4	0	0.79	50	2.3	1.5	0.9		157	14	2.1
S-69	12	0	0.37	66	3.6	1.9	1.8		211	12	2
S-83	22.2			34.7	2.14	4.16		109	133	4.78	3.18
S-83	22.2			34.7	2.14	4.16		109	133	4.78	3.18
S-84	11.2			17.3	2.48	1.61		51	62	5.31	1.63
S-84	11.2			17.3	2.48	1.61		51	62	5.31	1.63

Appendix A2. Water Quality from Cold Springs in the Vicinity of Hot Springs National Park--Continued

Well (W), spring (S), or hot spring (HS) number	Zinc (mg/L)	Strontium (mg/L)	Ammonia as NH_4	Fluoride (mg/L)	Nitrate (NO_3)	Ortho-phosphate (PO_4)	Organic Nitrogen a N	Residue on evaporation at 180°C	Sum of constituents	Specific conductance (µmho/cm at 25°C
S-5	0.08	0.11		0.2	0.1	0.03		196	202	339
S-7	0.01	0.1	0.08	0.2	0.1	0.12	0.04	146	149	219
S-7										
S-8	0.03	0		0.1	0	0.03		14	11	22
S-9	0	0.01		0.1	0.7	0.01		47	60	104
S-10	0.1	0.01		0.2	0.1	0.35		36	41	47
S-10	0.041	<0.08								63
S-10				0.1						63
S-11	0.06	0.07	0.06	0.2	0.1	0.39	0.01	131	141	232
S-26	0.1	0.2		0.2	0.1	0.12		157	164	276
S-69	0.06	0.11		0.3	0.1	0		204	212	354
S-83		0.083		0.18						
S-83		0.083		0.18						
S-84		0.037		0.13						
S-84		0.037		0.13						

Appendix A2. Water Quality from Cold Springs in the Vicinity of Hot Springs National Park--Continued

Well (W), spring (S), or hot spring (HS) number	pH (units) (field)	Dissolved oxygen (DO)	Deuterium/ Protium ratio (per mil)	Tritium pCi/L	$^{18}O/^{16}O$ ratio (per mil)	$^{13}C/^{12}C$ ratio (per mil)	^{14}C (% modern)	$^{87}Sr/^{86}Sr$ ratio	Data Source
S-5	7.25	0							Bedinger et al., 1977
S-7	6.72	0							Bedinger et al., 1977
S-7									Raley, 2018
S-8	4.58	6.3							Bedinger et al., 1977
S-9	7.12								Bedinger et al., 1977
S-10	4.82	3.3							Bedinger et al., 1977
S-10	6.1		-29.5	7	-5.11			0.70937	Kresse & Hays, 2009
S-10	6.1		-29.5	7	-5.11			0.70937	Kresse & Hays, 2009
S-11	7.15	0							Bedinger et al., 1977
S-26	6.69	0							Bedinger et al., 1977
S-69	7.08	0							Bedinger et al., 1977
S-83				2	-5.58			0.7121	Kresse & Hays, 2009
S-83				2	-5.58			0.7121	Kresse & Hays, 2009
S-84								0.71211	Kresse & Hays, 2009
S-84								0.71211	Kresse & Hays, 2009

Appendix A3. Water Quality from Shallow Wells in the Vicinity of Hot Springs National Park

Well (W), spring (S), or hot spring (HS) number	Latitude (ddmmss)	Longitude (ddmmss)	Name of well or spring	Sampling Date (mm/dd/yyyy)	Well Depth (in feet above LSD)	Geologic Formation	Water Temp (°C)	Water Temp (°F)
W-1	343230	930007	Thomas well	9/12/2007	150	350SLRN?	16.5	61.7
W-1	343230	930007	Thomas well	6/27/2018	150	350SLRN?		
W-3	343256	925542	Appel well	9/10/2007	35	330HSPG	20	68
W-5	343124	925803	Schnick well	9/13/2007	300	330HSPG	18.4	65.12
W-12	343347	925942	Elizabeth Brown well	9/24/1972			17.4	63.32
W-16	343056	930017	Thornton well	9/11/2007	74	330STNL	18.7	65.66
W-16B	343327	930004	R. B. Yates' well	9/25/1972			21.2	70.16
W-17	343227	930022	Bill Sargo's well	9/24/1972			18.1	64.58
W-19	343252	910023	Belvedere County Club well	9/25/1972			16.8	62.24
W-20	343204	930055	Frank Thompson's house well	9/24/1972			16.8	62.24
W-21	343130	930208	Gulpha Gorge Well	9/27/1972			20.4	68.72
W-24	343047	925711	Bratton well	9/5/2007	200	330STNL	19.1	66.38
W-25	343056	930406	Whittington Park well	1/28/1972			18.6	65.48
W-30	343224	925623	Sharp well	9/10/2007		330STNL	18.3	64.94
W-34	343047	925712	Bratton 2 well	9/5/2007	165	330STNL	20.4	68.72
W-40	343238	925352	Bratton 4 well	9/11/2007		364BGFK	17.1	62.78
W-41	343458	925602	Gates well	9/6/2007		367WMBL	16.7	62.06
W-45	343350	925607	King well	9/7/2007		364BGFK	19.5	67.1
W-46	343330	925911	Ester-Trusty-Carlin well	9/7/2007	50	364BGFK	17.49	63.482
W-49	343132	925854	Greer 1 well	9/5/2007	200	364BGFK	19.2	66.56

Appendix A3. Water Quality from Shallow Wells in the Vicinity of Hot Springs National Park--Continued

Well (W), spring (S), or hot spring (HS) number	Latitude (ddmmss)	Longitude (ddmmss)	Name of well or spring	Sampling Date (mm/dd/yyyy)	Well Depth (in feet above LSD)	Geologic Formation	Water Temp (°C)	Water Temp (°F)
W-51	343132	925855	Greer 2 well	9/7/2007	120	364BGFK	18.3	64.94
W-52	343132	925854	Greer 3 well	9/6/2007	160	364BGFK	17.9	64.22
W-52	343511	925809	Rigsby well	9/7/2007		364BGFK	19.5	67.1
W-100	343205	930437	Randy Jeffers well	6/27/2018				
W-100	343205	930437	Randy Jeffers well (dup)	6/27/2018				
W-101	343156	930416	Budd Kerry well	6/27/2018				
W-102	343314	930131	Jim Carter well	6/27/2018				
W-103	343402	930106	Judy Hawkins well	6/27/2018				
W-104	343206	930054	Nova Stone Place well	6/27/2018				
W-105	343004	925846	? None yet assigned	6/25/2018				
W-106	343329	925851	? None yet assigned	6/27/2018				
W-107	343158	925855	? Thousand Dr. 6 well?	6/26/2018				
W-109	343057	930311	Arlington Hotel well?	8/3/1993	200	330HSPG	30	86

Appendix A3. Water Quality from Shallow Wells in the Vicinity of Hot Springs National Park--Continued

Well (W), spring (S), or hot spring (HS) number	Silica (mg/L)	Aluminum (mg/L)	Iron total (mg/L)	Calcium (mg/L)	Magnesium (mg/L)	Sodium (mg/L)	Potassium (mg/L)	Alkalinity (field) as $CaCO_3$	Field Bicarbonate (mg/L)	Sulfate (mg/L)	Chloride (mg/L)
W-1	10.7	0.003	0.038	0.31	2.62	1		10	13	1.02	1.48
W-1											
W-3	9.08	0.059	0.029	0.12	0.208	1.53		0	2	1.11	2.92
W-5	7.76	0.08	0.089	0.81	0.364	1.6		0	1	2.67	2.12
W-12	8.7	0	2.1	55	1.9	1.6	0.7		183	7	2
W-16	31.3	0.002	0.216	27.16	4.01	10.83		78	95	22.71	2.86
W-16B	7.9	0.04	0.04	5.9	1.5	5.4	1.4		9	10	6.4
W-17	8.1	0.2	2	0.8	0.5	2.8	1.4		0	7.4	3.6
W-19	6.9	0.05	0.98	0.1	0.1	1	0.2		5	1.6	1.4
W-20	7.5	0.04	0.02	0.2	0.1	0.7	0.3		[2] 0	1.6	0.9
W-21	13	0	1.2	46	2.8	2.9	1.5		157	10	2.3
W-24	15.8	0.03	0.096	12.4	2.19	11.3					11.2
W-25	11	0	1.6	63	3.4	1.6	1.4		227	9.8	1.9
W-30	31.3	0.003	0.611	19.5	4.56	14.8		68	83	26.17	4.73
W-34	18.3	0.003	0.158	44.7	5.92	14.3		149	180	11.5	2.57
W-40	7.23	0.01		0.3	0.137	0.69		0	1	1.32	0.98
W-41	8.34	0.055	0.798	4.1	0.326	0.91		11	14	4.11	1.49
W-45	8.38	0.012		0.9	0.609	1.03		3	4	2.95	1.52
W-46	12.33	0.214	0.696	0.078	0.151	1.756		0.3	3.6	12.05	3
W-49	11.8	0.003	2.51	0.39	0.21	1.12		4	5	4.87	1.83

Appendix A3. Water Quality from Shallow Wells in the Vicinity of Hot Springs National Park--Continued

Well (W), spring (S), or hot spring (HS) number	Silica (mg/L)	Aluminum (mg/L)	Iron total (mg/L)	Calcium (mg/L)	Magnesium (mg/L)	Sodium (mg/L)	Potassium (mg/L)	Alkalinity (field) as $CaCO_3$	Field Bicarbonate (mg/L)	Sulfate (mg/L)	Chloride (mg/L)
W-51	13.5	0.005	0.008	0.01	0.007	9.17		14	17	3.51	1.71
W-52	10.8	0.005	1.22	6.11	0.288	1.46		16	20	3.6	1.22
W-52	10.7	0.002	0.012	78.1	8	11.5		205	249	35.4	9.95
W-100											
W-101											
W-102											
W-103											
W-104											
W-105											
W-106											
W-107											
W-109	25		2.8	30	3.6	7.5	2.1	89	109	28	3.5

Appendix A3. Water Quality from Shallow Wells in the Vicinity of Hot Springs National Park--Continued

Well (W), spring (S), or hot spring (HS) number	Zinc (mg/L)	Strontium (mg/L)	Ammonia as NH_4	Fluoride (mg/L)	Nitrate (NO_3)	Ortho-phosphate (PO_4)	Organic Nitrogen a N	Residue on evaporation at 180°C	Sum of constituents	Specific conductance (µmho/cm at 25°C
W-1				E 0.1						29
W-1										
W-3				<0.1						23
W-5				<0.1						31
W-12	0.17	0.24	0.06	0.1	0.1	0.31	0.05	164	173	274
W-16				0.21						235
W-16B	0.06	0	0.02	0.1	8.3	0.02	0.01	51	54	77
W-17	0.02	0	0	0.1	1.7	0.06	0.1	26	36	44
W-19	0.04	0	0.04	0	0.3	0.04	0.08	12	15	15
W-20	0.02	0	0.04	0	0.2	0	0.04	12	18	36
W-21	0.02	0.08	0.02	0.2	0.1	0.07	0.08	152	165	247
W-24				0.15						154
W-25	0.12	0.26		0.2	0.1	0		193	200	331
W-30				0.18						184
W-34				0.18						295
W-40				<0.1						17
W-41				0.1						30
W-45				<0.1						22
W-46				< 0.1						50
W-49				<0.1						24

Appendix A3. Water Quality from Shallow Wells in the Vicinity of Hot Springs National Park--Continued

Well (W), spring (S), or hot spring (HS) number	Zinc (mg/L)	Strontium (mg/L)	Ammonia as NH4	Fluoride (mg/L)	Nitrate (NO3)	Ortho-phosphate (PO4)	Organic Nitrogen a N	Residue on evaporation at 180°C	Sum of constituents
W-51				0.17					
W-52				<0.1					
W-52				0.15					
W-100									
W-101									
W-102									
W-103									
W-104									
W-105									
W-106									
W-107									
W-109		0.095	0.09	0.2	<.05	<.031	<.011	140	156

Appendix A3. Water Quality from Shallow Wells in the Vicinity of Hot Springs National Park--Continued

Well (W), spring (S), or hot spring (HS) number	pH (units) (field)	Dissolved oxygen (DO)	Deuterium/Protium ratio (per mil)	Tritium pCi/L	$^{18}O/^{16}O$ ratio (per mil)	$^{13}C/^{12}C$ ratio (per mil)	^{14}C (% modern)	$^{87}Sr/^{86}Sr$ ratio	Data Source
W-1	4.8	6.8	-31	9	-5.6			0.72205	Kresse & Hays, 2009
W-1						-22.31685338			Raley, 2018
W-3	3.9	5.5	-31.3	7	-5.73			0.71812	Kresse & Hays, 2009
W-5	3.7	6.8	-30.7		-5.57			0.71435	Kresse & Hays, 2009
W-12	6.92	0							Bedinger et al., 1977
W-16	6.3	1	-28.1	12	-4.88	-17.37	66.1	0.71383	Kresse & Hays, 2009
W-16B	5.32	4.8							Bedinger et al., 1977
W-17	4.62	1.8							Bedinger et al., 1977
W-19	5.2	0.6							Bedinger et al., 1977
W-20	4.7	10.2							Bedinger et al., 1977
W-21	7.1	0							Bedinger et al., 1977
W-24	5.8	0.9		9		-19.43	79.5	0.71032	Kresse & Hays, 2009
W-25	7.6	3							Bedinger et al., 1977
W-30	5.9	0.5	-29.9		-5.41			0.71092	Kresse & Hays, 2009
W-34	7.4	0.6		1		-12.7	23.7	0.7103	Kresse & Hays, 2009
W-40	4.2	8.3	-32.2		-5.81			0.71319	Kresse & Hays, 2009
W-41	4.7	0.5	-29.6		-5.48			0.70969	Kresse & Hays, 2009
W-45	4.2	5.7	-29.3		-5.41			0.71258	Kresse & Hays, 2009
W-46	3.62	0.48	-30.4	9	-5.52			0.72242	Kresse & Hays, 2009
W-49	4.4	0.7	-30.2	7	-5.6	-23.49	77.8	0.71107	Kresse & Hays, 2009

Appendix A3. Water Quality from Shallow Wells in the Vicinity of Hot Springs National Park--Continued

Well (W), spring (S), or hot spring (HS) number	Specific conductance (µmho/cm at 25°C	pH (units) (field)	Dissolved oxygen (DO)	Deuterium/Protium ratio (per mil)		Tritium pCi/L	$^{18}O/^{16}O$ ratio (per mil)	$^{13}C/^{12}C$ ratio (per mil)	^{14}C (% modern)	$^{87}Sr/^{86}Sr$ ratio	Data Source
W-51	44	5.1	0.9	-30.6	8	-5.58	-23.09		85.2	0.7082	Kresse & Hays, 2009
W-52	38	5.6	0.5	-31.3	8	-5.63	-22.14		78.6	0.71064	Kresse & Hays, 2009
W-52	477	6.9	0.5	-28.7		-5.32				0.71108	Kresse & Hays, 2009
W-100							-22.12367175				Raley, 2018
							-22.2140055				Raley, 2018
W-101							-22.5229635				Raley, 2018
W-102							-23.6798985				Raley, 2018
W-103							-23.3324865				Raley, 2018
W-104							-24.10198088				Raley, 2018
W-105											Raley, 2018
W-106											Raley, 2018
W-107											Raley, 2018
W-109	232	6.3			8.6						NWIS

APPENDIX B

DB-Spreadsheet input data from sites that passed inspection in DB-WIN and produced successful calculated mass transfer NETPATH runs in NETPATH-WIN

Appendix B. Selected Model Input

Well Name	**Temp (°C)**	**pH (field)**	**Diss. 0_2** (mg/L)	**Alkalinity (Field) as $CaCO_3$**	**Tritium (TU)**	**Ca** (mg/L)	**Mg** (mg/L)	**Na** (mg/L)	**K** (mg/L)	**Cl** (mg/L)
Bratton2	20.4	7.4	0.6	149	3.22	44.7	5.92	14.3	n/a	2.57
Spring42	61.2	7	n/a	127	n/a	45.2	4.84	3.95	n/a	1.93
Spring46	57.4	7.2	n/a	132	n/a	45.4	4.83	4.01	n/a	1.86
Spring33	55.8	7.2	n/a	126	n/a	45.2	4.78	3.7	n/a	1.82
Spring25	62.5	7.1	n/a	132	n/a	45.3	4.83	3.92	n/a	1.83
Spring49	61.8	7.4	n/a	128	n/a	44.4	4.72	3.75	n/a	1.84
Spring9	62.1	7.5	n/a	131	0	44.7	4.79	3.88	n/a	1.77
Thornton	18.7	6.3	1	78	38.64	27.16	4.01	10.83	n/a	2.86
Spring8	61.9	7.5	n/a	132	1.923	44.8	4.78	3.88	n/a	1.84
Spring6	57.9	6.3	n/a	132	n/a	45.32	4.82	3.91	n/a	1.86
Spring17	54	7.3	n/a	124	-4.186	42	4.81	4.04	n/a	1.87
Spring47	61.3	7.2	n/a	138	n/a	45.9	4.88	3.91	n/a	1.84
Greer3	17.9	5.6	0.5	16	25.76	6.11	0.288	1.46	n/a	1.22
Greer2	18.3	5.1	0.9	14	25.76	0.01	0.007	9.17	n/a	1.71
HSSSCr	33.77	6.72	1.49	109	9.66	36.7	2.14	4.16	0.867	3.18
ARKSCr	20.4	7.1	0	109	1.3	34.7	2.8	2.9	1.5	2.3

Appendix B. Selected Model Input--Continued

Well Name	SO_4 (mg/L)	F (mg/L)	SiO_2 (mg/L)	B (mg/L)	Ba (mg/L)	Li (mg/L)	Sr (mg/L)	Fe (mg/L)	Mn (mg/L)	NO3-N (mg/L)
Bratton2	11.5	0.18	18.3	0.015	0.146	0.006	0.3245	0.158	0.0715	n/a
Spring42	7.79	0.14	39.8	0.011	0.139	0.0048	0.1055	0.018	0.223	n/a
Spring46	7.46	0.14	40.4	0.011	0.138	0.0047	0.1081	0.014	0.215	n/a
Spring33	7.66	0.15	41.3	0.012	0.143	0.005	0.1014	0.025	0.229	n/a
Spring25	7.48	0.13	39.7	0.01	0.141	0.0044	0.1055	0.02	0.226	n/a
Spring49	7.25	0.14	40.8	0.011	0.111	0.0049	0.098	<0.006	0.14	n/a
Spring9	7.53	0.13	39.8	0.011	0.075	0.0047	0.1067	<0.006	0.0011	n/a
Thornton	22.71	0.21	31.3	0.0097	0.0165	0.0167	0.2088	0.2164	1.115	n/a
Spring8	7.49	0.13	39.6	0.011	0.138	0.0047	0.1045	<0.006	0.213	n/a
Spring6	7.53	0.13	39.89	0.01077	0.086	0.0048	0.1054	<0.006	<0.0002	n/a
Spring17	7.6	0.13	39.7	0.01	0.081	0.0042	0.1024	<0.006	<0.0002	n/a
Spring47	7.32	0.13	39.7	0.011	0.138	0.0047	0.1064	<0.006	0.212	n/a
Greer3	3.6	<0.1	10.8	0.004	0.009	0.0004	0.0191	1.22	0.0227	n/a
Greer2	3.51	0.17	13.5	0.009	n/a	0.0014	0.0004	0.008	<0.0002	n/a
HSSSCr	4.78	0.18	22.2	0.0113	0.0106	n/a	0.083	<0.02	<0.0003	n/a
ARKSCr	5.31	0.2	13	0.0113	0.0106	n/a	0.08	1.2	0.13	0.1

Appendix B. Selected Model Input--Continued

Well Name	NH4-N (mg/L)	PO4-P (mg/L)	Sp. Cond. Field (µS/cm)	$\delta^{13}C$ TDIC	$\delta^{14}C$ (pmc)	δD ($^0/_{00}$)	$\delta^{18}O$ ($^0/_{00}$)	$^{87}Sr/^{86}Sr$	Al (mg/L)
Bratton2	n/a	n/a	295	-12.7	23.67	n/a	n/a	0.7103	0.0028
Spring42	n/a	n/a	286	-14.03	36.56	-28.9	-5.52	0.71192	0.0026
Spring46	n/a	n/a	297	-13.86	35.58	-28.6	-5.49	0.7119	0.0016
Spring33	n/a	n/a	298	-13.42	36.87	-30.2	-5.48	0.71191	0.0041
Spring25	n/a	n/a	302	-14.73	35.72	-29	-5.54	0.71196	0.0029
Spring49	n/a	n/a	290	-14.02	44.77	-29.7	-5.55	0.71192	0.0133
Spring9	n/a	n/a	311	-13.24	36.99	-28.2	-5.52	0.7119	0.0017
Thornton	n/a	n/a	235	-17.37	66.1	-28.1	-4.88	0.71383	0.0016
Spring8	n/a	n/a	284	-13.8	38.28	-28.3	-5.56	0.71189	0.0019
Spring6	n/a	n/a	302	-13.87	36.3	-28.6	-5.56	0.71196	0.00209
Spring17	n/a	n/a	290	-13.57	39.49	-29.4	-5.47	0.7119	0.0017
Spring47	n/a	n/a	316	-13.3	36.21	-29.5	-5.61	0.7119	0.002
Greer3	n/a	n/a	38	-22.14	78.6	-31.3	-5.63	0.71064	0.0053
Greer2	n/a	n/a	44	-23.09	85.2	-30.6	-5.58	0.7082	0.0051
HSSSCr	n/a	n/a	233	-23.7	98.9	-29.4	-5.58	0.71211	<0.02
ARKSCr	0.02	0.07	247	-23.7	98.9	-30	n/a	0.71211	0

APPENDIX C

NETPATH Outputs

Appendix C1. Non-Mixing Basics Geochemical System Outputs

Appendix C2. Non-Mixing Alkaline-Earth Geochemical System Outputs

Appendix C3. Non-Mixing Alkaline-Earth-plus-Sodium Geochemical System Outputs

Appendix C4. Mixing Outputs

Appendix C1. Non-Mixing Basics Geochemical System Outputs

Model Run No.	System	Initial Member	Final Member	Phases	Calculated Mass Transfer (mg/L) CO_2 gas	Calcite	SiO_2	Dolomite	Strontianite	Comp. $\delta^{13}C$ ($^0/_{00}$)	Observed $\delta^{13}C$ ($^0/_{00}$)	% error $\delta^{13}C$	Observed. $\delta^{14}C$ (pmc)
1	Basics	Bratton 2	Spring 25	Ca, Si		-0.235	0.356			-12.94	-14.73	12.19	35.72
2	Basics	Bratton 2	Spring 25	Dolo, Si			0.356	-0.117		-12.94	-14.73	12.19	35.72
3	Basics	Bratton 2	Spring 25	Stro, Si			0.356		-0.235	-12.94	-14.73	12.19	65.72
4	Basics	Greer3	Spring 25	Cal, Si		0.719	0.481			-16.82	-14.73	14.20	35.72
5	Basics	Bratton2	Spring 9	Cal, Si		-0.506	0.358			-13.17	-13.24	0.57	36.99
6	Basics	Bratton2	Spring 9	Dolo, Si			0.358	-0.253		-13.17	-13.24	4.00	36.99
7	Basics	Bratton2	Spring 9	Stro, Si			0.358		-0.506	-13.17	-13.24	0.57	36.99
8	Basics	Bratton2	Spring 8	Cal, Si		-0.486	0.355			-13.14	-13.8	4.75	38.28
9	Basics	Bratton2	Spring 8	Dolo, Si			0.355	-0.243		-13.14	-13.8	4.75	38.28
10	Basics	Bratton2	Spring 8	Stro, Si			0.355		-0.486	-13.14	-13.8	4.75	38.28
11	Basics	Bratton2	Spring 49	Cal, Si		-0.525	0.375			-13.19	-14.02	5.89	44.77
12	Basics	Bratton2	Spring 49	Dolo, Si			0.375	-0.263		-13.19	-14.02	5.89	44.77
13	Basics	Bratton2	Spring 49	Stro, Si			0.375		-0.525	-13.19	-14.02	5.89	44.77
14	Basics	Bratton2	Spring 47	Cal, Si		-0.185	0.356			-12.87	-13.3	3.20	36.21
15	Basics	Bratton2	Spring 47	Dolo, Si			0.356	-0.092		-12.87	-13.3	3.20	36.21
16	Basics	Bratton2	Spring 47	Stro, Si			0.356		-0.185	-12.87	-13.3	3.20	36.21
17	Basics	Bratton2	Spring 42	Cal, Si		-0.252	0.358			-12.96	-14.03	7.61	36.56
18	Basics	Bratton2	Spring 42	Dolo, Si			0.358	-0.126		-12.96	-14.03	7.61	36.56
19	Basics	Bratton2	Spring 42	Stro, Si			0.358		-0.252	-12.96	-14.03	7.61	36.56
20	Basics	HSSSCr	Spring 6	Cal, Si		2.013	0.295			-14.13	-13.87	1.86	36.3
21	Basics	ARKSCr	Spring 6	Cal, Si		2.425	0.448			-12.17	-13.87	12.28	36.3
22	Basics	Bratton2	Spring 46	Cal, Si		-0.317	0.368			-12.99	-13.86	6.25	35.58
23	Basics	Bratton2	Spring 46	Dolo, Si			0.368	-0.159		-12.99	-13.86	6.25	35.58
24	Basics	Bratton2	Spring 46	Stro, Si			0.368		-0.317	-12.99	-13.86	6.25	35.58
25	Basics	Bratton2	Spring 33	Cal, Si		-0.450	0.383			-13.12	-13.42	2.25	36.87
26	Basics	Bratton2	Spring 33	Dolo, Si			0.383	-0.225		-13.12	-13.42	2.25	36.87
27	Basics	Bratton2	Spring 33	Stro, Si			0.383		-0.450	-13.12	-13.42	2.25	36.87
28	Basics	Bratton2	Spring 17	Cal, Si		-0.552	0.356			-13.19	-13.57	2.79	39.49
29	Basics	Bratton2	Spring 17	Dolo, Si			0.356	-0.276		-13.19	-13.57	2.79	39.49
30	Basics	Bratton2	Spring 17	Stro, Si			0.356		-0.552	-13.19	-13.57	2.79	39.49

Appendix C1. Non-Mixing Basics Geochemical System Outputs-- Continued

Model Run No.	Original Data			Mass Balance (1990)			Tamers (1975)		Ingerson and Pearson (1964)		Mook (1972)		Fontes and Garnier (1979)		Eichinger (1983)	
	Ao TDC (pmc)	Ao TDC comp. (no decay)	Adjusted age (years)	Ao TDC (pmc)	Ao TDC comp. (no decay)	Adjusted age (years)	Ao TDC (pmc)	Adjusted age (years)	Ao TDC (pmc)	Adjusted age (years)	Ao TDC (pmc)	Adjusted age (years)	Ao TDC (pmc)	Adjusted age (years)	Ao TDC (pmc)	Adjusted age (years)
1	23.67	23.66	-3406	61.6	61.57	4501	54.03	3417	57.63	3990	57.55	4059	59.37	4252	55.53	3690
2	23.67	23.66	-3406	61.6	61.57	4501	54.03	3417	57.63	3950	57.55	3939	59.37	4196	55.53	3643
3	23.67	23.66	-3406	61.6	61.57	4501	54.03	3417	57.63	3950	57.55	3939	59.37	4196	55.53	3643
4	78.6	59.72	4248	94.42	71.74	5765	92.99	5632	92.99	5639	80.31	4426	93.03	5642	87.44	5129
5	23.67	23.65	-3698	61.6	61.54	4209	54.03	3124	57.63	3657	57.55	3646	59.37	3904	55.53	3351
6	23.67	23.65	-3698	64.6	61.54	4209	54.03	3124	57.63	3657	57.55	3646	59.37	394	55.53	3351
7	23.67	23.65	-3698	61.6	61.54	4209	54.03	3124	57.63	3657	57.55	3646	59.37	3904	55.53	3351
8	23.67	23.65	-3981	61.6	61.55	3926	54.03	2841	57.63	3374	57.55	3363	59.37	3621	55.53	3068
9	23.67	23.65	-3981	61.6	61.55	3926	54.03	2841	57.63	3374	57.55	3363	59.37	3621	55.53	3068
10	23.67	23.65	-3981	61.6	61.55	3926	54.03	2841	57.63	3374	57.55	3363	59.37	3621	55.53	3068
11	23.67	23.65	-5277	61.6	61.54	2630	54.03	1546	57.63	2079	57.55	2067	59.37	2325	55.53	1772
12	23.67	23.65	-5277	61.6	61.54	2630	54.03	1546	57.63	2079	57.55	2067	59.37	2325	55.53	1772
13	23.67	23.65	-5277	61.6	61.54	2630	54.03	1546	57.63	2079	57.55	2067	59.37	2325	55.53	1772
14	23.67	23.66	-3517	61.6	61.58	4390	54.03	3305	57.63	3823	57.55	3827	59.37	4085	55.53	3532
15	23.67	23.66	-3517	61.6	61.58	4390	54.03	3305	57.63	3838	57.55	3827	59.37	4085	55.53	3532
16	23.67	23.66	-3517	61.6	61.58	4390	54.03	3305	57.63	3838	57.55	3827	59.37	4085	55.53	3532
17	23.67	23.66	-3598	61.6	61.57	4309	54.03	3224	57.63	3757	57.55	3746	59.37	4004	55.53	3451
18	23.67	23.66	-3598	61.6	61.57	4309	54.03	3224	57.63	3757	57.55	3746	59.37	4004	55.53	3451
19	23.67	23.66	-3958	61.6	61.57	4309	54.03	3224	57.63	3757	57.55	3746	59.37	4004	55.53	3451
20	98.9	58.95	4009	67.88	40.46	897	63.37	329	98.84	4004	138.07	6767	112.14	5047	102.98	4343
21	98.9	50.77	2744	63.81	32.76	-849	57.52	-1706	98.84	2769	173.79	7434	118.88	4295	100.7	2923
22	23.67	23.66	-3374	61.6	61.57	4533	54.03	3448	57.63	3981	57.55	3970	59.37	4228	55.53	3675
23	23.67	23.66	-3374	61.6	61.57	4533	54.03	3448	57.63	3981	57.55	3970	59.37	4228	55.53	3675
24	23.67	23.66	-3374	61.6	61.57	4533	54.03	3448	57.63	3981	57.55	3970	59.37	4228	55.53	3675
25	23.67	23.65	-3671	61.6	61.55	4236	54.03	3152	57.63	3685	57.55	3674	59.37	3931	55.53	3378
26	23.67	23.65	-3671	61.6	61.55	4236	54.03	3152	57.63	3685	57.55	3674	59.37	3931	55.53	3378
27	23.67	23.65	-3671	61.6	61.55	4236	54.03	3152	57.63	3685	57.55	3674	59.37	3931	55.53	3378
28	23.67	23.65	-4239	61.6	61.54	3668	54.03	2583	57.63	3166	57.55	3105	59.37	3363	55.53	2809
29	23.67	23.65	-4239	61.6	61.54	3668	54.03	2583	57.63	3116	57.55	3105	59.37	3363	55.53	2809
30	23.67	23.65	-4239	61.6	61.54	3668	54.03	2583	57.63	3116	57.55	3105	59.37	3363	55.53	2809

Appendix C2. Non-Mixing Alkaline-Earth Geochemical System Outputs

Model Run No.	System	Initial Member	Final Member	Phases	Notes	Calculated Mass Transfer (mg/L)					Comp. $\delta^{13}C$ ($^{0}/_{00}$)	Observed $\delta^{13}C$ ($^{0}/_{00}$)	% error $\delta^{13}C$
						CO_2 gas	Calcite	SiO_2	Dolomite	Strontianite			
31	Alk. Earth	Thornton	Spring 25	Co2, Dolo, Stro, Cal, Si	Co2 diss./ con. Ig.	-0.844	0.419	0.140	0.0338	-0.0012	-14.00	-14.73	5.0
32	Alk. Earth	Bratton2	Spring 9	Co2, Dolo, Stro, Cal, Si	Co2 diss./ con. Ig.	-0.457	0.046	0.358	-0.0465	-0.0025	-11.97	-13.24	9.6
33	Alk. Earth	Thornton	Spring 9	Co2, Dolo, Stro, Cal, Si	Co2 diss./ con. Ig.	-1.099	0.406	0.142	0.0321	-0.0012	-13.51	-13.24	2.0
34	Alk. Earth	Bratton2	Spring 8	Co2, Dolo, Stro, Cal, Si	Co2 diss./ con. Ig.	-0.439	0.049	0.355	-0.0469	-0.0025	-11.98	-13.8	13.2
35	Alk. Earth	Thornton	Spring 8	Co2, Dolo, Stro, Cal, Si	Co2 diss./ con. Ig.	-1.081	0.409	0.138	0.0317	-0.0012	-13.53	-13.8	2.0
36	Alk. Earth	Bratton2	Spring 49	Co2, Dolo, Stro, Cal, Si	Co2 diss./ con. Ig.	-0.466	-0.042	0.375	-0.0494	-0.0026	-11.99	-14.02	14.5
37	Alk. Earth	Thornton	Spring 49	Co2, Dolo, Stro, Cal, Si	Co2 diss./ con. Ig.	-1.107	0.401	0.158	0.0292	-0.0013	-13.55	-14.02	3.3
38	Alk. Earth	Bratton2	Spring 47	Co2, Dolo, Stro, Cal, Si	Co2 diss./ con. Ig.	-0.169	0.073	0.356	-0.0428	-0.0025	-12.28	-13.3	7.6
39	Alk. Earth	Thornton	Spring 47	Co2, Dolo, Stro, Cal, Si	Co2 diss./ con. Ig.	-0.811	0.432	0.140	0.0358	-0.0012	-13.93	-13.3	4.7
40	Alk. Earth	Bratton2	Spring 42	Co2, Dolo, Stro, Cal, Si	Co2 diss./ con. Ig.	-0.218	0.057	0.358	-0.0444	-0.0025	-12.31	-14.03	12.2
41	Alk. Earth	Thornton	Spring 42	Co2, Dolo, Stro, Cal, Si	Co2 diss./ con. Ig.	-0.859	0.416	0.142	0.0342	-0.0012	-13.99	-14.03	0.3
42	Alk. Earth	Bratton2	Spring 46	Co2, Dolo, Stro, Cal, Si	Co2 diss./ con. Ig.	-0.287	0.062	0.368	-0.0449	-0.0025	-12.14	-13.86	12.4
43	Alk. Earth	Thornton	Spring 46	Co2, Dolo, Stro, Cal, Si	Co2 diss./ con. Ig.	-0.928	0.422	0.152	0.0338	-0.0012	-13.71	-13.86	1.1
44	Alk. Earth	Bratton2	Spring 33	Co2, Dolo, Stro, Cal, Si	Co2 diss./ con. Ig.	-0.413	0.059	0.383	-0.0469	-0.0025	-11.95	-13.42	10.9
45	Alk. Earth	Thornton	Spring 33	Co2, Dolo, Stro, Cal, Si	Co2 diss./ con. Ig.	-1.054	0.419	0.167	0.0317	-0.0012	-13.47	-13.42	0.4
46	Alk. Earth	Bratton2	Spring 17	Co2, Dolo, Stro, Cal, Si	Co2 diss./ con. Ig.	-0.436	-0.022	0.356	-0.0457	-0.0025	-12.13	-13.57	10.6
47	Alk. Earth	Thornton	Spring 17	Co2, Dolo, Stro, Cal, Si	Co2 diss./ con. Ig.	-1.078	0.337	0.140	0.0329	-0.0012	-13.66	-13.57	0.7

Appendix C2. Non-Mixing Alkaline-Earth Geochemical System Outputs--Continued

	Original Data			Mass Balance (1990)			Tamers (1975)		Ingerson and Pearson (1964)		Mook (1972)		Fontes and Garnier (1979)		Eichinger (1983)	
Model Run No.	Ao TDC (pmc)	Ao TDC comp. (no decay)	Adjusted age (years)	Ao TDC (pmc)	Ao TDC comp. (no decay)	Adjusted age (years)	Ao TDC (pmc)	Adjusted age (years)	Ao TDC (pmc)	Adjusted age (years)	Ao TDC (pmc)	Adjusted age (years)	Ao TDC (pmc)	Adjusted age (years)	Ao TDC (pmc)	Adjusted age (years)
31	66.1	56.8	3835	81.91	70.39	5608	76.74	5069	75.12	4893	59.7	2293	75.08	4888	70.48	4365
32	23.67	23.33	-3811	61.6	60.71	4096	54.03	3011	57.63	3544	57.55	3533	59.37	3791	55.53	3238
33	66.1	56.76	3540	81.91	70.34	5312	76.74	4774	75.12	4597	59.7	2698	75.08	4593	70.48	4070
34	23.67	23.3	-4102	61.6	60.65	3805	54.03	2720	57.63	3253	57.55	3242	59.37	3500	55.53	2946
35	66.1	56.75	3255	81.91	70.32	5028	76.74	4489	75.12	4313	59.7	2413	75.08	4308	70.48	3785
36	23.67	23.36	-5377	61.6	60.8	2530	54.03	1446	57.63	1979	57.55	1968	59.37	2225	55.53	1672
37	66.1	56.93	1986	81.91	70.54	3759	76.74	3220	75.12	3044	59.7	1144	75.08	3039	70.48	2516
38	23.67	23.13	-3704	61.6	60.2	4203	54.03	3118	57.63	3651	57.55	3640	59.37	3898	55.53	3345
39	66.1	56.57	3689	81.91	70.1	5461	76.74	4923	75.12	4746	59.7	2846	75.08	4742	70.48	4219
40	23.67	23.25	-3743	61.6	60.5	4164	54.03	3079	57.63	3612	57.55	3601	59.37	3859	55.53	3306
41	66.1	56.82	3645	81.91	70.41	5417	76.74	4879	75.12	4702	59.7	2803	75.08	4698	70.48	4175
42	23.67	23.21	-3532	61.6	60.4	4375	54.03	3290	57.63	3823	57.55	3812	59.37	4070	55.53	3517
43	66.1	56.67	3848	81.91	70.22	5620	76.74	5082	75.12	4905	59.7	3006	75.08	4901	70.48	4378
44	23.67	23.23	-3819	61.6	60.46	4088	54.03	3003	57.63	3536	57.55	3525	59.37	3783	55.53	3230
45	66.1	56.63	3547	81.91	70.17	5320	76.74	4781	75.12	4905	59.7	2705	75.08	4600	70.48	4077
46	23.67	23.7	-4222	61.6	61.67	3685	54.03	2601	57.63	3134	57.55	3123	59.37	3380	55.53	2827
47	66.1	57.98	3175	81.91	71.85	4947	76.74	4409	75.12	4232	59.7	2333	75.08	4228	70.48	3705

Appendix C3. Non-Mixing Alkaline-Earth-plus-Sodium Geochemical System Outputs

Model Run No.	System	Initial Member	Final Member	Phases	Notes	Calculated Mass Transfer (mg/L)								Comp. $\delta^{13}C$ ($^0/_{00}$)	Observed $\delta^{13}C$ ($^0/_{00}$)	% error $\delta^{13}C$
						CO_2 gas	Calcite	SiO_2	Dolomite	Strontianite	Ca/Na Exchange	Illite	NaCl			
48	Alk. Earth + Na	Bratton2	Spring 25	CO2, Si, Cal, Dolo, Stro, EX	Co2 diss.	0.02323	-0.166	0.356	-0.045	-0.0025	-0.226			-13.0489	-14.73	11.4
49	Alk. Earth + Na	Bratton2	Spring 25	CO2, Si, Cal, Dolo, Stro, EX, IL	Co2 diss.	0.18924		-1.968	-0.211	-0.0025	-0.226	0.664		-13.8379	-14.73	6.1
50	Alk. Earth + Na	Bratton2	Spring 25	CO2, Si, Cal, Dolo, Stro, EX, IL	Co2 diss.	0.04868	-0.141		-0.070	-0.0025	-0.226	0.102		-13.1726	-14.73	10.6
51	Alk. Earth + Na	Bratton2	Spring 25	Si, Cal, Dolo, Stro, EX, IL			-0.189	0.682	-0.022	-0.0025	-0.226	-0.093		-12.9351	-14.73	12.2
52	Alk. Earth + Na	Bratton2	Spring 25	Si, Cal, Dolo, Stro, EX, NaCl			-0.143	0.356	-0.045	-0.0025	-0.203		-0.046	-12.9351	-14.73	12.2
53	Alk. Earth + Na	Bratton2	Spring 25	Si, Cal, Stro, EX, IL, NaCl			-0.232	0.984		-0.0025	-0.247	-0.179	0.043	-12.9351	-14.73	12.2
54	Alk. Earth + Na	Bratton2	Spring 25	Si, Dolo, Stro, EX, IL, NaCl				-0.643	-0.116	-0.0025	-0.131	0.286	-0.189	-12.9351	-14.73	12.2
55	Alk. Earth + Na	Bratton2	Spring 25	Cal, Dolo, Stro, EX, IL, NaCl			-0.092		-0.070	-0.0025	-0.177	0.102	-0.097	-12.9351	-14.73	12.2
56	Alk. Earth + Na	Thornton	Spring 25	Si, Cal, Dolo, Stro, EX, IL			0.962	-9.570	-0.660	-0.00118	-0.150	2.774		-13.9357	-14.73	5.4
57	Alk. Earth + Na	Thornton	Spring 25	Si, Cal, Dolo, Stro, IL, NaCl			1.263	-11.676	-0.810	-0.00118	3.375		-0.301	-12.9701	-14.73	11.9
58	Alk. Earth + Na	Bratton2	Spring 9	Si, Cal, Dolo, Stro, EX, IL			0.051	-2.873	-0.277	-0.00248	-0.227	0.923		-12.9926	-13.24	1.9
59	Alk. Earth + Na	Bratton2	Spring 9	Si, Cal, Dolo, Stro, EX, NaCl			-0.411	0.358	-0.047	-0.00248	-0.457	0.462		-13.1651	-13.24	0.6
60	Alk. Earth + Na	Bratton2	Spring 9	Si, Cal, Stro, EX, IL, NaCl			-0.504	1.009		-0.00248	-0.504	-0.186	0.555	-13.1651	-13.24	0.6
61	Alk. Earth + Na	Bratton2	Spring 9	Si, Dolo, Stro, EX, IL, NaCl				-2.519	-0.252	-0.00248	-0.252	0.822	0.051	-13.1651	-13.24	0.6
62	Alk. Earth + Na	Bratton2	Spring 9	Cal, Dolo, Stro, EX, IL, NaCl			-0.360		-0.072	-0.00248	-0.432	0.102	0.410	-13.1651	-13.24	0.6
63	Alk. Earth + Na	Thornton	Spring 9	Si, Cal, Dolo, Stro, EX, IL			1.202	-13.125	-0.915	-0.00116	-0.151	3.790		-13.0336	-13.24	1.6
64	Alk. Earth + Na	Thornton	Spring 9	Si, Cal, Dolo, Stro, IL, NaCl			1.504	-15.241	-1.067	-0.00116		4.395	-0.302	-12.077	-13.24	8.8
65	Alk. Earth + Na	Thornton	Spring 8	Si, Cal, Dolo, Stro, EX, IL			1.187	-12.876	-0.898	-0.00119	-0.151	3.718		-13.0781	-13.8	5.2
66	Alk. Earth + Na	Thornton	Spring 8	Si, Cal, Dolo, Stro, IL, NaCl			1.489	-14.993	-1.049	-0.00119		4.323	-0.302	-12.1189	-13.8	12.2
67	Alk.Earth +Na	Bratton2	Spring 49	Si, Cal, Dolo, Stro, EX, IL			0.049	-2.936	-0.286	-0.00258	-0.230	0.946		-13.0281	-14.02	7.1
68	Alk.Earth +Na	Bratton2	Spring 49	Si, Cal, Dolo, Stro, EX, NaCl			-0.424	0.375	-0.049	-0.00258	-0.466		0.473	-13.1946	-14.02	5.9
69	Alk.Earth +Na	Bratton2	Spring 49	Si, Cal, Stro, EX, IL, NaCl			-0.523	1.066		-0.00258	-0.515	-0.198	0.572	-13.1946	-14.02	5.9
70	Alk.Earth +Na	Bratton2	Spring 49	Si, Dolo, Stro, EX, IL, NaCl				-2.594	-0.261	-0.00258	-0.254	0.848	0.049	-13.1946	-14.02	5.9
71	Alk.Earth +Na	Bratton2	Spring 49	Cal, Dolo, Stro, EX, IL, NaCl			-0.371		-0.076	-0.00258	-0.439	0.107	0.419	-13.1946	-14.02	5.9
72	Alk. Earth + Na	Thornton	Spring 49	Si, Cal, Dolo, Stro, EX, IL			1.200	-13.188	-0.924	-0.00126	-0.154	3.813		-13.0711	-14.02	6.8
73	Alk. Earth + Na	Thornton	Spring 49	Si, Cal, Dolo, Stro, IL, NaCl			1.508	-15.344	-1.078	-0.00126		4.429	-0.308	-12.0977	-14.02	13.7

Appendix C3. Non-Mixing Alkaline-Earth-plus-Sodium Geochemical System Outputs--Continued

		Original Data			Mass Balance (1990)			Tamers (1975)		Ingerson and Pearson (1964)		Mook (1972)		Fontes and Garnier (1979)		Eichinger (1983)	
Model Run No.	Observed $\delta^{14}C$ (pmc)	Ao TDC (pmc)	Ao TDC comp. (no decay)	Adjusted age (years)	Ao TDC (pmc)	Ao TDC comp. (no decay)	Adjusted age (years)	Ao TDC (pmc)	Adjusted age (years)	Ao TDC (pmc)	Adjusted age (years)	A_o TDC (pmc)	Adjusted age (years)	A_o TDC (pmc)	Adjusted age (years)	A_o TDC (pmc)	Adjusted age (years)
48	35.72	23.67	24.2259	-3210	61.6	61.86	4539	54.03	3469	57.63	3994	57.55	3983	59.37	4283	55.53	3692
49	35.72	23.67	28.16	-1967	61.6	63.82	4797	54.03	3819	57.63	4298	57.55	4288	59.37	4521	55.53	4022
50	35.72	23.67	24.84	-3002	61.6	61.16	4580	54.03	3525	57.63	4043	57.55	4032	59.37	4283	55.53	3745
51	35.72	23.67	23.66	-3406	61.6	61.57	4501	54.03	3417	57.63	3950	57.55	3939	59.37	4196	55.53	3643
52	35.72	23.67	23.66	-3406	61.6	61.57	4501	54.03	3417	57.63	3950	57.55	3939	59.37	4196	55.53	3643
53	35.72	23.67	23.66	-3406	61.6	61.57	4501	54.03	3417	57.63	3950	57.55	3939	59.37	4196	55.53	3643
54	35.72	23.67	23.66	-3406	61.6	61.57	4501	54.03	3417	57.63	3950	57.55	3939	59.37	4196	55.53	3643
55	35.72	23.67	23.66	-3406	61.6	61.57	4501	54.03	3417	57.63	3950	57.55	3939	59.37	4196	55.53	3643
56	35.72	66.1	48.66	2556	81.91	60.3	4328	76.74	3790	75.12	3613	59.7	1714	75.08	3609	70.48	3086
57	35.72	66.1	90.74	7707	81.91	112.45	9480	76.74	8942	75.12	8765	59.7	6865	75.08	8761	70.48	8238
58	36.99	23.67	23.25	-3840	61.6	60.5	4067	54.03	2982	57.63	3515	57.55	3504	59.37	3762	55.53	3209
59	36.99	23.67	23.65	-3698	61.6	61.54	4209	54.03	3124	57.63	3657	57.55	3646	59.37	3904	55.53	3351
60	36.99	23.67	23.65	-3698	61.6	61.54	4209	54.03	3124	57.63	3657	57.55	3646	59.37	3904	55.53	3351
61	36.99	23.67	23.65	-3698	61.6	61.54	4209	54.03	3124	57.63	3657	57.55	3646	59.37	3904	55.53	3351
62	36.99	23.67	23.65	-3698	61.6	61.54	4209	54.03	3124	57.63	3657	57.55	3646	59.37	3904	55.53	3351
63	36.99	66.1	44.28	1487	81.91	54.87	3259	76.74	2721	75.12	2545	59.7	645	75.08	2540	70.48	2017
64	36.99	66.1	135.59	10738	81.91	168.02	12511	76.74	11973	75.12	11796	59.7	9896	75.08	11792	70.48	11269
65	38.28	66.1	44.57	1257	81.91	55.22	3029	76.74	3790	75.12	3613	59.7	1714	75.08	3609	70.48	3086
66	38.28	66.1	130.77	10156	81.91	162.04	11928	76.74	8942	75.12	8765	59.7	6865	75.08	8761	70.48	8238
67	44.77	23.67	23.26	-5414	61.6	60.53	2493	54.03	1408	57.63	2941	57.55	1930	59.37	2188	55.53	1635
68	44.77	23.67	23.65	-5277	61.6	61.54	2630	54.03	1546	57.63	2079	57.55	2067	59.37	2325	55.53	1772
69	44.77	23.67	23.65	-5277	61.6	61.54	2630	54.03	1546	57.63	2079	57.55	2067	59.37	2325	55.53	1772
70	44.77	23.67	23.65	-5277	61.6	61.54	2630	54.03	1546	57.63	2079	57.55	2067	59.37	2325	55.53	1772
71	44.77	23.37	23.65	-5277	61.6	61.54	2630	54.03	1546	57.63	2079	57.55	2067	59.37	2325	55.53	1772
72	44.77	66.1	44.24	-99	81.91	54.82	1674	76.74	11136	75.12	959	59.7	-941	75.08	955	70.48	432
73	44.77	66.1	141.01	9484	81.91	174.73	11257	76.74	10542	75.12	8642	59.7	10537	75.08	10014	70.48	12906

Appendix C3. Non-Mixing Alkaline-Earth-plus-Sodium Geochemical System Outputs--Continued

Model Run No.	System	Initial Member	Final Member	Phases	Notes	Calculated Mass Transfer (mg/L)								Comp. $\delta^{13}C$ ($^0/_{00}$)	Observed $\delta^{13}C$ ($^0/_{00}$)	% error $\delta^{13}C$
						CO_2 gas	Calcite	SiO_2	Dolomite	Strontianite	Ca/Na Exchange	Illite	NaCl			
74	Alk. Earth + Na	Bratton2	Spring 47	CO2, Si, Cal, Dolo, Stro, EX	Co2 diss.	0.05673	-0.153	0.356	-0.043	-0.00249	-0.226			-13.146	-13.3	1.2
75	Alk. Earth + Na	Bratton2	Spring 47	CO2, Si, Cal, Stro, EX, IL	Co2 diss.	0.01394	-0.196	0.955	-0.196	-0.00249	-0.226	-0.171		-12.9413	-13.3	2.7
76	Alk. Earth + Na	Bratton2	Spring 47	CO2, Si, Dolo, Stro, EX, IL	Co2 diss.	0.21004		-1.790	-0.196	-0.00249	-0.226	0.613		-13.8567	-13.3	4.2
77	Alk. Earth + Na	Bratton2	Spring 47	CO2, Cal, Dolo, Stro, EX, IL	Co2 diss.	0.08218	-0.128		-0.068	-0.00249	-0.226	0.102		-13.2664	-13.3	0.3
78	Alk. Earth + Na	Bratton2	Spring 47	Si, Cal, Dolo, Stro, EX, IL			-0.210	1.151	0.014	-0.00249	-0.226	-0.227		-12.7869	-13.3	3.9
79	Alk. Earth + Na	Bratton2	Spring 47	Si, Cal, Dolo, Stro, EX, NaCl			-0.097	0.356	-0.043	-0.00249	-0.169		-0.113	-12.874	-13.3	3.2
80	Alk. Earth + Na	Bratton2	Spring 47	Si, Cal, Dolo, Stro, IL, NaCl			0.242	-2.014	-0.212	-0.00249		0.677	-0.452	-12.1433	-13.3	8.7
81	Alk. Earth + Na	Bratton2	Spring 47	Si, Cal, Stro, EX, IL, NaCl			-0.182	0.955		-0.00249	-0.212	-0.171	-0.028	-12.874	-13.3	3.2
82	Alk. Earth + Na	Bratton2	Spring 47	Si, Dolo, Stro, EX, IL, NaCl				-0.320	-0.091	-0.00249	-0.121	0.193	-0.210	-12.874	-13.3	3.2
83	Alk. Earth + Na	Bratton2	Spring 47	Cal, Dolo, Stro, EX, IL, NaCl			-0.046		-0.068	-0.00249	-0.144	0.102	-0.164	-12.874	-13.3	3.2
84	Alk. Earth + Na	Thornton	Spring 47	Si, Cal, Dolo, Stro, EX, IL			0.941	-9.101	-0.624	-0.00117	-0.151	2.640		-13.9343	-13.3	4.8
85	Alk. Earth + Na	Thornton	Spring 47	Si, Cal, Dolo, Stro, IL, NaCl			1.243	-11.208	-0.775	-0.00117		3.242	-0.301	-12.9585	-13.3	2.6
86	Alk. Earth + Na	Bratton 2	Spring 42	CO2, Si, Cal, Dolo, Stro, EX	Co2 diss.	0.00745	-0.168	0.358	-0.044	-0.0025	-0.225			-12.9989	-14.03	7.3
87	Alk. Earth + Na	Bratton 2	Spring 42	CO2, Si, Dolo, Stro, EX, IL	Co2 diss.	0.17572		-1.998	-0.213	-0.0025	-0.225	0.673		-13.8097	-14.03	1.6
88	Alk. Earth + Na	Bratton 2	Spring 42	CO2, Cal, Dolo, Stro, EX, IL	Co2 diss.	0.03302	-0.143		-0.070	-0.0025	-0.225	0.102		-13.1249	-14.03	6.5
89	Alk. Earth + Na	Bratton 2	Spring 42	Si, Cal, Dolo, Stro, EX, IL			-0.176	0.462	-0.037	-0.0025	-0.225	-0.030		-12.9619	-14.03	7.6
90	Alk. Earth + Na	Bratton 2	Spring 42	Si, Cal, Dolo, Stro, EX, NaCl			-0.161	0.358	-0.044	-0.0025	-0.218		-0.015	-12.9619	-14.03	7.6
91	Alk. Earth + Na	Bratton 2	Spring 42	Si, Cal, Dolo, Stro, IL, NaCl			0.275	-2.690	-0.262	-0.0025		0.871	-0.450	-12.1472	-14.03	13.4
92	Alk. Earth + Na	Bratton 2	Spring 42	Si, Cal, Stro, EX, IL, NaCl			-0.250	0.980			-0.262	-0.178	0.074	-12.9619	-14.03	7.6
93	Alk. Earth + Na	Bratton 2	Spring 42	Si, Dolo, Stro, EX, IL, NaCl				-0.768	-0.125	-0.0025	-0.137	0.322	-0.176	-12.9619	-14.03	7.6
94	Alk. Earth + Na	Bratton 2	Spring 42	Cal, Dolo, Stro, EX, IL, NaCl			-0.110		-0.070	-0.0025	-0.192	0.102	-0.066	-12.9619	-14.03	7.6
95	Alk. Earth + Na	Thornton	Spring 42	Si, Cal, Dolo, Stro, EX, IL			0.976	-9.789	-0.675	-0.00118	-0.150	2.837		-13.9367	-14.03	0.7
96	Alk. Earth + Na	Thornton	Spring 42	Si, Cal, Dolo, Stro, IL, NaCl			1.275	-11.884	-0.825	-0.00118		3.436	-0.299	-12.9835	-14.03	7.5
97	Alk. Earth + Na	Bratton2	Spring 46	CO2, Si, Dolo, Stro, EX, IL	Co2 diss.	0.09825	-0.206	-1.894	-0.002	-0.22386		0.646		-13.4658	-13.86	2.8
98	Alk. Earth + Na	Bratton2	Spring 46	Si, Cal, Dolo, Stro, EX, IL			-0.098	-0.518	-0.108	-0.00247	-0.224	0.253		-12.9932	-13.86	6.3
99	Alk. Earth + Na	Bratton2	Spring 46	Si, Cal, Dolo Stro, EX, NaCl			-0.225	0.368	-0.045	-0.00247	-0.287		0.127	-12.9932	-13.86	6.3
100	Alk. Earth + Na	Bratton2	Spring 46	Si, Cal, Dolo, Stro, IL, NaCl			0.349	-3.652	-0.332	-0.00247		1.149	-0.448	-11.9151	-13.86	14.0
101	Alk. Earth + Na	Bratton2	Spring 46	Si, Cal, Stro, EX, IL, NaCl			-0.315	0.996		-0.00247	-0.332	-0.179	0.216	-12.9932	-13.86	6.3
102	Alk. Earth + Na	Bratton2	Spring 46	Si, Dolo, Stro, EX, IL, NaCl				-1.206	-0.157	-0.00247	-0.175	0.450	-0.098	-12.9932	-13.86	6.3
103	Alk. Earth + Na	Bratton2	Spring 46	Cal, Dolo, Stro, EX, IL, NaCl			-0.172		-0.071	-0.00247	-0.261	0.105	0.074	-12.9932	-13.86	6.3
104	Alk. Earth + Na	Thornton	Spring 46	Si, Cal, Dolo, Stro, EX, IL			1.053	-10.770	-0.746	-0.00115	-0.148	3.120		-13.5493	-13.86	2.2
105	Alk. Earth + Na	Thornton	Spring 46	Si, Cal, Dolo, Stro, IL, NaCl			1.350	-12.847	-0.895	-0.00115		3.714	-0.297	-12.5954	-13.86	9.1

Appendix C3. Non-Mixing Alkaline-Earth-plus-Sodium Geochemical System Outputs--Continued

		Original Data			Mass Balance (1990)			Tamers (1975)		Ingerson and Pearson (1964)		Mook (1972)		Fontes and Garnier (1979)		Eichinger (1983)	
Model Run No.	Observed $\delta^{14}C$ (pmc)	Ao TDC (pmc)	Ao TDC comp. (no decay)	Adjusted age (years)	Ao TDC (pmc)	Ao TDC comp. (no decay)	Adjusted age (years)	Ao TDC (pmc)	Adjusted age (years)	Ao TDC (pmc)	Adjusted age (years)	A_o TDC (pmc)	Adjusted age (years)	A_o TDC (pmc)	Adjusted age (years)	A_o TDC (pmc)	Adjusted age (years)
74	36.21	23.67	25.03	-3053	61.6	62.26	4481	54.03	3430	57.63	3946	57.55	3935	59.37	4185	55.53	3649
75	36.21	23.67	24	-3400	61.6	61.75	4412	54.03	3336	57.63	3865	57.55	3854	59.37	4110	55.53	3561
76	36.21	23.67	28.6	-1951	61.6	64.05	4714	54.03	3746	57.63	4220	57.55	4210	59.37	4440	55.53	3647
77	36.21	23.67	25.63	-2856	61.6	62.56	4521	54.03	3484	57.63	3993	57.55	3982	59.37	4229	55.53	3700
78	36.21	23.67	23.45	-3591	61.6	61.03	4316	54.03	3231	57.63	3764	57.55	3753	59.37	4011	55.53	3458
79	36.21	23.67	23.66	-3517	61.6	61.58	4390	54.03	3305	57.63	3838	57.55	3827	59.37	4085	55.53	3532
80	36.21	23.67	38.2	443	61.6	99.42	8350	54.03	7265	57.63	7798	57.55	7787	59.37	8045	55.53	7492
81	36.21	23.67	23.66	-3517	61.6	61.58	4390	54.03	3305	57.63	3838	57.55	3827	59.37	4085	55.53	3532
82	36.21	23.67	23.66	-3517	61.6	61.58	4390	54.03	3305	57.63	3838	57.55	3827	59.37	4085	55.53	3532
83	36.21	23.67	23.66	-3517	61.6	61.58	4390	54.03	3305	57.63	3838	57.55	3827	59.37	4085	55.53	3532
84	36.21	66.1	49.11	2520	81.91	60.86	4292	76.74	3754	75.12	3577	59.7	1678	75.08	3573	70.48	3050
85	36.21	66.1	85.49	7102	81.91	105.94	8874	76.74	8336	75.12	8159	59.7	6259	75.08	8155	70.48	7632
86	36.56	23.67	23.84	-3535	61.6	61.66	4321	54.03	3241	57.63	3722	57.55	3760	59.37	4017	55.53	3466
87	36.56	23.67	27.85	-2248	61.6	63.66	4585	54.03	3600	57.63	4083	57.55	4073	59.37	4307	55.53	3805
88	36.56	23.67	24.46	-3321	61.6	61.97	4363	54.03	3292	57.63	3821	57.55	3810	59.37	4063	55.53	3520
89	36.56	23.67	23.66	-3598	61.6	61.57	4309	54.03	3224	57.63	3757	57.55	3746	59.37	4004	55.53	3451
90	36.56	23.67	23.66	-3598	61.6	61.57	4309	54.03	3224	57.63	3757	57.55	3746	59.37	4004	55.53	3451
91	36.56	23.67	143.78	11320	61.6	374.21	19227	54.03	18142	57.63	18675	57.55	18664	59.37	18922	55.53	18369
92	36.56	23.67	23.66	-3598	61.6	61.57	4309	54.03	3224	57.63	3757	57.55	3746	59.37	4004	55.53	3451
93	36.56	23.67	23.66	-3598	61.6	61.57	4309	54.03	3224	57.63	3757	57.55	3746	59.37	4004	55.53	3451
94	36.56	23.67	23.66	-3598	61.6	61.57	4309	54.03	3224	57.63	3757	57.55	3746	59.37	40004	55.53	3451
95	36.56	66.1	48.4	2320	81.91	59.98	4092	76.74	3554	75.12	3377	59.7	1478	75.08	3373	70.48	2850
96	36.56	66.1	92.7	7691	81.91	114.87	9464	76.74	8926	75.12	8749	59.7	6849	75.08	8756	70.48	8222
97	35.58	23.67	26.06	-2575	61.6	62.77	4692	54.03	3666	57.63	4169	57.55	4159	59.37	4403	55.53	3880
98	35.58	23.67	23.66	-3374	61.6	61.57	4533	54.03	3448	57.63	3981	57.55	3970	59.37	4228	55.53	3675
99	35.58	23.67	23.66	-3374	61.6	61.57	4533	54.03	3448	57.63	3981	57.55	3970	59.37	4228	55.53	3675
100	35.58	23.67	189.56	13829	61.6	493.34	21736	54.03	20652	57.63	21185	57.55	21174	59.37	21431	55.53	20878
101	35.58	23.67	23.66	-3374	61.6	61.57	4533	54.03	3448	57.63	3981	57.55	3970	59.37	4228	55.53	3675
102	35.58	23.67	23.66	-3374	61.6	61.57	4533	54.03	3448	57.63	3981	57.55	3970	59.37	4228	55.53	3675
103	35.58	23.67	23.66	-3374	61.6	61.57	4533	54.03	3448	57.63	3981	57.55	3970	59.37	4228	55.53	3675
104	44.77	66.1	44.24	-99	81.91	54.82	1674	76.74	3546	75.12	3370	59.7	1470	75.08	3366	70.48	2843
105	44.77	66.1	141.1	9484	81.91	174.73	11257	76.74	9823	75.12	9646	59.7	7746	75.08	9642	70.48	9119

Appendix C3. Non-Mixing Alkaline-Earth-plus-Sodium Geochemical System Outputs--Continued

Model Run No.	System	Initial Member	Final Member	Phases	Notes	Calculated Mass Transfer (mg/L)								Comp. $\delta^{13}C$ ($^0/_{00}$)	Observed $\delta^{13}C$ ($^0/_{00}$)	% error $\delta^{13}C$
						CO_2 gas	Calcite	SiO_2	Dolomite	Strontianite	Ca/Na Exchange	Illite	NaCl			
106	Alk. Earth + Na	Bratton2	Spring 33	Si, Cal, Dolo, Stro, EX, IL			0.011	-2.166	-0.229	-0.00254	-0.231	0.728		-13.0818	-13.42	2.5
107	Alk. Earth + Na	Bratton2	Spring 33	Si, Cal, Dolo, Stro, EX, NaCl			-0.353	0.383	-0.047	-0.00254	-0.413		0.364	-13.1184	-13.42	2.2
108	Alk. Earth + Na	Bratton2	Spring 33	Si, Cal, Dolo, Stro, IL, NaCl			0.472	-5.395	-0.460	-0.00254		1.651	-0.461	-11.6435	-13.42	13.2
109	Alk. Earth + Na	Bratton2	Spring 33	Si, Cal, Stro, EX, IL, NaCl			-0.447	1.040		-0.00254	-0.460	-0.188	0.458	-13.1184	-13.42	2.2
110	Alk. Earth + Na	Bratton2	Spring 33	Si, Dolo, Stro, EX, IL, NaCl				-2.090	-0.224	-0.00254	-0.236	0.707	0.011	-13.1184	-13.42	2.2
111	Alk. Earth + Na	Bratton2	Spring 33	Cal, Dolo, Stro, EX, IL, NaCl			-0.299		-0.074	-0.00254	-0.385	0.109	0.309	-13.1184	-13.42	2.2
112	Alk. Earth + Na	Thornton	Spring 33	Si, Cal, Dolo, Stro, EX, IL			1.162	-12.418	-0.867	-0.00122	-0.155	3.596		-13.1888	-13.42	1.7
113	Alk. Earth + Na	Thornton	Spring 33	Si, Cal, Dolo, Stro, IL, NaCl			-0.635	0.167	0.032	-0.00122	-1.054		1.798	-12.2072	-13.42	9.0
114	Alk. Earth + Na	Bratton2	Spring 17	CO2, Si, Dolo, Stro, EX, IL	Co2 diss.	0.03186		-3.073	-0.296	-0.00253	-0.222	0.980		-13.3497	-13.57	1.6
115	Alk. Earth + Na	Bratton2	Spring 17	Si, Cal, Dolo, Stro, EX, IL			-0.032	-2.627	-0.259	-0.00253	-0.223	0.852		-13.1917	-13.57	2.8
116	Alk. Earth + Na	Bratton2	Spring 17	Si, Cal, Dolo, Stro, EX, NaCl			-0.458	0.356	-0.046	-0.00253	-0.436	0.426		-13.1917	-13.57	2.8
117	Alk. Earth + Na	Bratton2	Spring 17	Si, Cal, Dolo, Stro, IL, NaCl			0.415	-5.752	-0.482	0.00253		1.745	-0.446	-11.8352	-13.57	12.8
118	Alk. Earth + Na	Bratton2	Spring 17	Si, Cal, Stro, EX, IL, NaCl			-0.549	0.996		-0.00253	-0.048	-0.183	0.518	-13.1917	-13.57	2.8
119	Alk. Earth + Na	Bratton2	Spring 17	Si, Dolo, Stro, EX, IL, NaCl				-2.850	-0.275	-0.00253	-0.207	0.916	-0.032	-13.1917	-13.57	2.8
120	Alk. Earth + Na	Bratton2	Spring 17	Cal, Dolo, Stro, EX, IL, NaCl		-0.407			-0.071	-0.00253	-0.411	0.102	0.375	-13.1917	-13.57	2.8
121	Alk. Earth + Na	Thornton	Spring 17	Si, Cal, Dolo, Stro, EX, IL		1.120	-12.878		-0.897	-0.00121	-0.148	3.720		-13.2673	-13.57	2.2
122	Alk. Earth + Na	Thornton	Spring 17	Si, Cal, Dolo, Stro, Il, NaCl		1.145	-14.946		-1.045	-0.00121		4.310	-0.295	-12.2939	-13.57	9.4

Appendix C3. Non-Mixing Alkaline-Earth-plus-Sodium Geochemical System Outputs--Continued

		Original Data			Mass Balance (1990)			Tamers (1975)		Ingerson and Pearson (1964)		Mook (1972)		Fontes and Garnier (1979)		Eichinger (1983)	
Model Run No.	Observed $\delta^{14}C$ (pmc)	Ao TDC (pmc)	Ao TDC comp. (no decay)	Adjusted age (years)	Ao TDC (pmc)	Ao TDC comp. (no decay)	Adjusted age (years)	Ao TDC (pmc)	Adjusted age (years)	Ao TDC (pmc)	Adjusted age (years)	A_o TDC (pmc)	Adjusted age (years)	A_o TDC (pmc)	Adjusted age (years)	A_o TDC (pmc)	Adjusted age (years)
106	36.87	23.67	23.56	-3701	61.6	61.33	4206	54.03	3122	57.63	3655	57.55	3643	59.37	3901	55.53	3348
107	36.87	23.67	23.65	-3671	61.6	61.55	4236	54.03	3152	57.63	3685	57.55	3674	59.37	3931	55.53	3378
108	36.87	23.67	7180.61	43580	61.6	18687.86	51487	54.03	50402	57.63	50935	57.55	50924	59.37	51182	55.53	50628
109	36.87	23.67	23.65	-3671	61.6	61.55	4236	54.03	3152	57.63	3685	57.55	3674	59.37	3931	55.53	3378
110	36.87	23.67	23.65	-3671	61.6	61.55	4236	54.03	3152	57.63	3685	57.55	3674	59.37	3931	55.53	3378
111	36.87	23.67	23.65	-3671	61.6	61.55	4236	54.03	3152	57.63	3685	57.55	3674	59.37	3931	55.53	3378
112	36.87	66.1	45.04	1655	81.91	55.81	3428	76.74	2889	75.12	2713	59.7	813	75.08	2708	70.48	2185
113	36.87	66.1	122.37	9917	81.91	151.64	11690	76.74	11152	75.12	10975	59.7	9075	75.08	10971	70.48	10448
114	39.49	23.67	24.47	-3958	61.6	61.95	3722	54.03	2658	57.63	3181	57.55	3170	59.37	3423	55.53	2880
115	39.49	23.67	23.65	-4239	61.6	61.54	3668	54.03	2583	57.63	3116	57.55	3105	59.37	3363	55.53	2809
116	39.49	23.67	23.65	-4239	61.6	61.54	3668	54.03	2583	57.63	3116	57.55	3105	59.37	3363	55.53	2809
117	39.49	23.67	7.42	-13823	61.6	19.3	-5916	54.03	-7001	57.63	-6468	57.55	-6479	59.37	-6221	55.53	-6774
118	39.49	23.67	23.65	-4239	61.6	61.54	3668	54.03	2583	57.63	3116	57.55	3105	59.37	3363	55.53	2809
119	39.49	23.67	23.65	-4239	61.6	61.54	3688	54.03	2583	57.63	3116	57.55	3105	59.37	3363	55.53	2809
120	39.49	23.67	23.65	-4239	61.6	61.54	3668	54.03	2583	57.63	3116	57.55	3105	59.37	3363	55.53	2809
121	39.49	66.1	45.37	1148	81.91	56.22	2921	76.74	2382	75.12	2206	59.7	306	75.08	2201	70.48	1678
122	39.49	66.1	156.72	11395	81.91	194.21	13168	76.74	12629	75.12	12453	59.7	10553	75.08	12448	70.48	11925

Appendix C4. Mixing Scenario Outputs

Model Run No.	System	Initial Member 1	Initial Member 2	Initial Member 3	Final Member	Phases	Notes
123	Basics	Greer3	Bratton2	N/a	Spring 17	Init1, Init2, Si	Diss.1, 2 2(F)
124	Basics	Greer3	Bratton2	N/a	Spring 25	Init1, Init 2, Si	Diss. 1, Diss. 2, 2(F)
125	Basics	Bratton2	ARKSCr	N/a	Spring 25	Init1, Init2, Si	Diss 1&2
126	Basics	Bratton2	Greer3	HSSSCr	Spring 25	Init1, Init2, Init3, Si	Diss1,2, &3
127	Basics	Bratton2	Greer3	ARKSCr	Spring 25	Init1, Init2, Init3, Si	Diss1,2, &3
128	Alk. Earth	Greer3	Bratton2	N/a	Spring 17	Init1, Init2, Co2, Dolo, Stro, Si	Diss.1&2 2(F), Co2. diss, con. Ig.
129	Alk. Earth	Bratton2	Thornton	Greer3	Spring 17	Init1, Init2, Init3, Co2, Dolo, Stro	Diss.1,2&3 3(F), Co2. diss, con. Ig.
130	Alk. Earth	Bratton2	Thornton	Greer3	Spring 17	Init1, Init2, Init3, Co2, Stro, Cal	Diss.1,2&3 3(F), Co2. diss, con. Ig.
131	Alk. Earth	Bratton2	Thornton	N/a	Spring 17	Init1, Init2, Co2, Dolo, Stro, Si	Diss.1&2 2(F), Co2. diss, con. Ig.
132	Alk. Earth	Bratton2	Thornton	N/a	Spring 17	Init1, Init2, Co2, Stro, Cal, Si	Diss.1&2 2(F), Co2. diss, con. Ig.
133	Alk. Earth	Greer3	Bratton2	N/a	Spring 25	Init1, Init2, Co2, Stro, Cal, Si	Diss.1, Diss.2 2(F), Co2 diss
134	Alk. Earth	Bratton2	Thornton	Greer3	Spring 25	Init1, Init2, Init3, Co2, Stro, Cal	Diss.1,2, &3 3(F), Co2 diss
135	Alk. Earth	Bratton2	Thornton	N/a	Spring 25	Init 1, Init2, Co2, Stro, Cal, Si	Diss.1,2 2(F), Co2 diss, con. Ig.
136	Alk. Earth	Bratton2	HSSSCr	N/a	Spring 25	Init1, Init2, Co2, Stro, Cal, Si	Diss.1,2 2(F), Co2 diss, con. Ig.
137	Alk. Earth + Na	Greer3	Thornton	N/a	Spring 17	Init1, Init2, Si, Cal, Dolo, EX, IL	Diss.1&2 2(F)
138	Alk. Earth + Na	Greer3	Thornton	N/a	Spring 17	Init1, Init2, Si, Cal, Dolo, IL, NaCl	Diss.1&2 2(F)
139	Alk. Earth +Na	Greer3	Bratton2	N/a	Spring 17	Init1, Init2, Si, Cal, Dolo, EX, IL	Diss.1&2 2(F)
140	Alk. Earth +Na	Greer3	Bratton2	N/a	Spring 17	Init1, Init2, Si, Cal, Dolo, IL, NaCl	Diss.1&2 2(F)
141	Alk. Earth +Na	Greer3	Bratton2	N/a	Spring 17	Init1, Init2, Si, Cal, Stro, EX, NaCl	Diss.1&2 2(F)
142	Alk. Earth +Na	Greer3	Bratton2	N/a	Spring 17	Init1, Init2, Si, Dolo, Stro, EX, IL	Diss.1&2 2(F)
143	Alk. Earth +Na	Greer3	Bratton2	N/a	Spring 17	Init1, Init2, Cal, Stro, EX, IL, NaCl	Diss.1&2 2(F)
144	Alk. Earth + Na	Bratton2	Thornton	Greer3	Spring 17	Init1, Init2, Init3, Cal, Stro, EX, IL, NaCl	Diss.1,2&3 3(F)
145	Alk. Earth + Na	Bratton2	Thornton	N/a	Spring 17	Init1, Init2, Si, Dolo, Stro, EX, NaCl	Diss.1&2 2(F)
146	Alk. Earth + Na	Greer3	Thornton	N/a	Spring 25	Init1, Init2, Si, Cal, Dolo, EX, IL	Diss. 1, 2 2(F)
147	Alk. Earth + Na	Greer3	Thornton	N/a	Spring 25	Init1, Init2, Si, Cal, Dolo, IL, NaCl	Diss. 1, 2 2(F)

Appendix C4. Mixing Scenario Outputs--Continued

Model Run No.	Initial Water 1	Initial Water 2	Initial Water 3	Calculated Mass Transfer (mg/L) SiO_2	CO_2 gas	Dolomite	Strontianite	Calcite	Ca/Na Exchange	Illite	NaCl	Comp. $\delta^{13}C$ ($^0/_{00}$)	Observed $\delta^{13}C$ ($^0/_{00}$)	% error
123	0.421	0.579		0.429								-13.34	-13.57	1.69
124	0.754	0.246		0.387								-14.47	-14.73	1.79
125	0.649	0.351		0.387								-16.00	-14.73	8.62
126	0.754	0.246	0.000	0.387								-14.47	-14.73	1.79
127	0.754	0.246	0.000	0.387								-14.47	-14.73	1.79
128	0.970	0.029		0.360	-0.4436	-0.039	-0.00243					-12.28	-13.57	9.49
129	0.970	0.000	0.030		-0.4436	-0.039	-0.00243					-12.28	-13.57	9.49
130	0.803	0.000	0.197		-0.4845		-0.00184	0.1225				-12.75	-13.57	6.07
131	0.940	0.061		0.343	-0.4751	-0.041	-0.00245					-12.33	-13.57	9.11
132	0.419	0.581		0.231	-0.8090		-0.00176	0.1870				-13.32	-13.57	1.84
133	0.806	0.194		0.380	-0.2499		-0.00183	0.2014				-12.87	-14.73	12.65
134	0.806	0.000	0.194	0.380	-0.2499		-0.00183	0.2014				-12.87	-14.73	12.65
135	0.429	0.571		0.233	-0.5685		-0.00175	0.2648				-13.53	-14.73	8.14
136	0.712	0.288		0.338	-0.2316		-0.00171	0.0726				-15.05	-14.73	2.18
137	0.440	0.560		-11.173		-0.703		1.3342	-0.034	3.287		-13.04	-13.57	3.89
138	0.440	0.560		-11.642		-0.737		1.4012		3.421	-0.067	-12.79	-13.57	5.76
139	0.273	0.727		-7.867		-0.471		1.0837	-0.020	2.375		-13.21	-13.57	2.63
140	0.273	0.727		-8.148		-0.491		1.1240		2.456	-0.040	-13.05	-13.57	3.84
141	0.803	0.197		0.381			-0.00184	-0.3620	-0.484		0.633	-14.43	-13.57	6.31
142	0.979	0.021		-2.777		-0.265	-0.00246		-0.217	0.896		-13.31	-13.57	1.88
143	0.681	0.319					-0.00142	-0.2460	-0.486	0.113	0.704	-15.28	-13.57	12.57
144	0.681	0.000	0.319				-0.00142	-0.2460	-0.486	0.113	0.704	-15.28	-13.57	12.57
145	0.972	0.028		-2.911		-0.276	-0.00249		-0.221		1.259	-13.33	-13.57	1.78
146	0.454	0.546		-7.907		-0.471		1.1715	-0.039	2.352		-13.82	-14.73	6.18
147	0.454	0.546		-8.452		-0.510		1.2494		2.508	-0.078	-13.53	-14.73	8.15

Appendix C4. Mixing Scenario Outputs--Continued

		Original Data			Mass Balance (1990)			Tamers (1975)		Ingerson and Pearson (1964)		Mook (1972)		Fontes and Garnier (1979)		Eichinger (1983)	
Model Run No.	Observed $\delta^{14}C$ (pmc)	Ao TDC (pmc)	Ao TDC comp. (no decay)	Adjusted age (years)	Ao TDC (pmc)	Ao TDC comp. (no decay)	Adjusted age (years)	Ao TDC (pmc)	Adjusted age (years)	Ao TDC (pmc)	Adjusted age (years)	Ao TDC (pmc)	Adjusted age (years)	Ao TDC (pmc)	Adjusted age (years)	Ao TDC (pmc)	Adjusted age (years)
123	39.94	50.68	50.68	2062	77.74	77.85	5599	73.15	5096	75.01	5304	68.74	4582	75.92	5403	71.22	4875
124	35.72	33.95	33.95	-420	67.74	67.74	5291	61.31	4465	64.24	4852	61.81	4533	65.67	5034	61.5	4492
125	35.72	46.23	46.23	2133	62.26	62.26	4594	55.08	3579	69.99	5560	92.41	7858	77.22	6373	69.08	5452
126	35.72	33.95	33.95	-420	67.74	67.74	5291	61.31	4465	64.24	4852	61.81	4533	65.67	5034	61.5	4492
127	35.72	33.95	33.95	-420	67.74	67.74	5291	61.31	4465	64.24	4852	61.81	4533	65.67	5034	61.5	4492
128	39.49	24.83	24.86	-3825	62.3	62.37	3779	54.85	2726	58.37	3241	58.03	3192	60.08	3480	53.2	2928
129	39.49	24.83	24.86	-3825	62.3	62.37	3779	54.85	2726	58.37	3241	58.03	3192	60.08	3480	56.2	2928
130	39.49	31.77	61.17	-1957	66.44	65.18	4142	59.76	3267	62.84	3682	60.9	3423	64.33	3876	60.3	3332
131	39.49	26.33	26.36	-3340	62.87	62.96	3856	55.45	2817	58.72	3291	57.68	3143	60.36	3518	56.47	2967
132	39.49	48.72	47.34	1499	73.59	71.51	4909	67.44	4187	67.95	4251	58.82	3057	68.65	4334	64.35	3801
133	35.72	31.61	61.26	-1103	66.35	65.6	5025	59.65	4145	58.98	4563	60.84	4308	64.24	4758	60.14	4213
134	65.72	31.61	31.26	-1103	66.35	65.6	5025	59.65	4145	62.74	4563	60.84	4308	64.24	4758	60.14	4213
135	35.72	48.27	46.83	2239	73.38	71.19	5701	67.2	4974	67.77	5044	58.79	3870	68.48	5130	64.2	4596
136	35.72	44.1	43.66	1660	63.31	62.67	4648	56.56	3717	68.82	5338	79.42	6522	73.7	5905	68.42	5290
137	39.49	71.89	43.83	863	87.71	53.48	2507	84.24	2173	83.41	2091	69.25	553	83.4	2090	78.34	1573
138	39.49	71.89	76.04	5416	87.71	92.77	7060	84.24	6726	93.41	6644	69.25	5107	83.4	6644	78.34	6126
139	39.49	59.5	39.17	-67	83.01	54.65	2686	79.4	2318	80.7	2452	72.4	1555	81.33	2517	76.34	1994
140	39.49	59.5	54.01	2589	83.01	75.35	5341	79.4	4973	80.7	5108	72.4	421	81.33	5172	76.34	4649
141	39.49	31.77	31.75	-1804	66.44	66.4	4295	59.76	3420	62.84	3835	60.9	3576	64.33	4029	60.23	3485
142	39.49	24.48	24.45	-3962	62.09	62.03	3732	54.6	2670	58.15	3191	57.88	3153	59.87	3432	56	2879
143	39.49	37.31	37.29	-473	69.75	69.72	4699	63.69	3947	66.41	4293	63.2	3884	67.73	4456	63.45	3917
144	39.49	37.31	37.29	-473	69.75	69.72	4699	63.69	3947	66.41	4293	63.2	3884	67.73	4456	63.45	3917
145	39.49	24.89	24.86	-3825	62.18	62.12	3745	54.68	2682	58.13	3188	57.61	3114	59.82	3425	55.96	2873
146	35.72	71.72	47.63	2378	87.54	58.13	4026	84.02	3687	83.16	3602	68.97	2055	83.15	3601	78.11	3083
147	35.72	71.72	62.63	4643	87.54	76.45	6290	84.02	5951	83.16	5866	68.97	4319	83.15	5865	78.11	5348

Appendix C4. Mixing Scenario Outputs--Continued

Model Run No.	System	Initial Member 1	Initial Member 2	Initial Member 3	Final Member	Phases	Notes
148	Alk. Earth + Na	Greer3	Bratton2	N/a	Spring 25	Init1, Init2, Si, Cal, Dolo, Stro, EX	Diss.1,2 2(F)
149	Alk. Earth + Na	Greer3	Bratton2	N/a	Spring 25	Init1, Init2, Si, Cal, Dolo, EX, IL	Diss.1,2 2(F)
150	Alk. Earth + Na	Greer3	Bratton2	N/a	Spring 25	Init1, Init2, Si, Cal, Dolo, EX, NaCl	Diss.1,2 2(F)
151	Alk. Earth + Na	Greer3	Bratton2	N/a	Spring 25	Init1, Init2, Si, Cal, Dolo, IL, NaCl	Diss.1,2 2(F)
152	Alk. Earth + Na	Greer3	Bratton2	N/a	Spring 25	Init1, Init2, Si, Cal, Stro, EX, NaCl	Diss.1,2 2(F)
153	Alk. Earth + Na	Greer3	Bratton2	N/a	Spring 25	Init1, Init2, Si, Cal, EX, IL, NaCl	Diss.1,2 2(F)
154	Alk. Earth + Na	Greer3	Bratton2	N/a	Spring 25	Init1, Init2, Si, Dolo, Stro, EX, IL	Diss.1,2 2(F)
155	Alk. Earth + Na	Greer3	Bratton2	N/a	Spring 25	Init1, Init2, Si, Dolo, Stro, EX, NaCl	Diss.1,2 2(F)
156	Alk. Earth + Na	Greer3	Bratton2	N/a	Spring 25	Init1, Init2, Si, Stro, EX, IL, NaCl	Diss.1,2 2(F)
157	Alk. Earth + Na	Greer3	Bratton2	N/a	Spring 25	Init1, Init2, Cal, Dolo, Stro, EX, IL	Diss.1,2 2(F)
158	Alk. Earth + Na	Greer3	Bratton2	N/a	Spring 25	Init1, Init2, Cal, Stro, EX, IL, NaCl	Diss.1,2 2(F)
159	Alk. Earth + Na	Greer3	Bratton2	N/a	Spring 25	Init1, Init2, Dolo, Stro, EX, IL, NaCl	Diss.1,2 2(F)
160	Alk. Earth + Na	Bratton2	Thornton	Greer3	Spring 25	Init1, Init2, Init3, Si, Cal, Dolo, Stro, EX	Diss.1, 2,3 3(F)
161	Alk. Earth + Na	Bratton2	Thornton	Greer3	Spring 25	Init1, Init2, Init3, Si, Cal, Stro, EX, NaCl	Diss.1, 2,3 3(F)
162	Alk. Earth + Na	Bratton2	Thornton	Greer3	Spring 25	Init1, Init2, Init3, Si, Cal, EX, IL, NaCl	Diss.1, 2,3 3(F)
163	Alk. Earth + Na	Bratton2	Thornton	Greer3	Spring 25	Init1, Init2, Init3, Si, Stro, EX, IL, NaCl	Diss.1, 2,3 3(F)
164	Alk. Earth + Na	Bratton2	Thornton	Greer3	Spring 25	Init1, Init2, Init3, Cal, Stro, EX, NaCl	Diss.1, 2,3 3(F)
165	Alk. Earth + Na	Bratton2	Thornton	N/a	Spring 25	Init1, Init2, Si, Cal, Dolo, Stro, EX	Diss. 1,2 2(F)
166	Alk. Earth + Na	Bratton2	Thornton	N/a	Spring 25	Init1, Init2, Si, Cal, Stro, EX, NaCl	Diss. 1,2 2(F)
167	Alk. Earth + Na	Bratton2	Thornton	N/a	Spring 25	Init1, Init2, Si, Dolo, Stro, EX, IL	Diss. 1,2 2(F)
168	Alk. Earth + Na	Bratton2	Thornton	N/a	Spring 25	Init1, Init2, Cal, Dolo, Stro, EX, IL	Diss. 1,2 2(F)
169	Alk. Earth + Na	Bratton2	Thornton	N/a	Spring 25	Init1, Init2, Cal, Stro, EX, IL, NaCl	Diss. 1,2 2(F)
170	Alk. Earth + Na	Bratton2	HSSSCr	N/a	Spring 25	Init1, Init2, Si, Cal, Dolo, Stro, EX	Diss. 1,2 2(F)
171	Alk. Earth + Na	Bratton2	HSSSCr	N/a	Spring 25	Init1, Init2, Si, Cal, Stro, EX, NaCl	Diss. 1,2 2(F)
172	Alk. Earth + Na	Bratton2	HSSSCr	N/a	Spring 25	Init1, Init2, Si, Dolo, Stro, EX, IL	Diss. 1,2 2(F)
173	Alk. Earth + Na	Bratton2	HSSSCr	N/a	Spring 25	Init1, Init2, Cal, Dolo, Stro, EX, IL	Diss. 1,2 2(F)
174	Alk. Earth + Na	Bratton2	ARKSCr	N/a	Spring 25	Init1, Init2, Co2, Si, Cal, Stro, EX	Diss,1,2 2(F), Co2 diss
175	Alk. Earth + Na	Bratton2	ARKSCr	N/a	Spring 25	Init1, Init2, Co2, Si, Stro, EX, IL	Diss,1,2 2(F), Co2 diss
176	Alk. Earth + Na	Bratton2	ARKSCr	N/a	Spring 25	Init1, Init2, Co2, Si, Stro, EX, NaCl	Diss,1,2 2(F), Co2 diss
177	Alk. Earth + Na	Bratton2	ARKSCr	N/a	Spring 25	Init1, Init2, Si, Cal, Stro, EX, IL	Diss1&2 2(F)
178	Alk. Earth + Na	Bratton2	ARKSCr	N/a	Spring 25	Init1, Init2, Si, Cal, Stro, EX, NaCl	Diss1&2 2(F)
179	Alk. Earth + Na	Bratton2	ARKSCr	N/a	Spring 25	Init1, Init2, Si, Dolo, Stro, EX, NaCl	Diss1&2 2(F)
180	Alk. Earth + Na	Bratton2	ARKSCr	N/a	Spring 25	Init1, Init2, Si, Stro, EX, IL, NaCl	Diss1&2 2(F)
181	Alk. Earth + Na	Bratton2	ARKSCr	N/a	Spring 25	Init1, Init2, Dolo, Stro, EX, IL, NaCl	Diss1&2 2(F)

Appendix C4. Mixing Scenario Outputs--Continued

Model Run No.	Calculated Mass Transfer (mg/L)											Comp. $\delta^{13}C$ ($^0/_{00}$)	Observed $\delta^{13}C$ ($^0/_{00}$)	% error
	Initial Water 1	Initial Water 2	Initial Water 3	SiO_2	CO_2 gas	Dolomite	Strontianite	Calcite	Ca/Na Exchange	Illite	NaCl			
148	0.956	0.044		0.362		-0.035	-0.00235	-0.1212	-0.213			-13.19	-14.73	10.44
149	0.282	0.718		-4.496		-0.231		0.9131	-0.025	1.412		-13.92	-14.73	5.47
150	0.282	0.718		0.446		0.122		0.2071	-0.378		0.706	-15.94	-14.73	8.22
151	0.282	0.718		-4.848		-0.257		0.9634		1.513	-0.050	-13.72	-14.73	6.82
152	0.806	0.194		0.380			-0.00183	-0.0485	-0.250		0.156	-14.12	-14.73	4.16
153	0.282	0.718		-1.257				0.4503	-0.257	0.486	0.463	-15.94	-14.73	8.22
154	0.877	0.123		-0.207		-0.058	-0.00207		-0.191	0.165		-13.67	-14.73	7.19
155	0.707	0.293		0.393		0.023	-0.00148		-0.274		0.261	-14.61	-14.73	0.83
156	0.755	0.245		0.221			-0.00165		-0.251	0.047	0.186	-14.46	-14.73	1.87
157	0.905	0.095				-0.049	-0.00217	-0.4413	-0.199	0.105		-13.49	-14.73	8.39
158	0.684	0.316					-0.0014	0.0674	-0.251	0.113	0.228	-14.68	-14.73	0.36
159	0.818	0.182				-0.030	-0.00187		-0.220	0.108	0.090	-14.04	-14.73	4.67
160	0.956	0.000	0.044	0.362		-0.035	-0.00235	-0.1212	-0.213			-13.19	-14.73	10.44
161	0.806	0.000	0.194	0.380			-0.00183	-0.0485	-0.250		0.156	-14.12	-14.73	4.16
162	0.282	0.000	0.718	-1.257				0.4503	-0.257	0.486	0.463	-15.94	-14.73	8.22
163	0.610	0.128	0.261	0.000			-0.00142		-0.323	0.103	0.359	-15.25	-14.73	3.50
164	0.684	0.000	0.316				-0.0014	0.0674	-0.251	0.113	0.228	-14.68	-14.73	0.36
165	0.968	0.032		0.349		-0.042	-0.00246	-0.1519	-0.223			-13.10	-14.73	11.09
166	0.429	0.571		0.233			-0.00175	-0.3037	-0.569		0.772	-15.71	-14.73	6.65
167	0.836	0.164		-1.003		-0.127	-0.00228		-0.213	0.378		-13.75	-14.73	6.68
168	0.934	0.066				-0.064	-0.00241	-0.1127	-0.221	0.098		-13.26	-14.73	9.95
169	0.253	0.747					-0.00151	-0.3258	-0.668	0.056	0.997	-16.54	-14.73	12.32
170	0.928	0.072		0.352		-0.004	-0.0023	-0.1469	-0.210			-13.62	-14.73	7.51
171	0.712	0.288		0.338			-0.00171	-0.1590	-0.232		0.139	-15.85	-14.73	7.60
172	0.677	0.323		-0.791		-0.075	-0.00161		-0.155	0.322		-16.21	-14.73	10.04
173	0.851	0.149				-0.046	-0.00209	-0.1017	-0.193	0.099		-14.43	-14.73	2.05
174	0.651	0.349		0.387	0.0375		-0.00153	-0.0370	-0.139			-16.14	-14.73	9.54
175	0.576	0.424		0.260	0.0501		-0.00132		-0.121	0.038		-16.89	-14.73	14.66
176	0.651	0.349		0.387	0.0005		-0.00153		-0.102		-0.074	-15.99	-14.73	8.53
177	0.872	0.128		0.766			-0.00214	-0.1473	-0.194	-0.114		-14.00	-14.73	4.99
178	0.349	0.387					-0.00153	0.0005	-0.102		-0.075	-15.98	-14.73	8.50
179	0.652	0.348		0.387		0.000	-0.00153		-0.102		-0.075	-15.97	-14.73	8.44
180	0.651	0.349		0.388			-0.00153		-0.102	0.000	-0.075	-15.98	-14.73	8.47
181	0.783	0.217				-0.044	-0.00189		-0.113	0.107	-0.118	-14.78	-14.73	0.31

Appendix C4. Mixing Scenario Outputs--Continued

		Original Data			Mass Balance (1990)			Tamers (1975)		Ingerson and Pearson (1964)		Mook (1972)		Fontes and Garnier (1979)		Eichinger (1983)	
Model Run No.	Observed $\delta^{14}C$ (pmc)	Ao TDC (pmc)	Ao TDC comp. (no decay)	Adjusted age (years)	Ao TDC (pmc)	Ao TDC comp. (no decay)	Adjusted age (years)	Ao TDC (pmc)	Adjusted age (years)	Ao TDC (pmc)	Adjusted age (years)	Ao TDC (pmc)	Adjusted age (years)	Ao TDC (pmc)	Adjusted age (years)	Ao TDC (pmc)	Adjusted age (years)
148	35.72	25.41	25.4	-2819	62.64	62.62	4640	55.26	3604	58.75	4110	58.27	4042	60.44	4344	56.54	3793
149	35.72	58.96	42.32	1401	82.69	59.35	4197	79.01	3821	80.35	3959	72.17	3072	81	4026	76.03	3503
150	35.72	58.96	50.09	2795	82.69	70.25	5591	79.01	5215	80.35	5353	72.17	4466	81	5420	76.03	4897
151	35.72	58.96	47.19	2303	82.69	66.19	5098	79.01	4723	80.35	4861	72.17	3974	81	4928	76.03	4404
152	35.72	31.61	31.61	-1010	66.35	66.34	5118	59.65	4239	62.74	4656	60.84	4401	64.24	4851	60.14	4306
153	35.72	58.96	46.92	2255	82.69	65.8	5050	79.01	4675	80.35	4813	72.17	3926	81	4880	76.03	4356
154	35.72	28.62	28.62	-1833	64.56	64.55	4891	57.53	3939	60.82	4397	59.6	4230	62.41	4610	58.41	4063
155	35.72	36.09	35.53	-43	69.02	67.96	5317	62.82	4539	65.62	4899	62.69	4522	66.98	5069	62.74	4528
156	35.72	33.87	33.74	-470	67.7	67.44	5254	61.25	4427	64.19	4815	61.78	4497	65.62	4997	61.46	4454
157	35.72	27.43	27.43	-2184	63.85	63.83	4799	56.69	3816	60.05	4292	59.11	4161	61.68	4513	57.72	3964
158	35.72	37.13	36.31	135	69.65	68.1	5334	63.56	4578	66.3	4926	63.13	4521	67.62	5090	63.35	4550
159	35.72	31.11	31.11	-1143	66.05	66.04	5080	59.3	4189	62.42	4613	60.63	4373	63.93	4811	59.85	4266
160	35.72	25.41	25.4	-2819	62.64	62.62	4640	55.26	3604	58.75	4110	58.27	4042	60.44	4344	56.54	3793
161	35.72	31.61	31.61	-1010	66.35	66.34	5118	59.65	4239	62.74	4656	60.84	4401	64.24	4851	60.14	4306
162	35.72	58.96	46.92	2255	82.69	65.8	5050	79.01	4675	80.35	4813	72.17	3926	81	488	76.03	4356
163	35.72	40.66	40.66	1071	71.03	71.03	5682	65.01	4950	67.16	5219	62.38	4608	68.31	5359	64.01	4822
164	35.72	37.13	36.31	135	69.65	68.1	5334	63.56	4578	66.3	4926	63.13	4521	67.62	5090	63.35	4550
165	35.72	25.1	25.08	-2922	62.28	62.25	4592	54.79	3533	58.21	4034	57.62	3949	59.9	4269	56.03	3718
166	35.72	48.27	48.24	2484	73.38	73.33	5946	67.2	5219	67.77	5289	58.79	4115	68.48	5375	64.2	4841
167	35.72	30.86	30.85	-1212	65.05	65.01	4951	57.88	3986	60.59	4364	57.91	3990	62.04	4559	58.06	4012
168	35.72	26.59	26.58	-2444	63	62.97	4687	55.59	3653	58.83	4121	57.7	3960	60.45	4345	56.56	3795
169	35.72	55.68	55.64	3664	76.92	76.87	6336	71.71	5693	70.83	5653	59.17	4167	71.22	5700	66.81	5171
170	35.72	28.71	28.7	-1810	62.02	62	4558	54.65	3512	60.39	4337	62.94	4679	62.9	4675	58.71	4104
171	35.72	44.1	44.09	1740	63.31	63.29	4728	56.56	3797	68.82	5418	79.42	6602	73.7	5985	68.42	5370
172	35.72	46.62	46.61	2199	63.52	63.5	4756	56.88	3843	70.2	5583	82.11	6878	75.47	6181	70.01	5560
173	35.72	34.14	64.13	-377	62.48	62.13	4618	55.33	3614	63.36	4735	68.75	5410	66.72	5161	62.13	4573
174	35.72	46.13	46.79	2232	62.26	62.73	4655	55.07	3662	69.93	5597	92.25	7851	77.13	6394	69.01	5490
175	35.72	51.37	52.18	3133	62.41	63.04	4696	55.31	3726	72.8	5937	100.34	8538	81.28	6828	72.16	5866
176	35.72	46.13	46.14	2115	62.26	62.27	4594	55.07	3580	69.93	5554	92.25	7843	77.13	6364	69.01	5445
177	35.72	31.49	31.48	-1043	61.86	61.81	4533	54.39	3474	61.91	4544	69.64	5516	65.56	5017	60.23	4316
178	35.72	46.13	46.12	2112	62.26	62.25	4592	55.07	3577	69.93	5552	92.25	7842	77.13	6363	69.01	5443
179	35.72	46.04	46.04	2099	62.26	62.26	4593	55.07	3578	69.88	5548	92.12	7832	77.07	6357	68.96	5438
180	35.72	46.08	46.11	2110	62.26	62.3	4599	55.07	3584	69.9	5556	92.17	7842	77.09	6365	68.98	5446
181	35.72	37.24	37.23	343	62	61.99	4557	54.66	3515	65.06	4955	78.52	6509	70.11	5573	63.68	4778

APPENDIX D

Model Statistics

D1. Non-Mixing Scenario Summary Statistics

D2. Mixing Scenario Summary Statistics

D1. Non-Mixing Scenario Summary Statistics

	Original Data			Mass Balance (1990)			Tamers (1975)		Ingerson and Pearson (1964)		Mook (1972)		Fontes and Garnier (1979)		Eichinger (1983)	
	Ao TDC (pmc)	Ao TDC comp. (no decay)	Adjusted age (years)	Ao TDC (pmc)	Ao TDC comp. (no decay)	Adjusted age (years)	Ao TDC (pmc)	Adjusted age (years)	Ao TDC (pmc)	Adjusted age (years)	Ao TDC (pmc)	Adjusted age (years)	Ao TDC (pmc)	Adjusted age (years)	Ao TDC (pmc)	Adjusted age (years)
Basics																
Min	23.67	23.65	-5277	61.6	32.76	-849	54.03	-1706	57.63	2079	57.55	2067	59.37	394	55.53	1772
Max	98.9	59.72	4248	94.42	71.74	5765	92.99	5632	98.84	5639	173.79	7434	118.88	5642	102.98	5129
Median	23.67	23.655	-3671	61.6	61.55	4236	54.03	3152	57.63	3685	57.55	3710	59.37	3967.5	55.53	3378
Average	30.516	26.937	-3121.4	63.077	60.233	3833.967	55.756	2805.833	61.556	3559.933	64.867	3758.6	64.235	3750.033	59.681	3282.633
Alkaline-Earth																
Min	23.67	23.13	-5377	61.6	60.2	2530	54.03	1446	57.63	1979	57.55	1144	59.37	2225	55.53	1672
Max	66.1	57.98	3848	81.91	71.85	5620	76.74	5082	75.12	4905	59.7	3812	75.08	4901	70.48	4378
Median	66.1	56.57	1986	81.91	70.1	4375	76.74	3290	75.12	3823	59.7	2846	75.08	4070	70.48	3517
Average	46.133	41.084	-105.294	72.352	65.866	4554	66.053	3758.471	66.889	3933.471	58.688	2863.824	67.687	4029.588	63.445	3492.412
Alkaline-Earth-plus-Sodium																
Min	23.37	7.42	-13823	61.6	19.3	-5916	54.03	-7001	57.63	-6468	57.55	-6479	59.37	-6221	55.53	-6774
Max	66.1	7180.61	43580	81.91	18687.86	51487	76.74	50402	75.12	50935	59.7	50924	75.08	51182	70.48	50628
Median	23.67	23.66	-3406	61.6	61.57	4328	54.03	3336	57.63	3764	57.55	3760	59.37	4063	55.53	3466
Average	33.849	137.630	-501.213	66.474	330.061	5852.72	59.480	5042.187	61.828	5257.52	58.066	4831.12	63.140	5928.72	59.118	4947.413

Appendix D2. Mixing Scenario Summary Statistics

	Original Data			Mass Balance (1990)			Tamers (1975)		Ingerson and Pearson (1964)		Mook (1972)		Fontes and Garnier (1979)		Eichinger (1983)	
	Ao TDC (pmc)	Ao TDC comp. (no decay)	Adjusted age (years)	Ao TDC (pmc)	Ao TDC comp. (no decay)	Adjusted age (years)	Ao TDC (pmc)	Adjusted age (years)	Ao TDC (pmc)	Adjusted age (years)	Ao TDC (pmc)	Adjusted age (years)	Ao TDC (pmc)	Adjusted age (years)	Ao TDC (pmc)	Adjusted age (years)
Basics																
Min	33.95	33.95	-420	62.26	62.26	4594	55.08	3579	64.24	4852	61.81	4533	65.67	5034	61.5	4492
Max	50.68	50.68	2133	77.74	77.85	5599	73.15	5096	75.01	5560	92.41	7858	77.22	6373	71.22	5452
Median	33.95	33.95	-420	67.74	67.74	5291	61.31	4465	64.24	4852	61.81	4533	65.67	5034	61.5	4492
Average	39.752	39.752	587	68.644	68.666	5213.2	62.432	4414	67.544	5084	69.316	5207.8	70.03	5375.6	64.96	4760.6
Alkaline-Earth																
Min	24.83	24.86	-3825	62.3	62.37	3779	54.85	2726	58.37	3241	57.68	3057	60.08	3480	53.2	2928
Max	48.72	61.26	2239	73.59	71.51	5701	67.44	4974	68.82	5338	79.42	6522	73.7	5905	68.42	5290
Median	31.61	43.66	-1103	66.35	65.18	4648	59.65	3717	62.74	4251	58.82	3423	64.24	4334	60.14	3801
Average	34.674	40.84	-1083.89	66.321	65.494	4540.44	59.49	3633.78	62.729	4134.89	61.483	3890.556	64.907	4359.89	60.38	3807.56
Alkaline-Earth-plus-Sodium																
Min	24.48	24.45	-3962	61.86	53.48	2507	54.39	2173	58.13	2091	57.61	421	59.82	488	55.96	1573
Max	71.89	76.04	5416	87.71	92.77	7060	84.24	6726	93.41	6644	100.34	8538	83.4	6828	78.34	6126
Median	37.31	39.17	135	66.35	63.83	4699	59.65	3821	66.41	4813	63.2	4319	68.31	4928	63.68	4356
Average	42.968	40.403	416.156	69.982	65.626	4828.089	63.925	4041.133	68.942	4683.511	69.1	4596.156	71.048	4863.756	66.0231	4358.24

Appendix E

Compilation Summary of Selected Previous Publications of the Hydrogeology of Hot Springs National Park

Appendix E Compilation Summary of Selected Previous Publications of the Hydrogeology of HSNP

Name	**What they did**	**Results**
Weed (1902), Purdue (1910), Purdue and Miser (1923)	Proponents of the theory of the meteoric origin of the spring waters	Proponents of the theory of the meteoric origin of the spring waters
Bryan (1922)	Posed the question as to the meteoric, juvenile, or mixed origin of the waters discharged from the Hot Springs.	Conceded that a definite conclusion could not be reached at that point in time.
Purdue and Miser (1923)	Wrote up a stratigraphic and structural description of the Hot Springs District.	Wrote up a stratigraphic and structural description of the Hot Springs District.
Bedinger, M.S.; Pearson, Jr., F.J., Reed, J.E.; Sniegocki, R.T.; Stone, C.G. (1979)	Measured the combined flow of the hot springs. Determined when the flow of the springs was the highest and the lowest. Measured the radioactivity and geochemical, and isotopic composition of the waters. Established the presence of radium and radon in the hot spring waters. Used mathematical models to test the various conceptual models of the hot springs flow system. Determined where the recharge zone is located.	The flow of the hot springs ranges from 750,000 to 950,000 gal/day. The flow is highest during the winter and spring and is the lowest during the summer and fall. Determined the radioactivity and chemical composition of the hot-water springs similar to the cold-water springs and wells in the area. TDS concentrations range from 175-200 mg/L. Cold waters range from 15.0-26.8°C. Silica concentrations for cold-water range from 2.6-13.0 mg/L; for hot-water they are ~42 mg/L. ^{3}H and ^{14}C analyses of the water indicated that the water is a mix of a small amount of water > 20 yrs and a preponderance of water ~4,400 yrs. ^{2}H and ^{18}O concentrations were not significantly different between hot-spring waters and cold ground waters. [Ra] = 2.1 picocuries/L. [Rn] range from 0.14-30.5 nanocuries/L. The geochemical data, flow measurements, and geologic structure of the region support the concept that virtually all the hot-springs water is of local, meteoric origin. The recharge zone occurs in the outcrop areas of the Bigfork Chert and the Arkansas Novaculite.
Bell and Hays (2007)	Used water-quality, water temperature, isotopic and radiochemical data to support the importance of the cold-water component of the hot springs.	Silica and TDS binary mixing models indicated that cold water recharge from storm events contributes an estimated 10-35% of the discharge issuing from the springs. Temperature modeling indicated that 1-35% of the discharge from various hot springs originated from cold water recharge.

Appendix E Compilation Summary of Selected Previous Publications of the Hydrogeology of HSNP-Continued

Name	What they did	Results
Yeatts (2006)	Measured the discharge of the springs and did continuous water temperature monitoring at the collection system reservoir inflow pipe. Monitored water temperatures at 4 thermal springs from August 2000-June 2005 & 4 additional thermal springs plus 1 thermal spring box was monitored from September 2003-June 2005. Determined where the cold-water component enters the ground. Estimated the size of the shallow cold-water recharge area from the hydrologic budget. Performed a Rhodamine dye trace on Hot Springs Mountain	The average collection discharge from 1990-1995 & 1998-2005 was 658,000 gal/day with an increasing rate of discharge. Temperature monitoring also showed a positive relation to discharge in 1990-1995 and an inverse relation to discharge from 1998-2005. The daily water temperature at the collection system reservoir flow ranged from 59.1-62.1°C. The data showed high seasonality. The thermal-water component enters the ground-water system and flows to estimated depths of 4,500 to 7,500 ft where the water is heated and rises along fault and fracture conduits. The cold-water component enters the ground-water system as locally derived recharge and flows along shallow NE trending faults, joints, and fractures to the thermal springs. The thermal springs are bounded on the SW, SE, and NW by shale barriers. The lower member of the Arkansas Novaculite was postulated to be the primary aquifer of the shallow groundwater flow. Groundwater levels generally indicated that the groundwater flow is towards Hot Springs Creek. The cold groundwater baseflow discharge is 17.8 million gal/year, with an estimated shallow cold-water recharge area of 0.10-0.20 mi^2. The shallow cold-water recharge area appears to be bounded on 3 sides by low permeability barriers and extends to the topographic divide. The estimated shallow ground-water recharge area based on the boundaries is ~0.14 mi^2. The dye trace was detected over a period of several weeks at several thermal water recovery sites. The flow path was postulated to be either along the western boundary contact with the Stanley Shale or along the NE-trending fractured lineaments. The presence of the dye verified that this area is part of the recharge area and that surface water enters the ground-water system at some point along the pathway of the rhodamine dye. Travel time from the release point to the thermal springs ranged from 1-3 weeks.

Appendix E Compilation Summary of Selected Previous Publications of the Hydrogeology of HSNP-Continued

Name	What they did	Results
Kresse and Hays (2009)	Characterized the water quality and geochemistry for the shallow groundwater system and provided a basis of comparison to the geochemistry of the hot springs by sampling fifteen shallow wells, two cold-water springs, and ten hot springs	Concluded that the hydrogeochemistry of the hot springs is the result of the rock/water interactions in the shale formations in the deeper sections of the of the flow path; the low strength ionic waters enter the ground through the quartz formations, travel through the upper formations and are modified by passage through shale formations present at depth. Mixing curves that used Sr, Li, and Mn data indicated that the shale formations were more significant than the quartz formations for much of the dissolved species content comprising the overall geochemistry. Mixing model analysis for Sr geochemistry indicated that 35%percent of the Sr came from the shale formations while the other 65% were contributed from the quartz formations.
Darrell Pennington written commun. (2009)	Pennington used the geochemical and isotopic data collected by Bell and Hays (2007) and Kresse and Hays (2009) in the integrated mass-balance model NetpathXL. Used an inverse mass-balance model approach and local isotopic values to calculate the MRT of the thermal springs in HSNP.	40 model runs provided ages ranging from 1281-5030 years old.
Raley, K.R.; Hays, P.D.; Brahana, J.V., Davis, R.K. (2019)	Used the mass-balance software NETPATH-WIN to make an improved age model using additional geological and geochemical data collected by Bell and Hays, 2007; Kresse and Hays, 2009. Calculations utilized 3 different geochemical systems, seven different A_0 models under both mixing and non-mixing scenarios. Calculated mass transfer NETPATH runs that contained higher than 15% error between observed and calculated $\delta^{13}C$ values were eliminated.	181 runs passed initial inspection. The Mass Balance (1990) A_0 model was determined to be the most applicable to this flow system while the Alkaline Earth geochemical system that contained carbon, Mg, Sr, Ca, and silica as constraints and CO_2 gas, dolomite, strontianite, calcite, and SiO_2 as phases was deemed the most realistic geochemical system due to its consistent calculated mass transfers. The median residence time calculated was 4,375 years.